

CAPITAL UNIVERSITY OF SCIENCE AND
TECHNOLOGY, ISLAMABAD



Proportional Load Sharing and Stability of DC Microgrid

by

Muhammad Rashad

A thesis submitted in partial fulfillment for the
degree of Doctor of Philosophy

in the

Faculty of Engineering

Department of Electrical Engineering

2019

Proportional Load Sharing and Stability of DC Microgrid

By

Muhammad Rashad
(PE123004)

Professor Dr. Adrian Traian

Gheorghe Asachi Technical University, Iasi, Romania
(Foreign Evaluator 1)

Senior Scientist Dr. Qadeer Ahmed
Ohio State University, Ohio, USA
(Foreign Evaluator 2)

Dr. Muhammad Ashraf
(Thesis Supervisor)

Dr. Noor Muhammad Khan
(Head, Department of Electrical Engineering)

Dr. Imtiaz Ahmed Taj
(Dean, Faculty of Engineering)

DEPARTMENT OF ELECTRICAL ENGINEERING
CAPITAL UNIVERSITY OF SCIENCE AND TECHNOLOGY
ISLAMABAD

2019

Copyright © 2019 by Muhammad Rashad

All rights reserved. No part of this thesis may be reproduced, distributed, or transmitted in any form or by any means, including photocopying, recording, or other electronic or mechanical methods, by any information storage and retrieval system without the prior written permission of the author.

To my parents



CAPITAL UNIVERSITY OF SCIENCE & TECHNOLOGY ISLAMABAD

Expressway, Kahuta Road, Zone-V, Islamabad
Phone: +92-51-111-555-666 Fax: +92-51-4486705
Email: info@cust.edu.pk Website: <https://www.cust.edu.pk>

CERTIFICATE OF APPROVAL

This is to certify that the research work presented in the thesis, entitled "**Proportional Load Sharing and Stability of DC Microgrid**" was conducted under the supervision of **Dr. Muhammad Ashraf**. No part of this thesis has been submitted anywhere else for any other degree. This thesis is submitted to the **Department of Electrical Engineering, Capital University of Science and Technology** in partial fulfillment of the requirements for the degree of Doctor in Philosophy in the field of **Electrical Engineering**. The open defence of the thesis was conducted on **January 22, 2019**.

Student Name: Mr. Muhammad Rashad (PE123004)

The Examining Committee unanimously agrees to award PhD degree in the mentioned field.

Examination Committee :

- (a) External Examiner 1: Dr. Shaikh Saqib Haroon
Associate Professor
UET, Taxila
- (b) External Examiner 2: Dr. Babar Hussain
Associate Professor
PIEAS, Islamabad
- (c) Internal Examiner : Dr. Umer Amir Khan
Assistant Professor
CUST, Islamabad

Supervisor Name : Dr. Muhammad Ashraf
Professor
CUST, Islamabad

Name of HoD : Dr. Noor Muhammad Khan
Professor
CUST, Islamabad

Name of Dean : Dr. Imtiaz Ahmad Taj
Professor
CUST, Islamabad

AUTHOR'S DECLARATION

I, **Mr. Muhammad Rashad (Registration No. PE-123004)**, hereby state that my PhD thesis titled, '**Proportional Load Sharing and Stability of DC Microgrid**' is my own work and has not been submitted previously by me for taking any degree from Capital University of Science and Technology, Islamabad or anywhere else in the country/ world.

At any time, if my statement is found to be incorrect even after my graduation, the University has the right to withdraw my PhD Degree.



(**Mr. Muhammad Rashad**)

Dated: **22** January, 2019

Registration No : PE123004

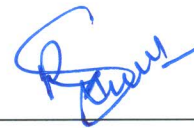
PLAGIARISM UNDERTAKING

I solemnly declare that research work presented in the thesis titled “**Proportional Load Sharing and Stability of DC Microgrid**” is solely my research work with no significant contribution from any other person. Small contribution/ help wherever taken has been duly acknowledged and that complete thesis has been written by me.

I understand the zero tolerance policy of the HEC and Capital University of Science and Technology towards plagiarism. Therefore, I as an author of the above titled thesis declare that no portion of my thesis has been plagiarized and any material used as reference is properly referred/ cited.

I undertake that if I am found guilty of any formal plagiarism in the above titled thesis even after award of PhD Degree, the University reserves the right to withdraw/ revoke my PhD degree and that HEC and the University have the right to publish my name on the HEC/ University Website on which names of students are placed who submitted plagiarized thesis.

Dated: 22 January, 2019



(**Mr. Muhammad Rashad**)
Registration No. PE123004

List of Publications

It is certified that following publication(s) have been made out of the research work that has been carried out for this thesis:-

Journal Publications

1. **M. Rashad**, M. Ashraf, A. I. Bhatti, and D. M. Minhas, "Mathematical Modeling and Stability Analysis of DC Microgrid Using SM Hysteresis Controller," *Electrical Power and Energy Systems*, vol. 95, pp. 507-522, 2018. (IF=3.61)
2. **M. Rashad**, U. Raouf, M. Ashraf, and B. A. Ahmed, "Proportional Load Sharing and Stability of DC Microgrid with Distributed Architecture Using SM Controller," *Mathematical Problems in Engineering*, vol. 2018, Article ID 2717129, pp. 16 pages, 2018. (IF=0.802)

Conference Publications

1. **M. Rashad**, D. M. Minhas, M. Ashraf, and S. Hussain, "PFC topologies for AC to DC converters in DC microgrid," *18th Mediterranean Electrotechnical Conference (MELECON 2016)*, Lemesos, Cyprus 2016.

Muhammad Rashad

(PE123004)

Acknowledgements

First of all my complements and thank to the Almighty ALLAH, WHO granted me the mental and physical abilities with the courage and wisdom of their execution. Regards to the all glory prophet MOHAMMAD (PBUH), for HIS enlightening teachings, that makes me focused and concentrated.

I am highly obliged to my supervisor Dr. Muhammad Ashraf for guiding me to the right things and pin pointed me at right. Also, by showing his belief in me, he provided me self motivating thoughts, which are more than helpful from my research perspective.

I am also thankful to Dr. Aamer Iqbal Bhatti. His valuable remarks is guiding me towards the peak of my research. His guidance in finding my research direction will always be unforgettable for me.

I am also thankful to Dr. Fazal-U-Rehman and Dr. Sajjad Hussain for providing me the background knowledge.

I am also thankful to Mr. Hassan Bin Ahmad and Mr. Daud Mustafa Minhas for their motivation and traveling support during my PhD Study.

Special thanks to my parents, brothers, sister, wife and my little kid Muhammad Burhan for their support and patience.

Abstract

AC electrical distribution system is presently dominating whose engineering foundations were planned above hundred years ago. However, the debate between ac and dc distribution system has started again due to the evolution of dc loads and increasing use of renewable energy sources (RESs). Currently, depleting threat of conventional fuels, growing energy demand and prices, and ecological changes necessitate that considerable power to be produced through RESs. Microgrids are modern form of distribution system which can function autonomously or in combination with main supply grid. Microgrids can operate in low or medium voltage range which have their own power generation with energy storage and loads. The unique property of the microgrids is that they can work in islanded mode under faulty grid conditions which increases the reliability of power supply. This inspires that microgrid is an effective way of power generation and consumption. In the near future, the distribution system may consist of some interconnected microgrids with local generation, storage and consumption of power.

Solar, wind and fuel cell technologies are playing an important role in electric power generation among various renewable sources. Most of these sources are inherently designed for dc or they are dc friendly. The growing use of these sources and fast evolution of domestic appliances from ac to dc attracting dc microgrids in the distribution system. DC microgrid system may be more efficient compared to the ac system because the integration of RESs in dc requires less conversion stages compared to ac. Additionally, the reactive power compensation and frequency synchronization circuits are not required in dc microgrids.

DC microgrids are not exempted from the stability concerns. In the first part of this thesis, voltage stability of dc microgrid based on decentralized control architecture is presented. Droop controllers are being used for voltage stability of dc microgrids. But droop control is not effective due to the error in steady state voltages and load power variations. Further, the voltage deviation increases with the increase in droop values which are not acceptable to the loads. Additionally, proportional integral (PI) controllers are being used to realize droop control for the

stability of dc microgrid. The main reason to use these control techniques is due to easy implementation of their tuning method in industrial applications. However, PI controllers cannot ensure global stability. They exhibit slower transient response and control parameters cannot be optimized with load power variations. To address the aforementioned limitation, sliding mode control (SMC) is proposed for voltage stability of dc microgrid in this thesis. Main advantages of SMC are high robustness, fast dynamic response and good stability for large load variations. To analyze the stability and dynamic performance, mathematical model of a dc microgrid is derived. Controllability and stability of the modeled system are verified. Hitting, existence and stability conditions are verified through SM. Modeled dynamics of the system are graphically plotted which shows that system trajectories converge to the equilibrium point. Detailed simulations are carried out to show the effectiveness of SM controller and results are compared with droop controller. SMC showed good voltage regulation performance in steady state condition. The effect of transient on a step load is also investigated which confirms the good performance of the proposed controller. Further, a small scale practical setup is developed, and results are presented.

In the second part of this thesis, distributed architecture using SM controller is proposed for proportional load sharing in dc microgrid. The key objectives of the dc microgrid include proportional load sharing and precise voltage regulation. Droop controllers are based on decentralized control architecture which are not effective to achieve these objectives simultaneously due to the voltage error and load power variations. Centralized controller can achieve these objectives using high bandwidth communication link. However, it loses reliability due to the single point failure. To address limitations, a distributed architecture using SM controller utilizing low bandwidth communication is proposed in this thesis. Main advantages are high reliability, load power sharing and precise voltage regulation. To analyze the stability and dynamic performance, system model is developed and its transversality, reachability and equivalent control condition are verified. Furthermore, the dynamic behavior of the modeled system is investigated for underdamped and critically damped response. Detailed simulation results are carried

out to show the effectiveness of the proposed controller.

Keywords: Microgrid, Droop controller, Proportional Integral (PI), Sliding Mode Control (SMC), Controllability, Stability, Transversality, Reachability, Underdamped, Critically damped.

Contents

| | |
|---|--------------|
| Author’s Declaration | iv |
| Plagiarism Undertaking | v |
| List of Publications | vi |
| Acknowledgements | vii |
| Abstract | viii |
| List of Figures | xv |
| List of Tables | xviii |
| Abbreviations | xix |
| Symbols | xxi |
| 1 Introduction | 1 |
| 1.1 Overview | 1 |
| 1.2 Generalized Model of DC Microgrid | 3 |
| 1.2.1 Grid Connected Mode | 3 |
| 1.2.2 Stand-alone Mode | 3 |
| 1.3 Control Architecture in DC Microgrid | 4 |
| 1.3.1 Centralize Control | 5 |
| 1.3.1.1 Tertiary Control (Energy Management System) | 7 |
| 1.3.1.2 Secondary Control (Power Sharing Control) | 7 |
| 1.3.2 Decentralized Control | 8 |
| 1.4 Overview of Factors Affecting Control Performance | 9 |
| 1.4.1 Switching Frequency | 9 |
| 1.4.2 Energy Storing Components | 10 |
| 1.4.3 Control Gain Parameters | 10 |
| 1.5 Commonly Available Control Techniques | 11 |
| 1.5.1 Hysteresis Control | 11 |
| 1.5.1.1 Hysteresis Voltage Control | 12 |

| | | |
|----------|--|-----------|
| 1.5.1.2 | Hysteresis Current Control | 12 |
| 1.5.2 | Pulse Width Modulation Control | 13 |
| 1.5.2.1 | Voltage Mode Controller | 13 |
| 1.5.2.2 | Current Mode Controller | 14 |
| 1.6 | Linear Control Techniques | 16 |
| 1.6.1 | Classical Control | 16 |
| 1.6.2 | Proportional Integral Derivative Control | 17 |
| 1.6.3 | Modern Control Techniques | 17 |
| 1.6.3.1 | State Feedback Control | 18 |
| 1.6.3.2 | Optimum Control Techniques | 18 |
| 1.6.4 | H Infinity Control | 19 |
| 1.6.5 | Linear Matrix Inequality | 19 |
| 1.7 | Control Techniques in Research | 20 |
| 1.7.1 | Adaptive Control | 20 |
| 1.7.2 | Fuzzy Logic Control | 20 |
| 1.7.3 | Artificial Neural Network Control | 21 |
| 1.7.4 | One Cycle Control | 21 |
| 1.7.5 | Genetic Algorithm | 21 |
| 1.7.6 | Passivity Based Control | 22 |
| 1.7.7 | Sliding Mode Control | 22 |
| 1.8 | Motivation | 22 |
| 1.9 | Statement of Problem | 23 |
| 1.10 | Statement of Contribution | 24 |
| 1.11 | Application of the Research | 26 |
| 1.12 | Thesis Organization | 26 |
| 2 | Feasibility of DC Distribution System | 28 |
| 2.1 | Overview | 28 |
| 2.2 | Motivation for DC Distribution | 29 |
| 2.2.1 | Electrical Loads | 29 |
| 2.2.1.1 | Electronic Appliances | 30 |
| 2.2.1.2 | Resistive Appliances | 31 |
| 2.2.1.3 | Universal Motor Based Appliances | 31 |
| 2.2.1.4 | Lighting Loads | 31 |
| 2.2.1.5 | Inverter Based Appliances | 32 |
| 2.2.1.6 | Plugged-in Electrical Vehicles | 32 |
| 2.2.2 | Renewable Energy Sources | 33 |
| 2.2.3 | Energy Storage | 33 |
| 2.2.4 | Data Centers | 33 |
| 2.2.5 | Shipyards System | 34 |
| 2.3 | Microgrid | 34 |
| 2.3.1 | AC Microgrid | 34 |
| 2.3.2 | DC Microgrid | 36 |
| 2.3.3 | DC Standardization Efforts | 37 |

| | | |
|----------|---|-----------|
| 2.4 | Summary | 37 |
| 3 | Control Architecture for Load Sharing | 39 |
| 3.1 | Overview | 39 |
| 3.2 | Passive Load Sharing Control | 40 |
| 3.2.1 | Implementation of droop controller | 44 |
| 3.2.1.1 | Voltage Droop by Adding External Series Resistance | 44 |
| 3.2.1.2 | Converters with Inherent Droop Characteristics | 45 |
| 3.2.1.3 | Current Mode Control with Low DC Gain | 46 |
| 3.2.1.4 | Voltage Droop by Output Feedback Current | 48 |
| 3.2.2 | Limitations of Droop Control in DC Microgrid | 49 |
| 3.2.2.1 | Current Sharing Inaccuracy | 49 |
| 3.2.2.2 | Output Voltage Deviation | 51 |
| 3.3 | Active Load Sharing Control | 52 |
| 3.3.1 | Centralized Control | 52 |
| 3.3.2 | Distributive Control | 53 |
| 3.4 | Summary | 55 |
| 4 | Voltage Stability of DC Microgrid using Sliding Mode Control | 57 |
| 4.1 | Overview | 57 |
| 4.2 | Sliding Mode Control | 59 |
| 4.3 | General Theory of Sliding Mode | 60 |
| 4.3.1 | Reaching Phase | 62 |
| 4.3.2 | Sliding Phase | 62 |
| 4.4 | Sliding Motion Properties | 62 |
| 4.4.1 | Sliding Motion Through Ideal Control | 62 |
| 4.4.2 | Practical Limits of Sliding Motion and Chattering Phenomena | 63 |
| 4.5 | Mathematical Formulation | 63 |
| 4.5.1 | Hitting Condition | 65 |
| 4.5.2 | Existence Condition | 66 |
| 4.5.3 | Stability Condition | 67 |
| 4.5.3.1 | Stability with Linear Sliding Surface | 68 |
| 4.5.3.2 | Stability with Nonlinear Sliding Surface | 69 |
| 4.6 | Implementation types of SM controller | 70 |
| 4.6.1 | Relay and Signum Function | 70 |
| 4.6.2 | Hysteresis Function | 71 |
| 4.6.3 | Equivalent Control Function | 73 |
| 4.7 | DC Microgrid Architecture | 74 |
| 4.8 | Modeling of DC Microgrid | 76 |
| 4.8.1 | Interconnection Structure | 77 |
| 4.8.2 | System Dynamic Equations | 78 |
| 4.9 | Stability Analysis | 79 |
| 4.9.1 | Controllability | 80 |
| 4.9.2 | Eigen values | 80 |

| | | |
|----------|---|------------|
| 4.10 | Voltage Stability Through Sliding Mode Control | 81 |
| 4.10.1 | System Design using Sliding Mode Controller | 81 |
| 4.10.1.1 | Sliding Surface Design | 81 |
| 4.10.1.2 | Control Law | 82 |
| 4.10.1.3 | Hitting Condition | 82 |
| 4.10.1.4 | Existence Condition | 83 |
| 4.10.1.5 | Stability Condition | 84 |
| 4.10.1.6 | Sliding Mode Hysteresis Control | 85 |
| 4.11 | Simulation Results and Discussion | 86 |
| 4.11.1 | Results using Droop Control | 86 |
| 4.11.2 | Results using Sliding Mode Control | 88 |
| 4.12 | Experimental Setup | 98 |
| 4.12.1 | Hardware Design Procedure | 99 |
| 4.12.2 | Practical Issues in Sliding Mode Implementation | 101 |
| 4.13 | Summary | 102 |
| 5 | Proportional Load Sharing using Sliding Mode Control | 106 |
| 5.1 | Overview | 106 |
| 5.1.1 | Proposed Distributive Control Architecture | 107 |
| 5.2 | Sliding Mode Control | 109 |
| 5.2.1 | Modeling | 109 |
| 5.2.2 | Sliding Mode Controller Analysis | 110 |
| 5.2.2.1 | Transversality Condition | 112 |
| 5.2.2.2 | Reachability Condition | 112 |
| 5.2.2.3 | Equivalent Control Condition | 113 |
| 5.2.3 | Sliding Mode Dynamics | 113 |
| 5.2.4 | Design of Sliding Mode Dynamic Behavior | 115 |
| 5.2.4.1 | Underdamped Response | 116 |
| 5.2.4.2 | Critically Damped Response | 117 |
| 5.2.5 | Sliding Mode Hysteresis Control | 117 |
| 5.3 | Simulation Results and Discussion | 118 |
| 5.3.1 | Results Using Droop Control | 119 |
| 5.3.2 | Results using Sliding Mode Control | 121 |
| 5.3.3 | Fail Safe Performance of Distributed Control Architecture | 126 |
| 5.3.4 | Performance Validation for More Sources | 126 |
| 5.4 | Summary | 129 |
| 6 | Conclusion and Future Work | 131 |
| 6.1 | Conclusion | 131 |
| 6.2 | Future Recommendations | 135 |
| | Bibliography | 136 |

List of Figures

| | | |
|------|---|----|
| 1.1 | Generic dc microgrid architecture | 4 |
| 1.2 | Hierarchical control architecture of a dc microgrid [10] | 6 |
| 1.3 | Hysteresis voltage control | 12 |
| 1.4 | Hysteresis current control | 13 |
| 1.5 | PWM voltage mode control | 14 |
| 1.6 | PWM peak current mode control | 15 |
| 1.7 | PWM average current mode control | 16 |
| | | |
| 2.1 | Power supply of electronic appliances | 31 |
| 2.2 | Power supply of Inverter based appliances | 32 |
| 2.3 | AC microgrid [126] | 35 |
| 2.4 | DC microgrid [126] | 36 |
| | | |
| 3.1 | Three sources in parallel configuration without any current sharing scheme | 41 |
| 3.2 | Steady state current distribution among sources | 41 |
| 3.3 | Parallel sources with droop control | 42 |
| 3.4 | Steady state characteristics with droop control | 42 |
| 3.5 | Step down dc to dc converter circuit and its output waveform [133] | 45 |
| 3.6 | Effective input resistance against duty cycle [133] | 46 |
| 3.7 | Voltage droop by current mode control with low dc gain | 47 |
| 3.8 | Voltage droop by output feedback current | 48 |
| 3.9 | Thevenin equivalent model of two-source dc microgrid | 49 |
| 3.10 | Current sharing inaccuracy using droop control [19] | 51 |
| 3.11 | Droop curves with different virtual resistances | 52 |
| 3.12 | Centralized control | 53 |
| 3.13 | Distributive control | 54 |
| | | |
| 4.1 | Reaching phase of SMC showing the system trajectory S moving towards the sliding surface irrespective of initial condition | 61 |
| 4.2 | Sliding phase of SMC showing the system trajectory S moving on the sliding surface directed and settles at the origin O | 61 |
| 4.3 | Practical SM with chattering in the system trajectory S moving along the sliding surface directed towards the origin O | 64 |
| 4.4 | System trajectory S in steady state bounded in periodically oscilating state near the origin O | 64 |

| | | |
|------|--|-----|
| 4.5 | System trajectory S converging to the sliding surface upon satisfying the hitting condition | 66 |
| 4.6 | System trajectory S inside the locality $0 < S > \delta$ and converging to sliding surface upon satisfying the existence condition | 67 |
| 4.7 | System trajectory S moving on sliding surface with stable and unstable behavior | 68 |
| 4.8 | Relay function using SMC | 71 |
| 4.9 | Hysteresis function using SMC | 72 |
| 4.10 | Chattering in trajectory S through hysteresis function | 72 |
| 4.11 | Low and high frequency components of trajectory in sliding phase | 73 |
| 4.12 | Structure of a node | 75 |
| 4.13 | Model of source- j with dc microgrid | 76 |
| 4.14 | Phase trajectories for (a) ideal SM; (b) actual SM with chattering | 85 |
| 4.15 | Three-source dc microgrid | 86 |
| 4.16 | Voltage controlled dc to dc buck converter using droop control | 87 |
| 4.17 | Node voltages using droop control in (a) with droop 0.04Ω (b) with droop 0.4Ω and (c) with droop 1.9Ω | 88 |
| 4.18 | Phase trajectories with $u = 1$ | 89 |
| 4.19 | Phase trajectories with $u = 0$ | 89 |
| 4.20 | Voltage controlled dc to dc buck converter using SM hysteresis control | 90 |
| 4.21 | Node voltages using hysteresis modulation based SMC | 90 |
| 4.22 | Average node voltage for different values of k | 91 |
| 4.23 | Average node voltage for different values of R_L | 91 |
| 4.24 | Source power variations applied to dc microgrid | 92 |
| 4.25 | Node voltages with the variation in source power | 92 |
| 4.26 | Transient response when a step load is applied to dc to dc converter at $0.2s$ | 93 |
| 4.27 | Output voltage when step load is changed from $R_L = 6.4\Omega$ to $R_L = 1.6\Omega$ with different values of α | 93 |
| 4.28 | Source currents for step change in power of load-3 | 95 |
| 4.29 | A dc microgrid with eight sources | 96 |
| 4.30 | Node voltages V1, V2, V3 and V4 | 97 |
| 4.31 | Node voltages V5, V6, V7 and V8 | 97 |
| 4.32 | Small scale experimental setup | 98 |
| 4.33 | Voltage controlled dc to dc buck converter using hysteresis based SMC | 104 |
| 4.34 | Experimental results: node voltages. Voltages: $10V/div$, x-axis: $20ns/div$ | 105 |
| 4.35 | Experimental results: control law u . Voltages: $10V/div$, x-axis: $50us/div$ | 105 |
| 5.1 | Distributive control architecture | 108 |
| 5.2 | Equivalent model of one source with dc microgrid | 110 |
| 5.3 | Block diagram of SM controller | 111 |
| 5.4 | System trajectory during SM operation | 118 |

| | | |
|------|---|-----|
| 5.5 | A two-source dc microgrid | 119 |
| 5.6 | DC to dc buck converter using droop control | 120 |
| 5.7 | Node voltages and source currents with droop gain 0.2Ω | 121 |
| 5.8 | DC to dc buck converter with distributed architecture using SM controller | 122 |
| 5.9 | Node voltages and source currents with distributed architecture using SM controller | 123 |
| 5.10 | Source 1 with 25% and source 2 with 75% load sharing of the rated load | 123 |
| 5.11 | Transient response when a step load of 3Ω is applied at 0.5 seconds | 124 |
| 5.12 | Voltage response of a source when load resistance is changed from 6 to 3Ω at 0.5 seconds | 125 |
| 5.13 | A three-source dc microgrid | 126 |
| 5.14 | Transient response during fault on source 2 at 0.5 seconds | 127 |
| 5.15 | A dc microgrid with eight sources sharing a load | 128 |
| 5.16 | Load voltages and current shared by source 1, 2, 3 and 4 | 128 |
| 5.17 | Current shared by source 5, 6, 7 and 8 | 129 |

List of Tables

| | | |
|-----|---|----|
| 2.1 | Classification of domestic appliances and loads | 30 |
| 3.1 | Summary of control architectures | 55 |

Abbreviations

| | |
|-------------|----------------------------------|
| RESs | Renewable Energy Sources- |
| DS | Distribution System |
| DC | Direct Current |
| AC | Alternating Current |
| VFDs | Variable Frequency Drives |
| PFC | Power Factor Correction |
| PECs | Power Electronic Converters |
| DSO | Distribution System Operator |
| TSO | Transmission System Operator |
| SoC | State of Charge |
| EMS | Energy Management System |
| HVDC | High Voltage DC |
| EMI | Electromagnetic Interference |
| PLC | Power Line Communication |
| P | Proportional |
| PI | Proportional Integral |
| PID | Proportional Integral Derivative |
| D | Derivative |
| CAN | Controller Area Network |
| PWM | Pulse Width Modulation |
| DBS | DC Bus Signaling |
| PV | Photovoltaic |
| CPLs | Constant Power Loads |
| SMC | Sliding Mode Control |

| | |
|-------------|--------------------------------------|
| VSSs | Variable Structured Systems |
| rms | Root Mean Square |
| UPS | Uninterruptable Power Supply |
| DCM | Discontinuous Current Condition Mode |
| ACS | Average Current Sharing |
| LAN | Local Area Network |
| SISO | Single Input Single Output |
| LTI | Linear Time Invariant |
| LQR | Linear Quadratic Regulator |
| LQG | Linear Quadratic Gaussian |
| MPC | Model Predictive Control |
| LMI | Linear Matrix Inequality |
| GA | Genetic Algorithm |

Symbols

| | |
|-----------------|----------------------------|
| u | Control Input |
| α, β | Sliding Coefficients |
| β | Sensing Ratio |
| ζ | Damping Ratio |
| ω_0 | Undamped Natural Frequency |
| S, Ψ | Sliding Surface |
| τ | Time Constant |
| t | Time |
| t_0 | Initial Time |
| n | Number of Nodes |
| m | Number of Branches |
| k | Positive Integer |

Chapter 1

Introduction

1.1 Overview

In the 19th century, the discussion between dc and ac distribution system (DS) had started [1], [2], [3], [4]. The advantages of ac system were remained dominant up to 20th century. However, due to the depleting threat of conventional fuels, growing electricity prices and demand, ecological fear of burning fossil fuels and apprehensions over climatic changes, it seems logical that a significant amount of power should be produced through RESs. Generating power close to the end user reduces power losses associated with transmitting and distribution of electricity and hence, increases system efficiency [1–13]. Microgrids can operate with main supply grid or autonomously as they have their own power generation i.e. RESs along with energy storage, non-renewable sources and power electronic (PE) controlled loads [14]. The unique property of the microgrids is that they can work in islanded mode under faulty grid conditions which increases the reliability of power supply [1, 2, 15]. In near future, the DS may consist of some interconnected microgrids with local generation, storage and consumption of power [9–13, 16].

Solar, wind and fuel cell technologies are playing an important role in electric power generation among various RESs. Most of these sources are inherently designed for dc or they are dc friendly. In ac microgrid, the DS is ac. Therefore, a

conversion stage is required to interconnect these sources with ac microgrid. The losses associated with these conversions decrease overall system efficiency. On the load side, many electrical loads are inherently designed for dc. A conversion stage is required for these loads in ac microgrid. This conversion can be avoided if these loads are powered directly by dc. Most of electronic, domestic and industrial loads convert ac to dc before consuming it. AC to dc rectifiers are nonlinear load which derate the transformers and cause damage to other devices due to produced harmonics. Hence, efficiency can be improved if these loads are directly powered by dc. Resistive loads can be powered both on ac and dc. Resistive loads will operate at same output power if the root mean square (rms) value of ac supply voltage is same as dc voltage. Hence most of the loads can be directly powered by dc.

Growing demand of RESs and unavailability of the main supply grid necessitates energy storage. Normally used energy storage devices are batteries. The operation and control of these devices require dc power. An extra conversion stage is required to interface these devices with ac microgrid. This is not required if these devices are directly powered by dc.

Due to the above-mentioned reasons, dc microgrids are becoming popular in the residential complexes, data centers [17] and commercial buildings [18]. It is expected that the efficiency of dc distribution will be 10 – 22% high than ac distribution [19]. Further, reactive power compensation and frequency synchronization circuits are not required in dc distribution which are prominent in ac distribution. Furthermore, skin effect problems are absent in dc. Due to these advantages, dc microgrid is an attractive subject for the researchers [1–19]. DC microgrid faces certain problems for practical realization which are given below.

- Financial cost associated with the replacement of ac distribution lines with new dc lines.
- Protection design of dc system is more difficult because dc circuit breakers are not evolved as ac circuit breakers are.

1.2 Generalized Model of DC Microgrid

DC microgrids are becoming popular due to availability of efficient PV systems and with the development of dc loads. DC microgrids are better suited for integration of RESs with loads and energy storage [1-5]. A generalized dc microgrid configuration [10] connecting different sources and loads is shown in Fig. 1.1. This configuration allows that any source can be interconnected within the microgrid. Every source in Fig. 1.1 contains a local load. Sources can be characterized as ac and dc sources. Wind and ac grid are ac sources. AC to dc power electronic converters (PECs) are required to interconnect these sources with a dc microgrid. While, fuel cell, PV and battery are dc sources. Since, the operating voltage of dc sources can vary, dc to dc PECs are required to interconnect these sources with dc microgrid. Further, sources and loads with dissimilar electrical characteristics are interconnected through PECs. Main utility grid can be interconnected to dc microgrid through ac to dc PEC with bi-directional power flow ability. There can be two modes of operation in dc microgrid which are described below.

1.2.1 Grid Connected Mode

In this mode, shortfall of power in dc microgrid is shared by utility grid. The role of batteries can be considered idle because utility grid is responsible for maintaining stable bus voltage within the limits [11, 16]. This mode is relatively simple because there is no need of complex bidirectional dc to dc controller to make decisions according to the state of charge (SOC) of batteries. Cost and maintenance cost of the batteries is also eliminated in this mode.

1.2.2 Stand-alone Mode

In this mode of operation, utility grid is no more available. Batteries role for both power balance and voltage stability is very important in this case. The control objective of the battery interface converter is to maintain stable voltage and make

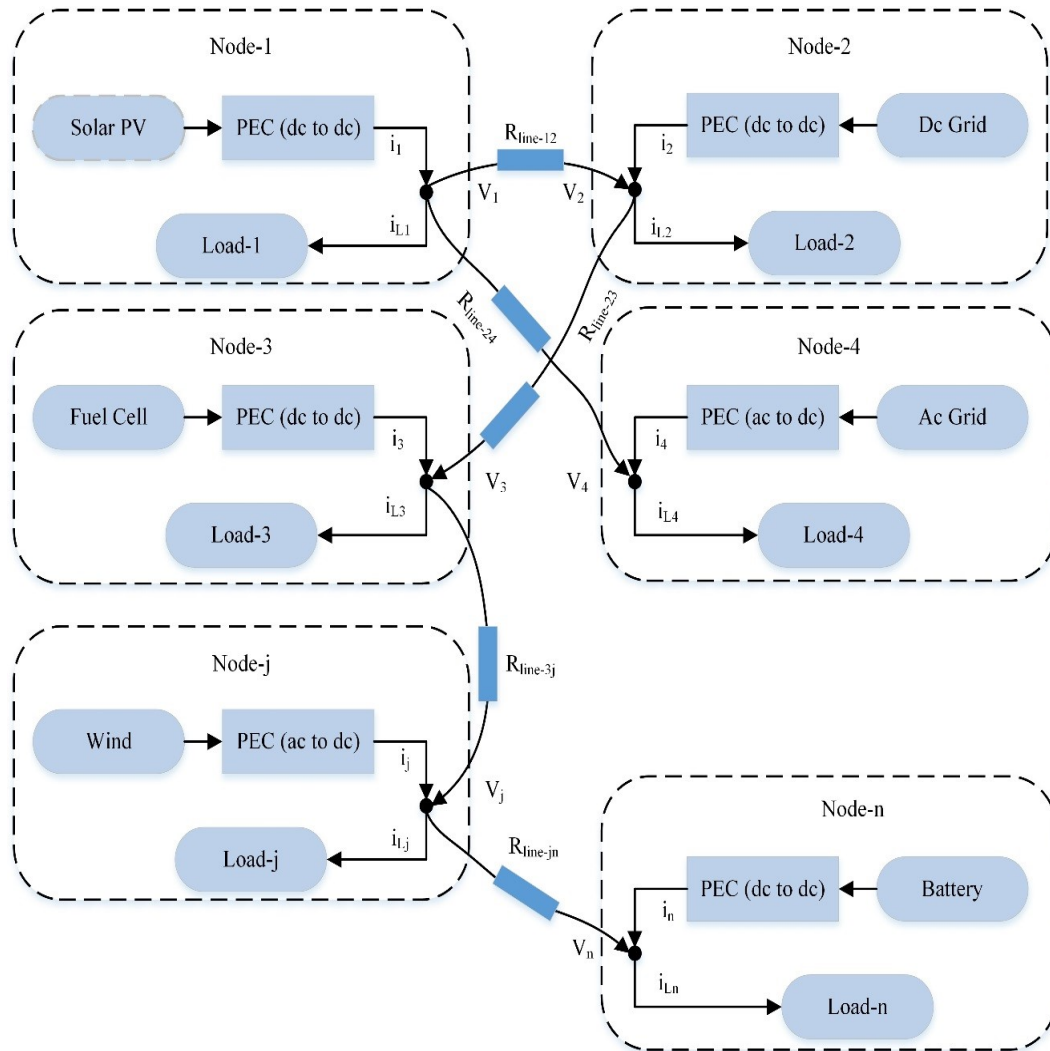


FIGURE 1.1: Generic dc microgrid architecture

decisions on the bases of SOC of battery [11, 16]. If there is shortage of power and battery is at low level of SOC, a non-renewable dc source is available for backup supply. For remote sites, stand-alone microgrids can be cost effective.

1.3 Control Architecture in DC Microgrid

Distributed generation can be connected to the dc microgrid through power PECs in parallel configuration. It is required to find efficient control to coordinate among various sources, loads and energy storage devices. There are two major concerns

of parallel connected sources which deals with actual power flow in a dc microgrid. The first concern is stability of the dc microgrid as electronic loads are very sensitive to voltage regulation. And second concern is load sharing among various sources [10, 17]. However, it is the nature of sources that only one unit can establish the voltage level in a paralleling system. The reason is the output resistances of the power sources which are extremely low. Thus, even a small difference in the output voltages between the paralleled sources will cause the one that is a few mili volt higher to hog all the current. If the output voltage of source is low, this problem will be more serious [20].

To address the aforementioned challenges, different control architectures are proposed in literature which can be categorized as centralized and decentralized control architectures [9, 11, 12], [20–22]. Fig. 1.2 shows the hierarchy of the control architecture used for a dc microgrid.

1.3.1 Centralize Control

In centralized control, a high bandwidth communication link is used to collect the system information. Centralized controller schedules the tasks based on the collected information and directs control decisions [9-11]. Centralize control can be divided into two controls: tertiary control and secondary control as shown in Fig. 1.2.

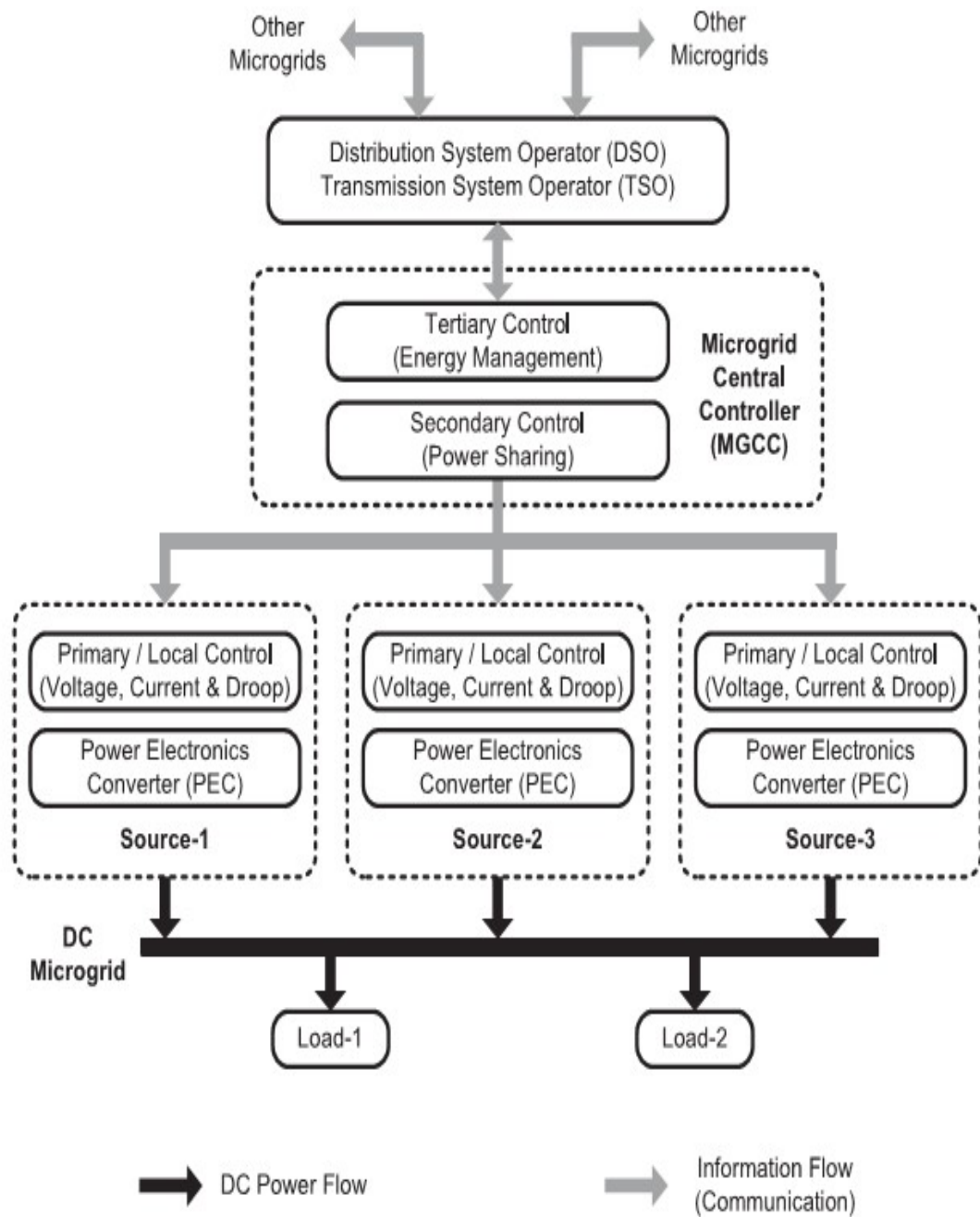


FIGURE 1.2: Hierarchical control architecture of a dc microgrid [10]

1.3.1.1 Tertiary Control (Energy Management System)

Tertiary control converses between secondary control and distribution system operator (DSO) or transmission system operator (TSO). DSO or TSO make decisions of power interchange among other microgrids. The main task of the DSO is to optimally control the operations of distributed sources and demand response. The demand response is responsible to accommodate the growing penetration of RESs, peak shaving and load balancing [23]. Demand response is an old idea, but it is attracting attention due to the extensive applications of smart meters and wireless communication [24]. Applying the demand response in the modern DS will help to optimally consume power generated by the RESs, reduce the peak demand hours and define schedule for the energy requirements. Improper management of DS will result in congestion, voltage disturbances and many other problems [25].

Energy management system (EMS) is responsible to optimize the demanded power to be fulfilled from the power available from the distributed sources. It is also responsible for peak shaving or load balancing and defines schedules for the demanded power to minimize the energy cost. Tertiary control collects system information and makes decisions of the tasks to be scheduled. These schedules are communicated to the secondary controller [9, 10, 21].

1.3.1.2 Secondary Control (Power Sharing Control)

Secondary control is responsible for proportional load sharing among various sources according to the schedules defined and communicated by the tertiary control. For proportional load sharing, secondary control defines the constraints of primary control (droop control) so that the bus voltage of the dc microgrid is maintained to acceptable tolerance [9, 10, 21]. Primary control is responsible for the compensation of the sudden mismatches among the scheduled and demanded power. Based on these mismatches, local controllers of various sources sets the reference voltage to share load

proportionally. However, secondary control depends on the power flow properties of the microgrid. In ac system, power flow depends on the voltage angle across the connecting lines/cables. Whereas in dc system, power flow depends on the voltage magnitude across connecting lines/cables. Further, there is no involvement of frequency parameter in dc systems. Due to the above-mentioned reasons, secondary control for ac grids cannot be adopted for dc grids.

However, if single central controller fails, it will degrade the system performance and reliability. Further, local area network (LAN)/Internet may be used for communication [26]. But for remote sites, the availability of infrastructure cannot be ensured for this mode of communication. Therefore, to use these schemes within or with other microgrids may not be feasible. Power line communication (PLC) as a communication scheme is becoming popular in ac systems [27]. Feasibility of PLC for dc systems is discussed in [28]. However, in dc microgrids, there can be various interconnections of cables, thus, making the channel complex [29].

1.3.2 Decentralized Control

The problem of single point failure can be avoided in decentralized control [12, 16]. In decentralized control, the control input of the individual source can be computed without the knowledge of states of all other sources. In this type of control, PECs operate on physical measured quantities. High reliability, scalability and low cost are significant advantages achieved in decentralized control. However, the advantages are achieved at the cost of partial stability and losing optimum operation due to the lack of operational information and status of the other sources [30, 31]. In [32–36], droop control for an ac microgrid is reported. Their extensive use in conventional ac system is an attraction for use in dc microgrids [37–39]. A drooped controlled dc system dealing with small zone is reported in [40]. The effect of connecting line resistances is not considered in case of a dc system. The effect of line resistances become prominent for low voltage dc. In [41], the effect of line resistances is reported which is limited to one source and on load.

1.4 Overview of Factors Affecting Control Performance

Each source in a dc microgrid consists of a dc to dc PEC as shown in Fig. 1.1. Mostly, closed loop feedback controllers are used to design these converters to regulate the output. Main objectives of these controller are to ensure low steady state error, fast dynamic response and high efficiency. These objectives can be reached through the suitable selection of a control technique, circuit components and parameters.

Factors which affect the control performance of a dc to dc converter are switching frequency, energy storing components and control gain parameters of the controller. These factors are discussed below.

1.4.1 Switching Frequency

Theoretically, the switching frequency of a dc to dc converter is selected infinitely to achieve ideal control performance i.e., perfect steady state regulation and extremely fast dynamic response. Since in practical systems, slew rate and time delays of circuit components limit the switching operation of the converters. Therefore, the switching frequency is limited by the bandwidth of the controller and circuit components of the converter (i.e., power switch, diode, etc.). Additionally, converter power loss increases with the increase in switching frequency. Hysteresis and eddy current losses associated with magnetic elements and skin effect losses will be increased as switching frequency increases. Further, high switching frequency may generate the undesirable electromagnetic interferences. Switching frequency also limits the power rating of a PEC. Aforementioned factors limit the realization of extremely high switching frequency to achieve the ideal performance of the converters. Mostly, in practical applications, converters are designed to meet certain objectives i.e., load regulation, output ripple, transient response and efficiency, weight and size requirements [42, 43]. Therefore, there will always be

a tradeoff between switching frequency and desired control performance requirements. An optimum combination of both these may produce desired results.

1.4.2 Energy Storing Components

The performance of the dc to dc converters is also affected by the size of the energy storing components (i.e., capacitance C and inductance L). This can be examined while analyzing the operation principle of these components. Since the size is directly related to the energy charging and discharging rate (i.e., $\tau = R_L C$ for capacitor and $\tau = L/R_L$ for inductor) of these components, the ability to respond against load variation is also affected by the size of these components. Particularly, for fixed frequency fast dynamic response, small values of L and C are required and small components require small time for energy charging and discharging.

On the other side, high ripple will be produced in inductor current with small value of L . Further, small value of L leads to smaller overshoot or undershoot in the output when a step change is applied to the load. Similarly, large value of C leads to smaller overshoot or undershoot in the output voltage for a step change in load. Hence, size of the energy storing components along with the control parameters determine the dynamic response of the dc to dc converter.

1.4.3 Control Gain Parameters

Controller gain parameters play significant role in determining the dynamic behavior of the system. Generally, the parameters in feedback controlled system are classified as control variables and control gains. The control variables are usually state variables which needs to be controlled. For dc to dc converters, these variables are typically output voltage and inductor current errors. The key objective of the controller is to nullify these errors in a short time for any disturbance or change in load. To achieve this, control variables are manipulated by the proportional, integral and derivative actions in the control computations [44]. These

control gains are multiplied to amplify the manipulated variables which are used to investigate the response with varying manipulating variables. This is required to shape the dynamic behavior as desired.

In classical control theory, increasing the proportional gain K_P , improves the transient response and reduces the steady state error. But, selecting high K_P lowers the systems stability. Therefore, a tradeoff is required in selection of gain K_P among better transient response and lower stability. Next, if the gain K_I is increased, it will boost the removal of steady state errors but at the cost of reduction in systems stability. Finally, if the gain K_D is increased, it will reduce the overshoot and oscillations produced in the transient response. Control gain K_D does not affect the performance of steady state error, but it generates noise [38, 39], [45–47].

1.5 Commonly Available Control Techniques

Commonly used control techniques for the designing of dc to dc converters are discussed below.

1.5.1 Hysteresis Control

The dc to dc converters are usually controlled through hysteresis controller. Hysteresis controller is classified into two types which are discussed below.

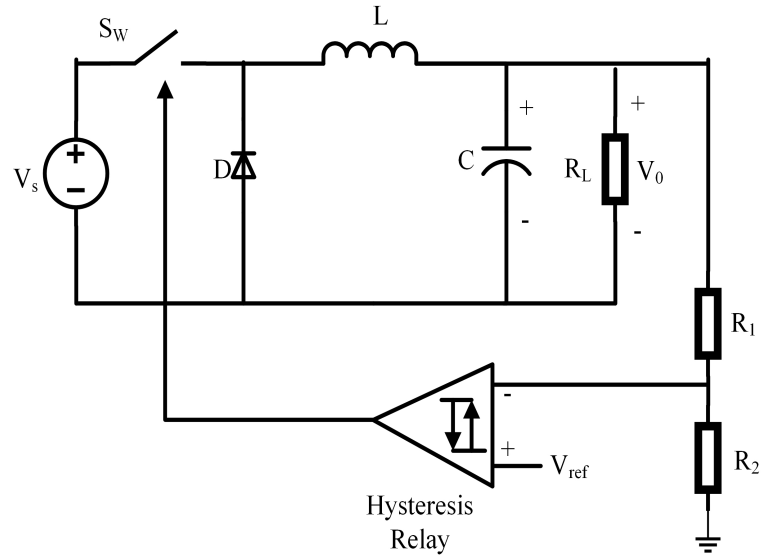


FIGURE 1.3: Hysteresis voltage control

1.5.1.1 Hysteresis Voltage Control

It is the simplest method to regulate the dc to dc converter and is shown in Fig. 1.3. It consists on a hysteresis relay which works as a comparator to compare actual voltage with reference voltage and generate the switching signal for the converter switch. But this technique is only effective for dc to dc buck converter where there is no involvement of phase lag during energy transfer [42, 48].

1.5.1.2 Hysteresis Current Control

This type of controller is effective for dc to dc boost and buck-boost converters where phase lag is involved in energy transfer (i.e., phase lag between controller action and voltage response). These types of converters show right half plane zero characteristics for which hysteresis voltage controller becomes insufficient for good regulation [42, 43, 48]. Therefore, hysteresis current controller is required for these types of converters and is shown in Fig. 1.4. In this controller, compensated voltage error is compared with inductor current to generate the switching signal for the converter switch. This ensures the precise inductor current regulation which leads to voltage regulation.

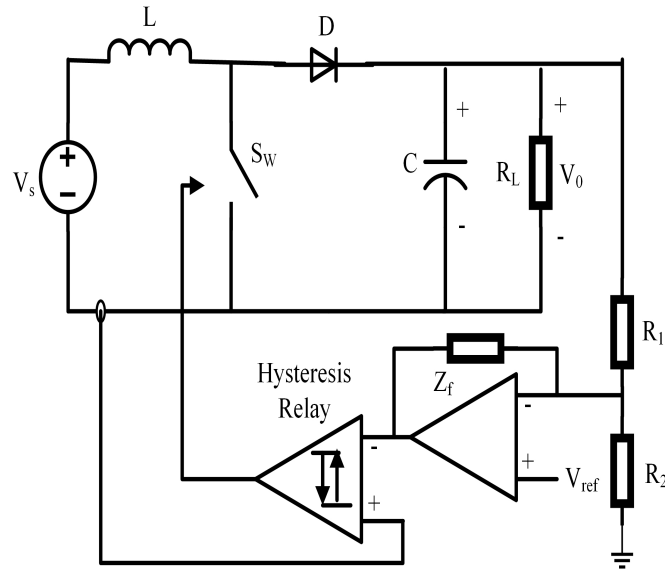


FIGURE 1.4: Hysteresis current control

However, converters with hysteresis controllers are simple to implement and they respond quickly to load changes. Nevertheless, the turn on and off time are not fixed of the hysteresis relay, hence switching frequency within the hysteresis band is varying depending on the converter parameters. Further, they generate unpredictable noise, making the controller design more complex [42, 48].

1.5.2 Pulse Width Modulation Control

Like hysteresis controller, pulse width modulation (PWM) controller can also be classified into voltage mode control and current mode control which are discussed below.

1.5.2.1 Voltage Mode Controller

In this type of linear controller, actual output voltage of dc to dc converter is compared with reference voltage to produce error signal. This error signal is processed through compensation network Z_f to generate control signal which is then compared with ramp signal to generate switching signal for the converter switch as shown in Fig.1.5. In this type, peak value of the ramp signal in proportion

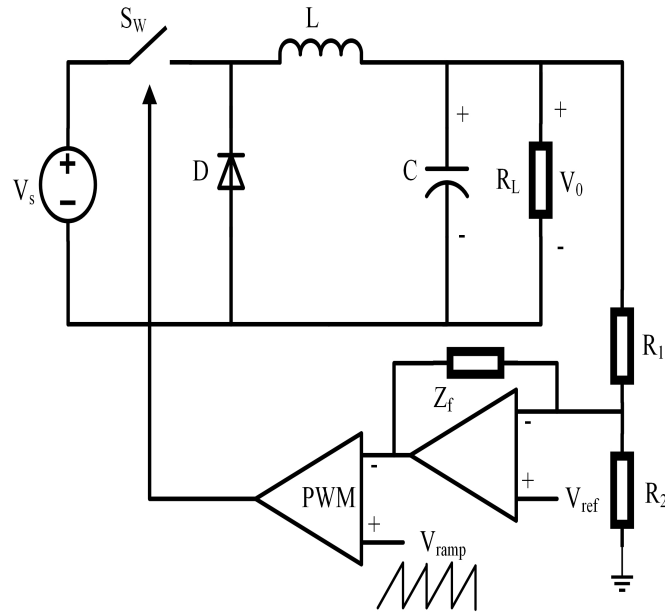


FIGURE 1.5: PWM voltage mode control

to the input voltage is required to increase the converters immunity against the disturbances in input voltage. This type of immunity is not required in current mode control [42, 48, 49].

1.5.2.2 Current Mode Controller

It is a two loop feedback nonlinear control which uses an outer voltage loop in addition to inner current loop. It is further classified into two types namely, peak and average mode control which are discussed below.

- Peak Current Mode Controller

In peak mode, the objective is to force the peak value of the instantaneous inductor current to follow the reference which is derived by the outer voltage loop as shown in Fig. 1.6. The converter switch is turned on as directed by the periodic clock signal of fixed frequency and turn off when instantaneous peak inductor current reaches the desired reference. The main disadvantage of current mode controller is that its noise susceptibility is high. Further, it shows inherent instability when

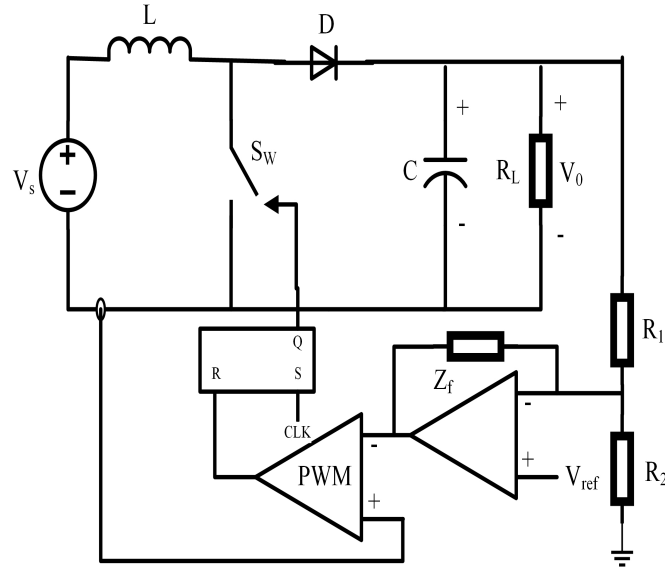


FIGURE 1.6: PWM peak current mode control

exceeding duty ratio over 0.5, which produces subharmonic oscillations. Furthermore, it shows non-ideal response due to the peak current detection instead of the average current detection [48], [50–54].

- Average Current Mode Controller

In average mode, there are two compensated networks Z_{f1} and Z_{f2} as shown in Fig. 1.7. Z_{f1} compensate the output voltage error at the first stage and generate the desired reference current which is compared with inductor current to produce current error. Z_{f2} at second stage compensate the produced current error and generate control signal for PW modulator where it is compared with the ramp signal to generate switching signal for the converter switch. The major advantage achieved is stability exceeding duty ratio over 0.5. Since, the two networks Z_{f1} and Z_{f2} are connected in series, the optimal design and analysis of these networks becomes nontrivial [48], [50–54].

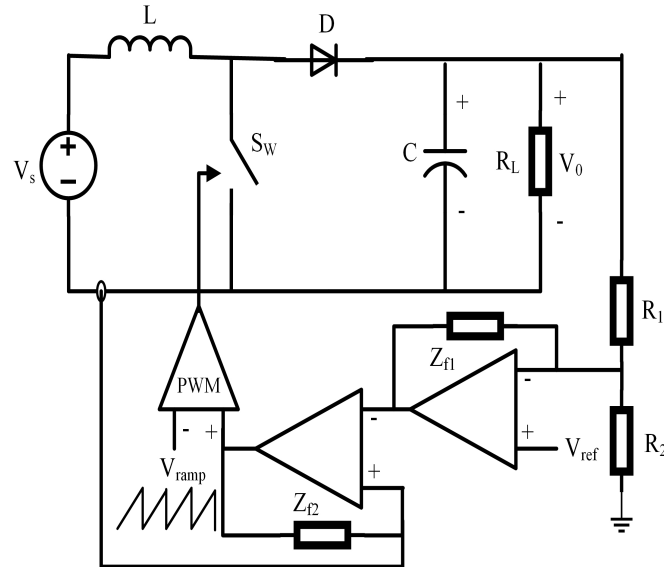


FIGURE 1.7: PWM average current mode control

1.6 Linear Control Techniques

Linear techniques can be categorized as classical, modern and robust control. In these techniques, an approximation of physically modeled system is used for the analysis and design of the controller. These techniques are based on certain systematic and generalized rules in which system behavior is known. Following are two major limitations of linearized control techniques.

- Linearized model is always an estimation (neglecting some of the dynamics) of nonlinear system model.
- Linearized controllers are stable on specified equilibrium points and hence, satisfies only local stability of the system.

1.6.1 Classical Control

Classical techniques which were familiarized in early 1930s provide solutions to the control problems in the form of graphical representation. Bode plots [55], Nyquist stability criterion [56] and Root Locus plots [57] are examples of these control techniques. In both Bode and Root locus plots, desired control response is

achieved using lead or lag compensation, or joint lead-lag compensation. Whereas, Nyquist stability criterion is polar representation of both magnitude and phase plots of bode diagram which can handle systems with delays and right half plane singularities. However, there are certain limitations of these techniques which are given below.

- Limited to LTI systems.
- Can handle only single input single output (SISO) systems.
- Both Root Locus and Bode plots cannot handle systems with delays.
- Preferred for simple systems with limited stability conditions.

1.6.2 Proportional Integral Derivative Control

PID controllers are commonly used linear techniques due to their easy implementation and available tuning methods. These techniques are based on the error tracking of the desired reference which generates input actions to address control problem. However, these controllers apply constant parameters in the feedback loop without direct knowledge of the modeled system dynamics. Thus, performance will be compromised [45–47].

1.6.3 Modern Control Techniques

In modern control techniques, the control problem is addressed through state space representation of a system model. State space formation deals with development of mathematical model which relates input, output and states of a physical system using first order differential or difference equations. The advantages of state space representation over classical techniques are given below.

- Can handle multi input and multi output (MIMO) systems.
- Controller analysis and design of a complex system becomes easier.

- Stability can be analyzed through Lyapunov Methods [58].

1.6.3.1 State Feedback Control

State or output feedback control is a technique in which states or outputs of a system are used in the feedback process to generate control input for desired response. In this type, poles of a system are placed in predetermined locations of s-plan. Since, poles location directly corresponds to eigen values. Therefore, pole placement will control the response of system. In order to apply state feedback controller, control input u must be present in modeled state space dynamics [58]. This technique can be applied to only single input systems. Moreover, arbitrarily selecting poles will not give optimum performance. This type lacks optimum selection of poles for desired system response [59].

1.6.3.2 Optimum Control Techniques

Optimal techniques deal with problem to find a suitable control law which satisfies certain optimal conditions. In optimal theory, control problem consists of a cost function consisting of state and control variables. These controllers adopt control parameters which minimize the cost function [58].

- Linear Quadratic Regulator

linear quadratic regulator (LQR) is state feedback optimal controller in which system dynamics consist of linear differential equations and cost is a quadratic function [60, 61]. However, LQR does not deal with system uncertainties and suffers the selection of control weights which limit to use it in converter applications.

- Linear Quadratic Gaussian

Linear quadratic gaussian (LQG) is optimal control which minimizes the expected value of quadratic cost function. In LQG, system dynamics are affected by gaussian noise [62]. However, LQG implementation becomes

difficult when state vector is of large dimension. Additionally, robustness is not ensured by LQG and needs to deal with it separately which limits to use in converter applications.

- **Linear Model Predictive Control**

Linear model predictive control (MPC) is based on process control theory and recently has been used in converter applications [63]. The major advantage of MPC is to optimize current control parameters while keeping future parameters in account which differentiate it from LQR. However, for analog implementation, fast response time is still a problem for MPC controller.

1.6.4 H Infinity Control

H infinity includes robust parameters in controller design which attracts it for converter applications [64]. In H infinity, control problem is formulated as an optimization problem which can handle cross coupling effects with guaranteed performance. However, H infinity controller shows optimal performance with reference to specified cost function. It does not address the control performance measure like settling time, energy consumed etc.

1.6.5 Linear Matrix Inequality

Linear matrix inequality (LMI) plays a central role in post-modern control techniques which deals the optimization problem with convex type objective function. The constraints of LMI can be solved with efficient available software tools which address the control problems numerically [65]. However, dc to dc converters are nonlinear in nature. Applying LMI in converter applications requires some linearization of system model which limits the desired performance.

1.7 Control Techniques in Research

The motivation behind the investigation of alternate control techniques is that conventional linear and partial nonlinear techniques fail to show satisfactory performance. Following are some techniques which are considered for the applications of dc to dc converters.

1.7.1 Adaptive Control

It is a controller which can adopt its control parameters with different operating conditions. Using this control, it is possible to optimize the performance of the controller for all operating conditions [66–68]. However, it is difficult to implement this type of control technique because it requires the sensors to detect the different instantaneous operating conditions. Further, to generate optimal conditions, complex mathematical operations are required. Therefore, complex analog circuit/digital controller is required to realize adaptive control. Due to this, adaptive control is unpopular for practical applications.

1.7.2 Fuzzy Logic Control

This type of control is based on heuristic reasoning which does not require complex computations of the system model. Its design becomes simple because experienced based rules are performed to create an output and Boolean logic is required for its computations. This extends the capability of controller for large operating conditions. This motivates the use of fuzzy logic controllers to control the dc to dc converters [69, 70]. However, the problem in using these controllers for converters is that these are impractical. These controllers involve digital processors and EEPROM for their practical realization [71, 72], [69, 70].

1.7.3 Artificial Neural Network Control

Artificial neural network is inspired by the human brain where biological nervous system processes information. It consists of many neurons which are linked through interconnection parameters called weights. If the weights are changed, it will not only change the neuron behavior but the entire system behavior. Thus, it is a self-tuned process which attracts to be used in dc to dc converters for desired output response [50, 71]. However, its practical implementation is nontrivial. Further, offline time-consuming training process is required before to use it.

1.7.4 One Cycle Control

One cycle is nonlinear PWM based technique which is designed to control the duty cycle of converter switch. In each cycle, average chopped waveform at the output of the converter switch is equal to the desired reference [73]. It is a straight forward technique and comparatively simple implementation is required. However, the behavior of converter switches e.g., transistors, diodes etc., is not ideal which makes the controller integration non-instantaneous. Therefore, it becomes difficult to achieve desired response of the controller.

1.7.5 Genetic Algorithm

Genetic algorithm (GA) is an optimization technique which is based on the theory of Darwins evolutionary process [74]. GA utilizes codes instead of parameters and requires population point for its operation. However, there is no guarantee that GA will show global optimization when the constraints in population are large. Additionally, GA cannot ensure constant response over time which limits to use it in converters applications.

1.7.6 Passivity Based Control

Passivity based controllers work with aim to make feedback loop look like passive system. These controllers simplify problem and reduces the complexity of control task. These controllers show stable control response over a wide operating range of system [75, 76]. However, selection of control parameters is based on trial and error approach. Therefore, it is difficult to optimize control parameters and not preferred for practical applications.

1.7.7 Sliding Mode Control

Sliding mode control (SMC) is a type of nonlinear control which is primarily used to control variable structure systems (VSSs) [72], [77], [78]. It is a state feedback control which switches from one state to another at a high frequency. The objective is to direct system dynamics to follow exactly what is desired. SM controller was first considered in 1983 [79] and 1986 [80] for the applications of dc to dc converters, since then, it has gained a key interest for the researchers regarding its development. SM controller implementation is relatively easy as compared to the other nonlinear controllers which attracts its use in dc to dc converter applications. However, the major problem in SM controller is produced chattering. If the chattering problem is controlled, it has a big potential for industrial applications.

1.8 Motivation

Microgrids are local energy networks that involve RESs and storage systems. They have the capability to be locally controlled. Therefore, they can be disconnected from the grid when there is a blackout, or a fault on the main supply grid, and continue to supply a portion of their local loads called stand-alone mode. Since microgrids typically include RESs and batteries, they will have the capability to increase the overall system efficiency [1-19], [81-83]. Various authors have shown that dc microgrids can play an effective role in solving some operational issues on

the main supply grid [84–88]. In conclusion, the aforementioned factors motivated many researchers to raise a fundamental yet essential question; is ac distribution still the most efficient means to distribute electrical power or it is time to reconsider deploying dc DSs? Researchers realized that dc DSs are not outdated anymore; they are more aligned with our today's needs than they were 100 years ago. A realistic proof is provided later in this report in chapter 2, where different existing dc systems are discussed in detail.

1.9 Statement of Problem

1. The use of dc microgrids in the residential and commercial complexes are increasing due to the high reliability, high efficacy, and easy integration with RESs. Stability of the dc microgrid is key challenge in the presence of various distributed sources. Droop controllers are being used for stability of dc microgrids. Droop controllers are not effective due to the error in steady state voltages and load power variations. Additionally, these controllers are realized through conventional classical controllers which cannot ensure global stability. One of the main reason to use these control techniques is easy implementation of tuning method in industrial applications. Further, these controllers suffer the optimization of the control gain parameters. Increasing the proportional gain K_P , improves the transient response and reduces the steady state error. But, selecting high K_P lowers the systems stability. Therefore, a tradeoff is required for selection of gain K_P among better transient response and lower stability. Next, if the gain K_I is increased, it will boost the removal of steady state errors but at the cost of reduction in systems stability. Finally, if the gain K_D is increased, it will reduce the overshoot and oscillations produced in the transient response. Control gain K_D does not affect the performance of steady state error, but it generates noise susceptibility. Furthermore, the parameters of classical controllers are calculated using current specifications of the system. These parameters vary with load and sources apply to the system. Hence it becomes difficult to optimize

controller parameters for different operating conditions. These controllers cannot ensure global stability of the desired equilibrium state. Hence, to use classical controllers for the stability of dc microgrid is not feasible. Therefore, nonlinear control techniques need to be explored for stability and better dynamic response in the dc microgrid applications.

2. Proportional load sharing and precise voltage regulation are the key objective to be achieved in dc microgrid. However, the problem in the parallel connected dc to dc sources is that these objectives cannot be achieved simultaneously. To address the challenge, different control architectures are proposed in literature which can be categorized as centralized and decentralized control. In centralized control, the controller collects system data using high bandwidth communication link, schedule the tasks based on the collected information and directs control decisions. However, if the single point failure exists, it will degrade the system performance and reliability. Additionally, these controllers are realized through proportional integral (*PI*) controllers which cannot ensure load sharing and stability in all operating conditions. Single central controller failure problem can be avoided in decentralized control. In this type of control architecture, PE converters operate on physical measured quantities. But, the improvement is achieved at the cost of partial stability and losing optimum operation due to the lack of operational information and status of the other converters. Therefore, a distributive type control architecture is required to be investigated for the load sharing and precise voltage regulation.

1.10 Statement of Contribution

Following are the main contributions presented in this research work.

1. Feasibility study of the household appliances for ac and dc DS is performed and the importance of dc DS is explored.

2. Voltage stability of dc microgrid is analyzed using SM Controller. Stability analysis contributes the following:

- A mathematical model is developed for dc microgrid and system dynamics are derived in state-space form.
- Controllability of the linearized model is investigated and eigen value stability is examined.
- Limitations of droop controlled dc microgrid are explored.
- SM controller is proposed for the stability of dc microgrid. Hitting, existence and stability conditions are verified.
- Simulations are carried out to compare the performance of droop controlled and SM controlled dc microgrid. Results of steady state and transient performance are presented. Further, dynamic behavior is investigated with different values of sliding parameter. Furthermore, the results with source power variation are presented which shows the performance of the proposed controller.
- Small scale experimental setup of dc microgrid is established using SM hysteresis controller and design procedure for implementation is also presented.

3. Proportional load sharing and voltage regulation of dc microgrid is done with distributed control architecture. It contributes the following:

- Limitations of centralized and decentralized control architecture are explored and a low bandwidth distributive control architecture is proposed for load sharing in dc microgrids.
- A model is developed and SMC technique is proposed for load sharing.
- A nonlinear sliding surface is proposed for load sharing purpose and Controllability, reachability and equivalent control conditions are verified.
- Closed loop system dynamics are developed and stability of sliding parameters is guaranteed through Laplace transform to ensure stable SM

operation. Further, the SM dynamic behavior is investigated for underdamped and critically damped response.

- Simulations are carried out to compare the performance of decentralized and distributive architecture. Results of steady state and transient performance are presented. Further, the results for better dynamic performance are presented for underdamped and critically damped response. Moreover, the fail-safe performance of distributed control architecture is explored and presented.

1.11 Application of the Research

Smart grids are becoming popular in the recent years. Smart grid is a modern electrical grid which comprises of smart meters, smart flexible appliances and RESs. Reliability, flexibility, efficiency (Load balancing, peak leveling and time of use pricing) and sustainability are smart grid features. This research work focuses on the efficient utilization of distributed energy sources and stability of the dc microgrid. This work will be a good addition to the solutions proposed to realize the smart grid and its features.

1.12 Thesis Organization

An overview of the contents of the chapters presented in this thesis is given below.

Chapter 2 presents the feasibility study of dc DS. This chapter emphasis on the motivation of dc distribution and investigates the efficient operation of different household appliances with dc power delivery. Further, the importance of dc distribution is over-viewed for RESs, energy storage, data centers and shipyard systems. Moreover, the concept of ac and dc microgrid is summarized.

Chapter 3 covers the literature about the control architectures for load sharing in dc microgrid system. Passive and active load sharing techniques are surveyed with

their limitations. Additionally, a distributive control architecture for proportional load sharing among sources is proposed in this chapter.

Chapter 4 presents the first contribution of this research thesis. First part of this chapter highlights the theory and mathematical formulation of SMC which will support the contribution in this thesis. The minimum conditions for a system to show SM property are presented. In second part of this chapter, a dc microgrid system is modeled and controllability and stability conditions are verified. Mathematical formulation of the modeled system using SMC is presented and existence of the SM is verified. Detailed simulations are carried out to show the effectiveness of SM controller and results are compared with droop controller. The transient behavior on step load is also investigated and presented. Furthermore, A scaled down experimental setup of a source is also presented in this chapter.

Chapter 5 comprises the second contribution of this research thesis. A distributed architecture using SM controller utilizing low bandwidth communication is proposed for dc microgrid in this chapter. System model is developed and its stability through SM is verified. Further, the dynamic behavior of the modeled system is investigated for underdamped and critically damped response. Detailed simulations are carried out to show the effectiveness of the proposed controller.

Finally, this thesis ends with Chapter 6 which concludes major contribution highlights the work presented. Moreover, some recommendations are suggested to work in this context.

Chapter 2

Feasibility of DC Distribution System

2.1 Overview

DS is the last stage in the electric power delivery. It transfers the electric power from transmission system to the end user. Depleting threat of fossil fuels and ecological fears increasing challenges to the traditional DS. In 19th century, the discussion between dc and ac DS had started again [4]. The advantages of ac system were remained dominant up to 20th century. In ac transmission system, the role of transformers is important in stepping up voltages to high which made possible transfer of power over a long distance. In early times, due to the lack of PECs, dc power transfer over a long distance was not possible. The debate on dc and ac system has started again because the latest developments in high power semiconductor technology has made it possible to develop high power electronic switches (e.g. MOSFETS, IGBTs, IGCTs etc.) which are widely used in power conversion circuits [89]. Advances in PECs increased the efficiency of transmission system through the high voltage direct current (HVDC) transmission. In HVDC transmission, the electric power transfer can be efficiently controlled using back to back PECs [89].

On the other hand, power losses in the low voltage ac DS and in domestic appliances are a hot issue in the growing energy concerns. At the same time due to the ecological fears of burning fossil fuels to produce energy and the increasing use of the RESs for power generation attracting dc distribution for power delivery to end user. Further, a shift of domestic appliances from ac to dc which requires ac to dc converter at first stage making dc distribution an attractive topic for the researchers. Most of the domestic and commercial appliances directly or indirectly run on dc power. Thus, the low voltage dc can be more efficient than ac distribution.

2.2 Motivation for DC Distribution

Power electronics is playing an important role in society's evolution for sustainable prospect. It is not only attractive solution to integrate RESs with electrical system but also opens the opportunities for safe, consistent and proficient power transfer to the end user. In ships [90], the transfer of power is already based on dc. While for data centers [91], hybrid vehicles [92] and aircrafts systems [93], the dc power is a promising solution.

The dc distribution is attractive solution in residential and commercial buildings [94, 95]. Further, the integration of the RESs with dc is easy as compared to ac distribution. There are several other reasons for the deployment of dc distribution which are discussed below.

2.2.1 Electrical Loads

Most of today's consumer loads are inherently supplied by dc. In this section, domestic appliances are investigated for dc distribution. Domestic loads based on their use can be classified into electronic, resistive, lighting, universal motor and VFD based appliances. In [96, 97], domestic appliances are discussed with their ratings and are listed in Table 2.1.

TABLE 2.1: Classification of domestic appliances and loads

| Type | Appliances |
|----------------------------------|--|
| Electronic appliances | Desktop PC, laptop, digital tv and monitors, printer, modem,(sound system, small battery chargers (cell phones, digital cameras, mp3 player etc.) cd and dvd player) |
| Resistive appliances | Electric stoves, toaster, electric rice cooker, electrical kettles, coffee makers, hand iron, heater |
| Universal motor based appliances | Juicer blender, vacuum cleaner, hair dryer |
| Inverter based appliances | Air conditioner, washing machine, fridge, energy saver, emergency light |
| Lighting loads | LED lights |

2.2.1.1 Electronic Appliances

All electronic appliances are inherently designed for dc power. These appliances are designed using switch mode power supplies which at first stage convert $220V_{rms}$, 50Hz supply to full wave rectified dc using rectifiers as shown in Fig. 2.1. A smoothing capacitor is used at the output of rectifier to smooth out rectified dc. At the second stage, dc to dc converter regulators are used to regulate rectified dc to the required level. Rectifiers with smoothing capacitors introduces undesirable current harmonics in the main supply current. Further, it reduces system efficiency due to low power factor (PF) and increases harmonic distortion. To improve PF, an extra PF correction circuit is used with regulators in these appliances [98], [99], [100], [101].

If electronic appliances are powered by dc distribution, dc can be directly applied to the regulation circuit. Therefore, there will be no requirement of rectifier circuits and hence, inefficiencies associated with these elements will be absent in dc. Further, there is no requirement of PF correction circuits and hence, efficient power will be delivered. Before utilizing ac generated power, about 30% of the power passes through PE converters as discussed in [102]. The amount of power losses in these converters varies generally in the range of 10-25% [103]. In [104], it is deliberated that the efficiency can be increased by 8% if these appliances

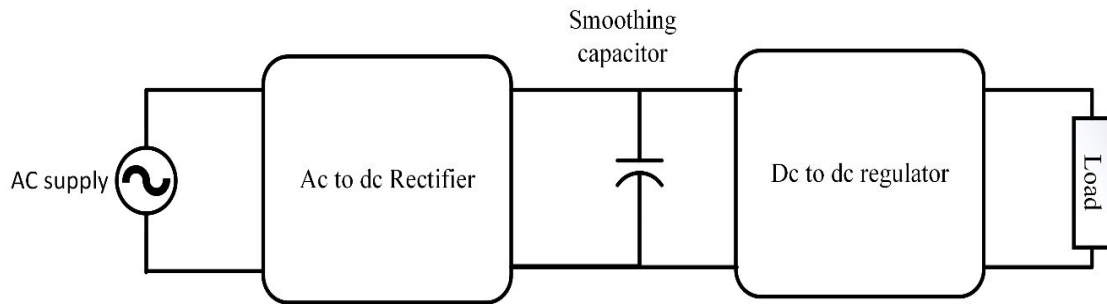


FIGURE 2.1: Power supply of electronic appliances

are powered by dc system. Further, efficiency can be increased to 25% after the removal of rectifier and PF correction stage.

2.2.1.2 Resistive Appliances

All the resistive appliances listed in Table 2.1 can operate both on ac and dc power. Presently, these appliances are being powered by ac DS. These appliances will operate at same output power if rms value of dc is equal to the rms value of ac. Hence, resistive appliances can be powered by dc line [96, 100, 101].

2.2.1.3 Universal Motor Based Appliances

Some of the domestic appliances are designed utilizing universal motor. Universal motor is an electrical motor which can run both on ac and dc supply. Universal motor produces high starting torque and runs at high speed. These motors are light weighted and compact in size which attracts them to be used in appliances like juicer blender, hair dryer and vacuum cleaner. So, these appliances can run both on dc and ac supply [96, 100, 101].

2.2.1.4 Lighting Loads

Most of currently used lights internally use dc power. So, these lights can be efficiently utilized if they are powered by dc supply. Further, newer lighting technologies such as compact fluorescent fixtures and solid-state lighting include dc

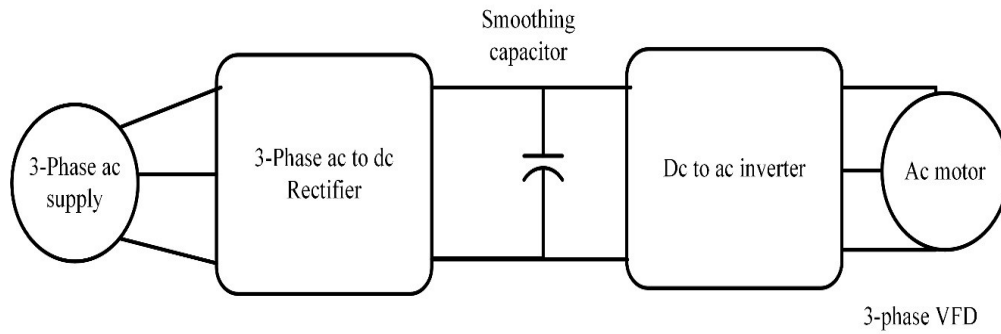


FIGURE 2.2: Power supply of Inverter based appliances

stage and hence, it is more efficient to use them in a dc powered system [105, 106].

2.2.1.5 Inverter Based Appliances

Modern air conditioners and washing machines are designed on VFD based technology. VFD uses two stage converters in which it converts ac supply to dc at first stage using rectifiers as shown in Fig. 2.2. At second stage, it converts dc to variable frequency using inverter which is used to run the motor. In dc system, rectifier stage is no more required and associated losses will be minimized. Hence, appliances with VFD based technology can be efficiently utilized if they are powered by dc supply [96, 100, 101].

2.2.1.6 Plugged-in Electrical Vehicles

Ecological fears and global call for reduction in CO_2 motivated many investors and automobile companies for plugged-in hybrid and electric vehicles. Fast charging stations are required to charge these vehicles which is still main concern for many researchers [107, 108]. Many authors believe that these vehicles should be connected with a common dc bus where any other distributed generator is integrated [109–112].

2.2.2 Renewable Energy Sources

Depleting threat of fossil fuels and ecological fears motivated the use of RESs for energy requirements. Some of these sources are inherently dc sources i.e., PV, fuel cell etc. PV can be efficiently integrated with dc distribution because dc to ac converter is required in the case of ac distribution. Wind turbines uses dc link for integration with ac distribution [113, 114]. A converter will be eliminated if wind turbines are integrated with dc and hence, efficiency will be improved. Further, there are three parameters (i.e., voltage, frequency and phase angle) of concern while integrating RESs with ac distribution. In the case of dc, frequency and phase angle are absent, hence controller design for converters will be relaxed. Furthermore, micro-turbines which generate high frequency ac signals are easy to integrate with dc distribution.

2.2.3 Energy Storage

One of the major benefit achieved in dc is that it facilitates the energy storage. Most of the energy storing devices are purely dc i.e., batteries and super capacitors. Further, mechanical energy storing devices such as flywheel use dc link for integration with DS. Integration efficiency of these devices will be improved in dc distribution [115, 116]. A study from the availability concern in [117] is carried out for comparison of uninterrupted ac and dc power supplies which shows that dc power is more reliable.

2.2.4 Data Centers

The main concern of power supplied in data centers is that reliable power should be maintained [117–119]. Therefore, uninterruptable power supplies (UPSs) are used in data centers. UPS requires multiple dc to dc and dc to ac converters to connect batteries with ac system. These converters and associated losses can be avoided if dc is used for distribution. Consequently, energy efficiency and cost

are optimized. Therefore, for data centers, dc distribution is more efficient and economical option [120–122].

2.2.5 Shipyard System

Usually in shipyards, electrical power is required for the communication, weapons, navigation and auxiliary loads. Reliability is major concern for the electrical power distributed in shipyards. In [123, 124], a medium dc voltage is investigated for the implementation of DS in future shipyards.

2.3 Microgrid

Microgrids are modern form of DS which can function autonomously or in combination with main supply grid. Microgrids can operate in low or medium voltage range which have their own power generation i.e. RESs along with energy storage, non-renewable sources and PE controlled loads [14]. The unique property of the microgrids is that they can work in islanded mode under faulty grid conditions which increases the reliability of power supply [15, 1, 2]. This inspires that microgrid is an effective way of power generation and consumption. In the near future, the DS may consist of some interconnected microgrids with local generation, storage and consumption of power [9-13], [16].

2.3.1 AC Microgrid

Presently, domestic and commercial buildings are facing problems to satisfy growing energy demands due to the increasing prices of electricity. In this scenario, homes and commercial buildings are using RESs together with main grid to satisfy their energy demands. Fig. 2.3 shows an ac microgrid which contains RESs such as PV and wind, and batteries for energy storage.

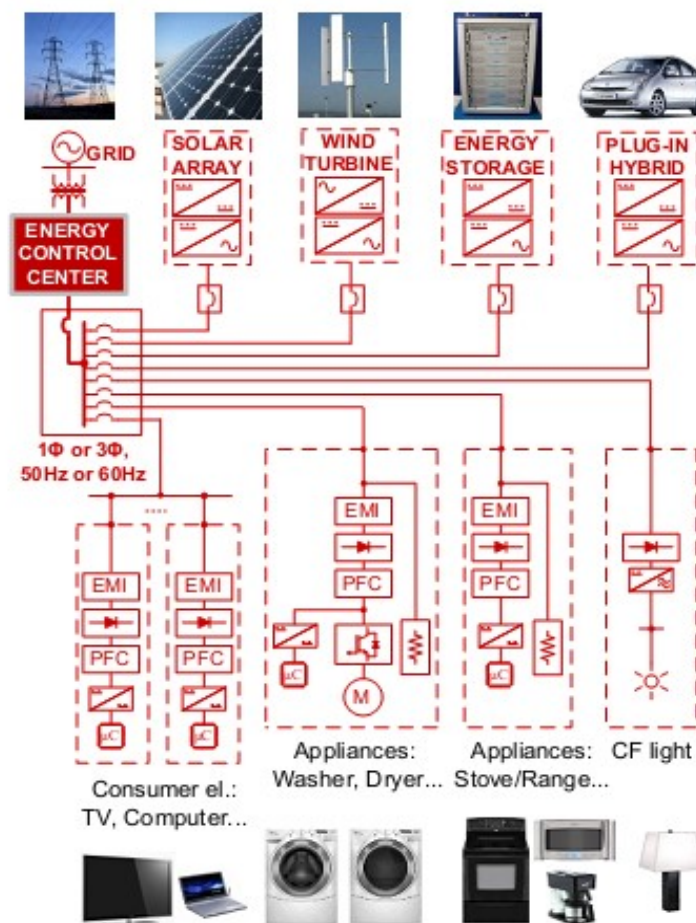


FIGURE 2.3: AC microgrid [126]

Energy control center performs the function of smart metering and remotely control operations in ac microgrid [125, 126]. It is also responsible for collection and recording of power flow data in microgrid. Further, it controls the operation of converters and appliances. Furthermore, it communicates with the distribution operator for power trading. Since the distribution is in ac, it does not solve the integration issues of RESs with ac system. Additionally, an extra electromagnetic interference (EMI) filter and PF correction stage is required in the appliances which increases the cost and reduces efficiency. Consequently, ac microgrid is a complex, high cost and suffers inefficiencies.

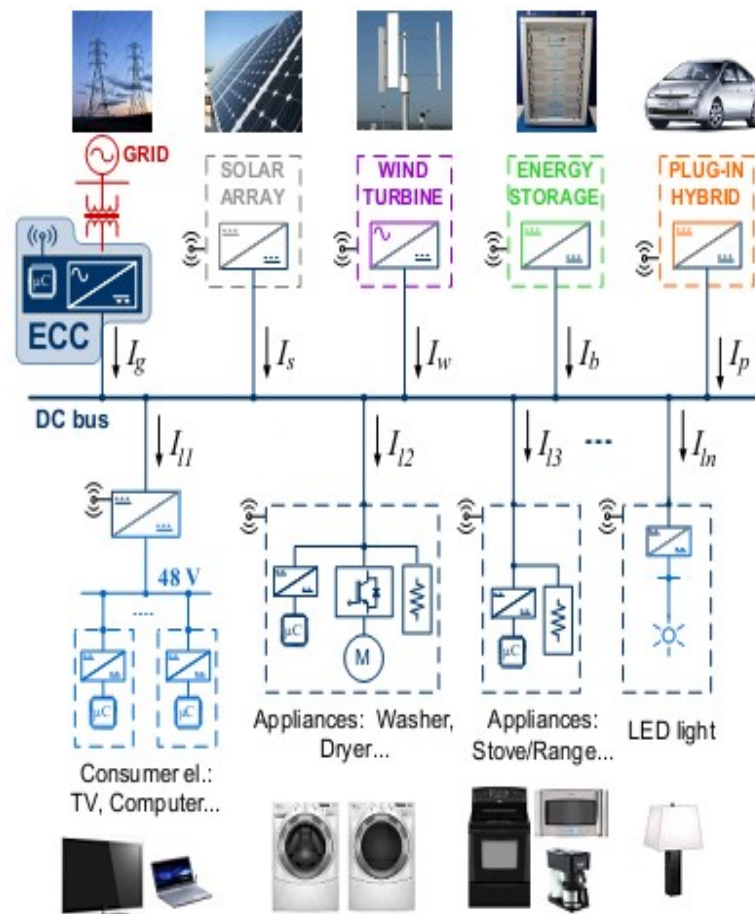


FIGURE 2.4: DC microgrid [126]

2.3.2 DC Microgrid

The problems and inefficiencies associated with ac can be addressed in dc microgrids as shown in the Fig. 2.4. The architecture is simplified and relaxed with dc distribution. The requirement of the dc to ac converter to interconnect RESs and batteries in ac microgrid is eliminated in dc microgrid as shown in Fig. 2.4. On the load side, EMI filter, rectifier and PF correction stage is eliminated in the dc microgrid which relaxes the appliances design, reduces cost and increases efficiency. Hence, dc microgrid is an attractive solution to optimize the reliability, complexity, efficiency and cost of the future commercial buildings and homes [126].

2.3.3 DC Standardization Efforts

Currently, ac system standards are much matured compared to dc because it is being utilized more than a hundred years. Major obstacle in the global acceptance of dc system is that it lacks the necessary standards. Particularly, the standards relating to the generation, transmission and distribution of dc power. DC standards are important which will provide a unified mechanism for the system design and installation.

There are different voltage standards proposed in literature for the bus voltage in dc microgrid. DC bus configuration can be realized through unipolar or bipolar scheme. Bipolar scheme can provide more options for voltage levels compared to unipolar scheme. Normally voltage levels can vary with the operation requirements of different systems. For example, a typical 380-400V is usually suitable for the data centers. While 48, 120, 325, 230V is suitable for the domestic and house installations. Other bipolar voltage level could be $\pm 230, \pm 170, \pm 110V$ etc. which can be preferred for protection measures [11, 13, 18, 96, 97, 122].

- 300V DC

As all loads convert $220V_{rms}$ ac supply into dc which is about 300V at first stage so, 300V is best suited voltage standard for domestic and industrial loads. With this voltage level, electrical loads can be operated with minimum modification. When dc DS gets matured, the converter circuits can be eliminated from the loads which will result in high efficiency and least cost.

2.4 Summary

Feasibility study of dc DS is presented in this chapter. This chapter emphasis on the motivation of the dc distribution and investigates the efficient operation of different household appliances with dc power delivery. Further, the importance of

dc distribution is over-viewed for RESs, energy storage, data centers and shipyard systems.

It is expected that the efficiency of dc distribution will be 10-22% high than ac distribution. Further, reactive power compensation and frequency synchronization circuits are not required in dc which have prominent role in ac power. Due to these advantages, dc is better suited for microgrid system. Furthermore, the concept of ac and dc microgrid is over-viewed.

Different voltage standards have been proposed in literature for dc microgrid based on operational requirement of the systems. As all loads convert $220V_{rms}$ ac into dc at first stage which is about 300V. So, this is best suited standard for domestic loads.

Chapter 3

Control Architecture for Load Sharing

3.1 Overview

PE converters play a significant role while integrating RESs with microgrid. RESs can be connected to microgrid through PE interface converters in parallel configuration. It is required to find an efficient control to coordinate among various sources, loads and energy storage. The key objective of parallel connected sources is to share load proportionally. However, it is the nature of power sources that only one source can establish the voltage in a parallel configuration. Further, the output resistances of sources are extremely low. Consequently, even a small difference in the output voltage among paralleled sources will cause the one which is a few mili volt higher to contribute most of the current. The lower the output voltage of a source, the more severe this problem is. Besides, even with same voltage references, the steady-state current sharing error is determined by the difference in output resistance of two paralleled sources[127].

If any source reaches its full load capacity, its current limiting circuit will be activated which causes its output voltage to drop and current of other sources increases to load. This situation is depicted in Fig. 3.1. Where, V_{s1} , V_{s2} and V_{s3}

are output voltages of three sources at no load and R_{o1}, R_{o2} and R_{o3} are output resistances of these sources respectively. These three sources are connected in parallel configuration to share a load without any current sharing scheme as shown in Fig. 3.1. Fig. 3.2 shows the steady state current sharing performance curves among these paralleled sources. These curves are plotted for equal output voltages of these source $V_{s1} = V_{s2} = V_{s3}$ and the relationship of the output resistances is as $R_{o1} < R_{o2} < R_{o3}$. Only source V_{s1} establishes the output voltage and share the maximum of load current while the other two are sharing small current which is not desired.

Without sharing control, stress is placed on the sources which will result in some sources operating at higher temperature level. This will reduce system reliability. Thus, the challenge in paralleled sources is to ensure uniform load sharing irrespective of number of sources and load conditions.

Therefore, the control scheme which is applied for coordination among sources in a dc microgrid should address the aforementioned challenge. There are two types of the control schemes: passive sharing control and active sharing control which are used for efficient load sharing and voltage regulation in dc microgrid. These control schemes are investigated below.

3.2 Passive Load Sharing Control

Different load sharing control schemes are presented in literature for paralleled dc to dc converters which are based on the droop control [128, 129], [12, 81]. In this control scheme, each source is designed with an output resistance R_d . Adding R_d in series with each source will cause the output voltage to drop in proportion with load current. The basic concept of droop control is shown in Fig. 3.3. Fig. 3.3(a) shows two parallel connected sources without droop resistance R_d . While Fig. 3.3(b) shows that a fixed droop resistance R_d is added in the output resistances of each source. Fig. 3.4 shows the steady state current sharing performance without

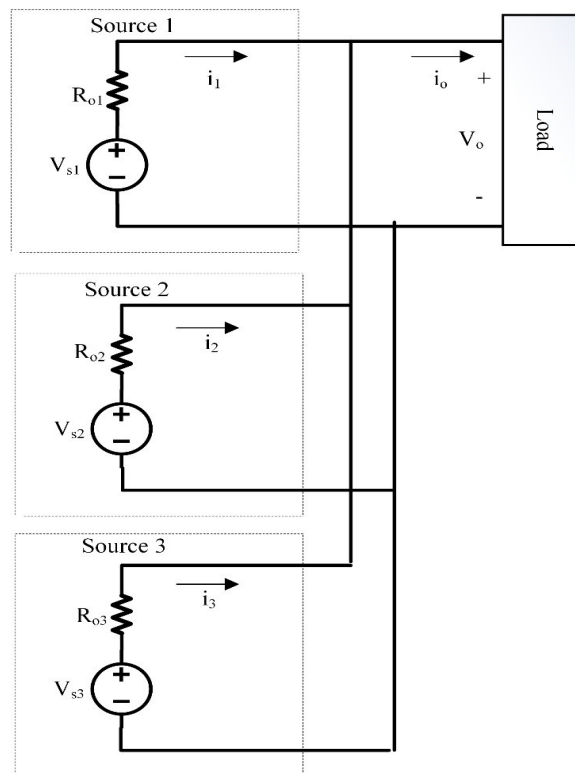


FIGURE 3.1: Three sources in parallel configuration without any current sharing scheme

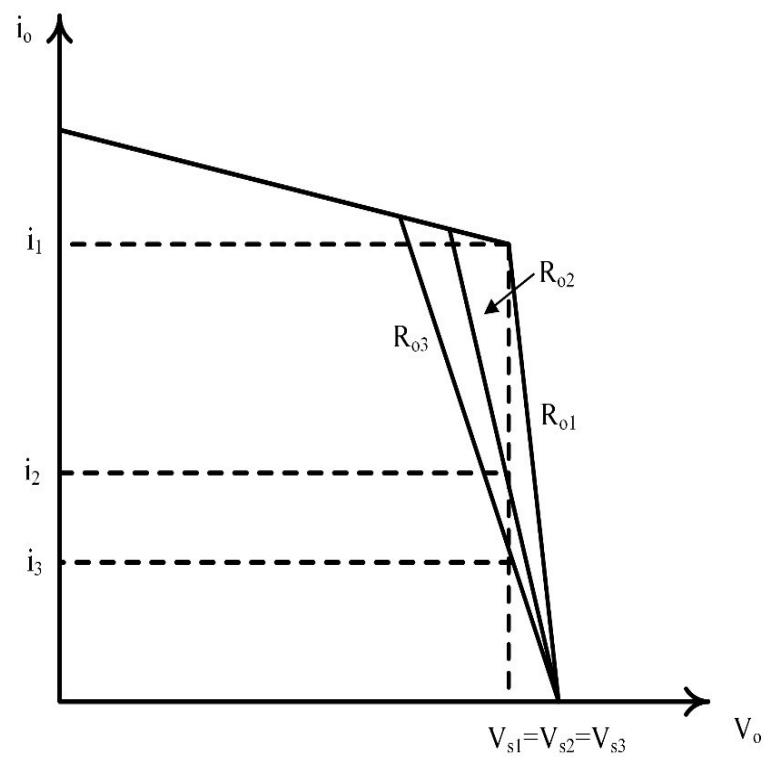


FIGURE 3.2: Steady state current distribution among sources

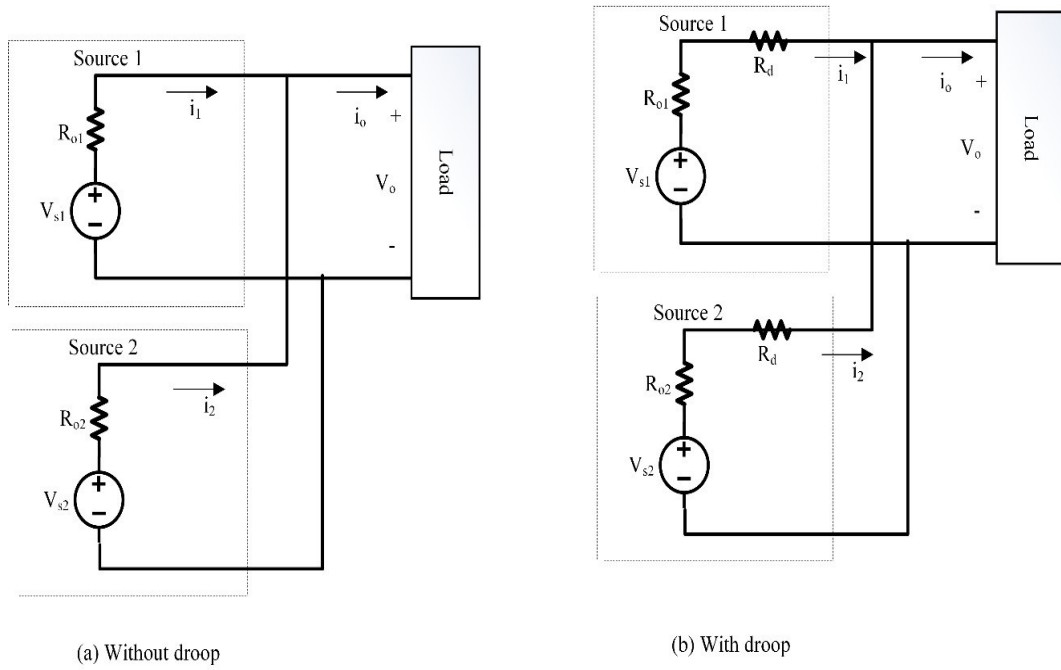


FIGURE 3.3: Parallel sources with droop control

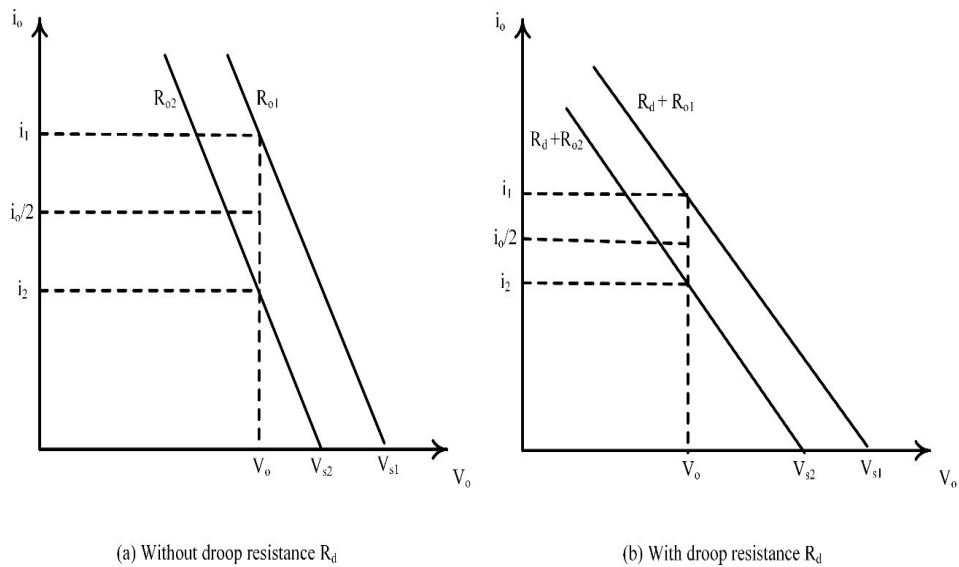


FIGURE 3.4: Steady state characteristics with droop control

and with droop resistance and shows how it improves with increasing R_d . Fig. 3.4 is plotted for source voltages $V_{s1} > V_{s2}$.

From Fig. 3.3(a), output voltage V_o can be written as:

$$V_o = V_{s1} - i_1 R_{o1} \tag{3.1}$$

$$V_o = V_{s2} - i_2 R_{o2} \quad (3.2)$$

Where, i_1 and i_2 are output current of source 1 and 2 respectively. After equating (3.1) and (3.2), it can be written as:

$$V_{s1} - V_{s2} = i_1 R_{o1} - i_2 R_{o2} \quad (3.3)$$

Substituting $i_2 = i_o - i_1$ in (3.3), it can be written as:

$$i_1 = \frac{V_{s1} - V_{s2}}{R_{o1} + R_{o2}} + \frac{i_o R_{o2}}{R_{o1} + R_{o2}} \quad (3.4)$$

Substituting $i_1 = i_o - i_2$ in (3.3), it can be written as:

$$-i_2 = \frac{V_{s1} - V_{s2}}{R_{o1} + R_{o2}} - \frac{i_o R_{o1}}{R_{o1} + R_{o2}} \quad (3.5)$$

Where, i_o is the total current of all the sources. Adding (3.4) and (3.5), the sharing error in currents can be calculated as:

$$i_1 - i_2 = \frac{2(V_{s1} - V_{s2})}{R_{o1} + R_{o2}} + \frac{i_o(R_{o2} - R_{o1})}{R_{o1} + R_{o2}} \quad (3.6)$$

The equation (3.6) shows the sharing error without droop effect. When the droop resistance R_d is added as shown in Fig. 3.3(b), the output resistances of both sources become $R_{o1} + R_d$ and $R_{o2} + R_d$ respectively. The sharing error with droop control can be written as:

$$i_1 - i_2 = \frac{2(V_{s1} - V_{s2})}{R_{o1} + R_{o2} + 2R_d} + \frac{i_o(R_{o2} - R_{o1})}{R_{o1} + R_{o2} + 2R_d} \quad (3.7)$$

It is clear from (3.7) that if the value of the output resistance is high, sharing error in currents is reduced. This situation is depicted in Fig. 3.4. In Fig. 3.4(a), when the output resistance is small, sharing error is high. Whereas, Fig. 3.4(b) shows that when the output resistance is increased by adding droop resistance, the sharing error is improved.

To determine the output voltage in Fig. 3.3(a), substitute $i_1 = \frac{(V_{s1}-V_o)}{R_{o1}}$ from (3.1) into (3.4), it can be expressed as:

$$V_o = \frac{(V_{s1}R_{o2} + V_{s2}R_{o1})}{R_{o1} + R_{o2}} + \frac{i_o(R_{o2}R_{o1})}{R_{o1} + R_{o2}} \quad (3.8)$$

And voltage regulation can be defined as:

$$\text{Voltage regulation}(\%) = \left(\frac{V_{NL} - V_o}{V_o} \right) \times 100 \quad (3.9)$$

Where, V_{NL} is the output voltage at no load. The advantage of droop control is that it is based on decentralized control architecture which does not require any communication channel. The disadvantages of droop control are based on (3.8) which states that voltage regulation will be degraded to achieve good current sharing performance. Therefore, current sharing among different power rating sources cannot be achieved using droop control [130, 131].

3.2.1 Implementation of droop controller

The resistance R_d in droop control can be implemented in different ways which are investigated below.

3.2.1.1 Voltage Droop by Adding External Series Resistance

In this scheme, the droop resistance R_d can be implemented by adding an external series resistance in each parallel connected source. The value of the resistance is set through variable resistor to make the output voltage of each source almost identical. Adding resistance in series will drop the voltage of each source. The major disadvantage of this scheme is high power loss in series resistance for high droop values which makes it impractical for high power applications. Thus, this scheme is only preferred for low power linear regulators [132–135].

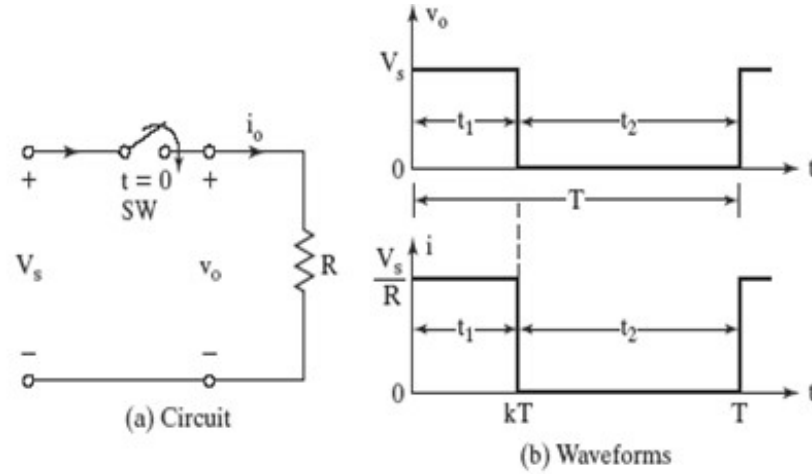


FIGURE 3.5: Step down dc to dc converter circuit and its output waveform [133]

3.2.1.2 Converters with Inherent Droop Characteristics

A simple scheme for parallel sources is to use converters with inherent droop characteristics. Converters such as resonant, dc to dc buck and boost converters when operated in discontinuous current condition mode (DCM) have the inherent droop capability. Therefore, these converters can be used for current sharing among parallel connected sources without any extra sharing requirement [130, 132].

The basic idea to improve current sharing among parallel connected sources is to vary the effective input resistances of the sources [136]. This idea can be accomplished by step down operation of a dc to dc converter as shown in the Fig. 3.5. When switch is closed for time t_1 in Fig. 3.5(a), the input voltage appears across the load as shown in Fig. 3.5(b). If the switch remains off for a time t_2 , the voltage across the load is zero.

From Fig. 3.5(b), the average output voltage V_a across the load can be expressed as:

$$V_a = \frac{1}{T} \int_0^{t_1} V_o dt = \frac{t_1}{T} V_s = k V_s \quad (3.10)$$

The rms output voltage across the load can be expressed as:

$$V_{o(rms)} = \sqrt{\frac{1}{T} \int_0^{t_1} V_o^2 dt} = \sqrt{k} V_s \quad (3.11)$$

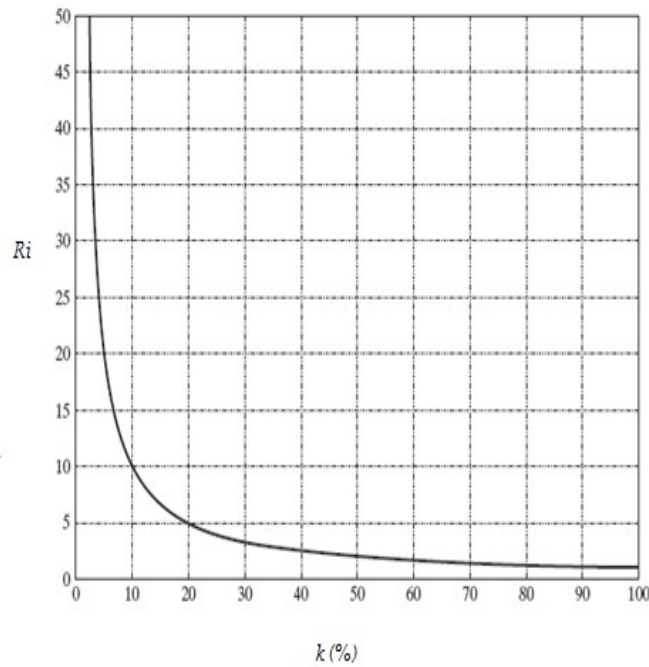


FIGURE 3.6: Effective input resistance against duty cycle [133]

Where, T and k are switching period and duty cycle respectively. The effective input resistance R_i seen by the source can be given as:

$$R_i = \frac{V_s}{I_a} = \frac{V_s}{kV_s/R} = \frac{R}{k} \quad (3.12)$$

The (3.12) shows that converter makes R_i as a variable resistance which is function of duty cycle k . The variation of effective input resistance against the duty cycle is shown in the Fig. 3.6. The same idea can be applied to improve current sharing error among parallel connected sources. The effective input resistance of sources can be increased by changing the duty cycle to increase current sharing.

3.2.1.3 Current Mode Control with Low DC Gain

This scheme is based on a fixed relationship between the change in PW and voltage error. It is realized by removing the series capacitor in the feedback path of an error amplifier [131, 133, 137]. Doing this significantly reduce the dc gain of the error amplifier and consequently, creating a droop effect in the output voltage. Fig. 3.7 shows the diagram of a source using current mode control with low dc

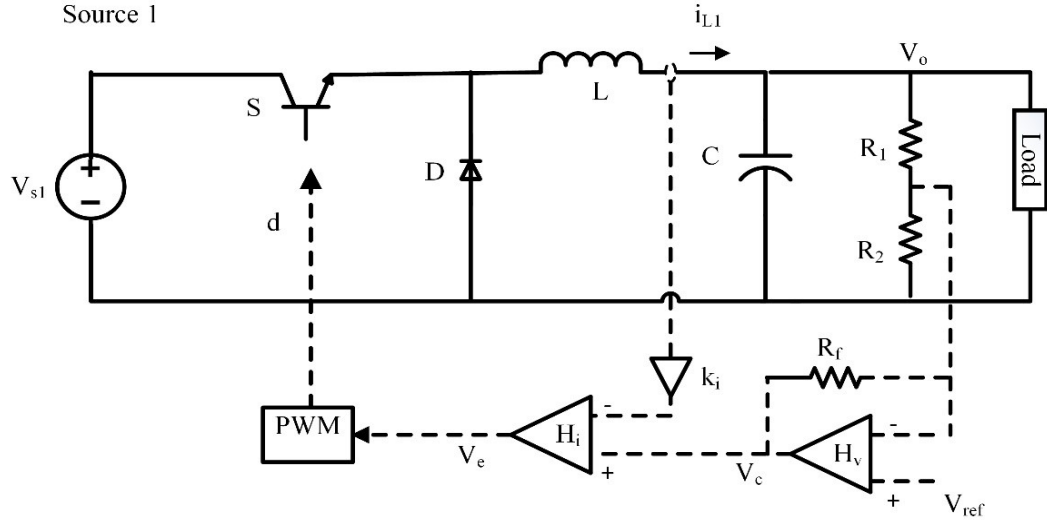


FIGURE 3.7: Voltage droop by current mode control with low dc gain

gain. From Fig. 3.7, the voltage signal V_c can be expressed as:

$$V_c = V_{ref} \left(\frac{1}{R_1} + \frac{1}{R_2} + \frac{1}{R_f} \right) R_f - \left(\frac{R_f}{R_1} \right) V_o \quad (3.13)$$

Where, V_{ref} and V_o are the reference and output voltage of dc to dc converter of source 1 respectively. The voltage error V_e can be expressed as:

$$V_e = V_c - k_i i_{L1} \quad (3.14)$$

Where, k_i and i_{L1} are the current sensing gain and inductor current of dc to dc converter of source 1 respectively. If error voltage V_e is Zero, then V_c can be expressed as:

$$V_c = k_i i_{L1} \quad (3.15)$$

Equating (3.15) and (3.13), the output voltage V_o can be expressed as:

$$V_o = V_{ref} \left(1 + \frac{R_1}{R_2} + \frac{R_1}{R_f} \right) - \left(\frac{R_1}{R_f} \right) k_i i_{L1} \quad (3.16)$$

Therefore, the droop resistance R_d created in the output voltage can be expressed as:

$$R_d = k_i \left(\frac{R_1}{R_f} \right) \quad (3.17)$$

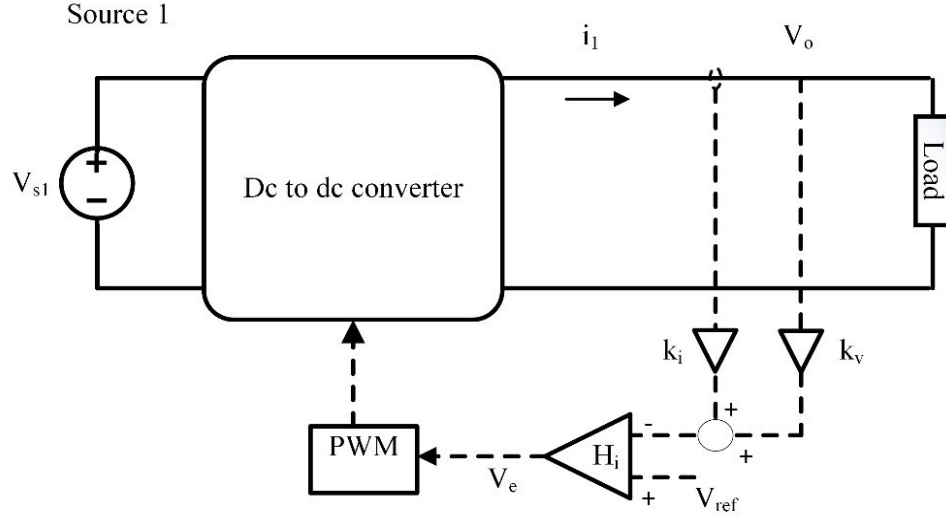


FIGURE 3.8: Voltage droop by output feedback current

3.2.1.4 Voltage Droop by Output Feedback Current

In this scheme, output current is sensed and this information is added in the voltage feedback loop. In this way the droop can be realized in proportion to output current [133]. Voltage droop of a source by output current feedback is shown in Fig. 3.8. The voltage error V_e can be expressed as:

$$V_e = V_{ref} - k_i i_1 - k_v V_o \quad (3.18)$$

Where, k_v and i_1 are voltage sensing gain and output current of source 1 respectively. Voltage droop created in the output voltage for $V_e = 0$, can be expressed as:

$$V_o = \frac{V_{ref} - k_i i_1}{k_v} \quad (3.19)$$

Therefore, the droop resistance R_d can be expressed as:

$$R_d = \left(\frac{k_i}{k_v} \right) \quad (3.20)$$

The performance of this scheme is the same as using R_d in series with output resistance.

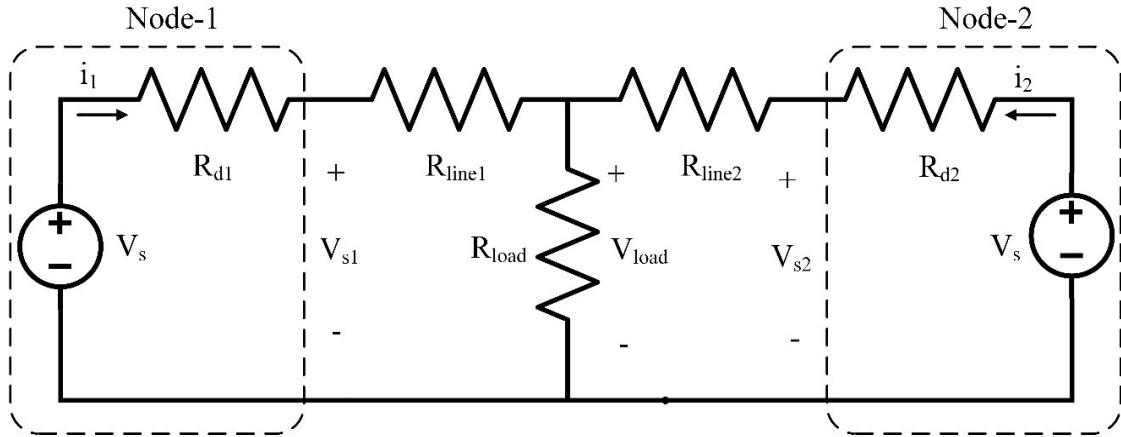


FIGURE 3.9: Thevenin equivalent model of two-source dc microgrid

3.2.2 Limitations of Droop Control in DC Microgrid

Although, different implementation schemes of droop control exist for parallel connected sources. Still, droop control cannot achieve the objectives of proportional load sharing and precise voltage regulation simultaneously in a dc microgrid. Therefore, it is required to study the limitation of droop control when used in dc microgrid application. The first limitation of this control is current sharing inaccuracy. Sources in dc microgrid are connected in parallel configuration through the connecting lines/cables. This will add a series resistance in each source. Due to this, output voltage of the parallel connected sources cannot be exactly same which lowers the load sharing accuracy. The second limitation is the output voltage deviation which occurs due to the droop action. Aforementioned limitations are investigated below.

3.2.2.1 Current Sharing Inaccuracy

Current sharing will be affected due to the voltage error in paralleled sources which are connected through dc to dc converters. This problem becomes challenging due to the extra voltage drop across the line connecting sources or when parameters of different sources are not same. Hence, current sharing among various sources is deteriorated. To analyze this problem, a dc microgrid with two-sources is shown in Fig. 3.9, where each source is modeled by its Thevenin equivalent circuit. The

commonly used droop control in dc system can be expressed as:

$$V_{sj} = V_s - i_j R_{dj} \quad (3.21)$$

Where, V_{sj} , V_s , i_j and R_{dj} are node voltage, source voltage, source current and droop resistance of each source respectively. The output resistance of source is embedded in droop resistance defined in (3.21). Output voltage of each source is represented by V_s , as shown in Fig. 3.9. Consider the load is drawing rated current and system has reached in steady state. Following can be derived from Fig. 3.9.

$$V_{load} = V_s - i_1 R_{d1} - i_1 R_{line1} \quad (3.22)$$

$$V_{load} = V_s - i_2 R_{d2} - i_2 R_{line2} \quad (3.23)$$

Comparing (3.22) and (3.33) and simplifying, these equations can be written as:

$$\frac{i_1}{i_2} = \frac{R_{d2}}{R_{d1}} + \frac{R_{line2} - (R_{d2}/R_{d1})R_{line1}}{R_{d1} + R_{line1}} \quad (3.24)$$

Above equation shows that in droop controlled dc grid, the current of both sources is inversely proportional to their droop resistances. Usually, it is assumed that dc microgrid is a small scale grid and connecting lines will contain resistances of small values. Hence, droop resistance R_{dj} can be selected large. Since $R_{dj} \gg R_{line}$, the above expression can be written as:

$$\frac{i_1}{i_2} = \frac{R_{d2} + R_{line2}}{R_{d1} + R_{line1}} \approx \frac{R_{d2}}{R_{d1}} \quad (3.25)$$

But the above-mentioned assumption is suitable for large R_{dj} . For small R_{dj} , precise current sharing cannot be ensured. Meanwhile, voltage regulation cannot be ensured with large droop resistance. This is graphically shown in Fig. 3.10.

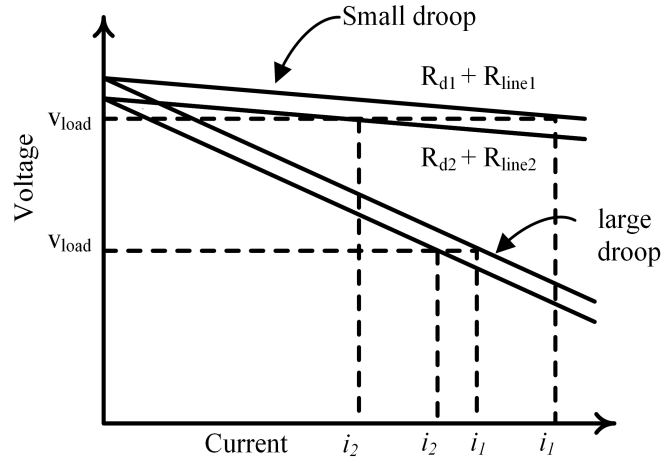


FIGURE 3.10: Current sharing inaccuracy using droop control [19]

3.2.2.2 Output Voltage Deviation

Voltage deviation can be written as:

$$\Delta v_j = V_s - V_{s_j} = i_j R_{d_j} \quad (3.26)$$

Fig. 3.11 shows the voltage deviation with different droop resistances. Voltage deviation is of zero value when sources operate at no load condition (source current is zero) as shown in Fig. 3.11. When the current by a source is not zero, voltage deviation appears and its value varies with the variation in load. To limit the output voltage deviation within acceptable levels, the droop coefficient R_{d_j} should be limited as:

$$R_{d_j} \leq \frac{\Delta v_{max}}{i_{fl_j}} \quad (3.27)$$

Where, i_{fl_j} is full load current of source-j. Therefore, the use of droop control method for current sharing in dc microgrid is limited by the challenge between current sharing efficiency and precise voltage regulation. Droop controllers are normally preferred in the applications where current sharing requirement is low.

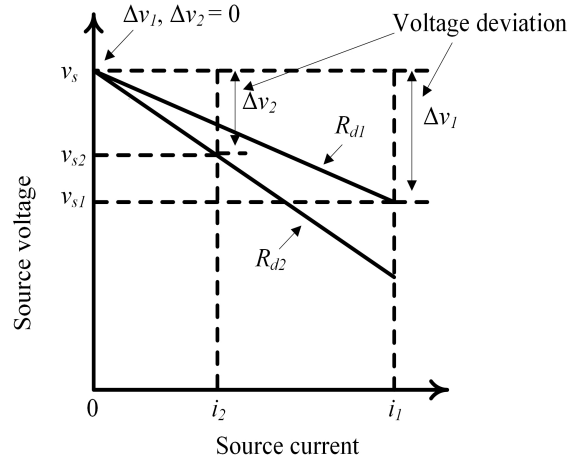


FIGURE 3.11: Droop curves with different virtual resistances

3.3 Active Load Sharing Control

Due to the limitations of droop control scheme, active sharing control is employed to achieve load sharing and precise voltage regulation simultaneously. Active sharing control provides load sharing accuracy utilizing a communication channel among parallel connected sources [138], [139], [140], [141], [9, 11, 12, 21], [128, 129]. Active control usually provides a current reference to each source which then adjust their own control parameters to follow the current reference. Consequently, the load current will be evenly shared among sources. It can be further classified in two types: centralized control and distributed control which are discussed below.

3.3.1 Centralized Control

In this type of control, the controller collects system data using real time high bandwidth communication channel and directs control decisions to the local controllers of each source. This type of architecture for dc microgrids is reported in [9, 11, 12, 139, 141] and is shown in Fig. 3.12. PE converter of each source contains droop control (primary control) and inner voltage and current control loop. Centralized control gives directions and control decision to the other primary controllers. Voltage of dc microgrid is communicated to the central controller, where it is compared with reference voltage. The error produced is transferred to PI

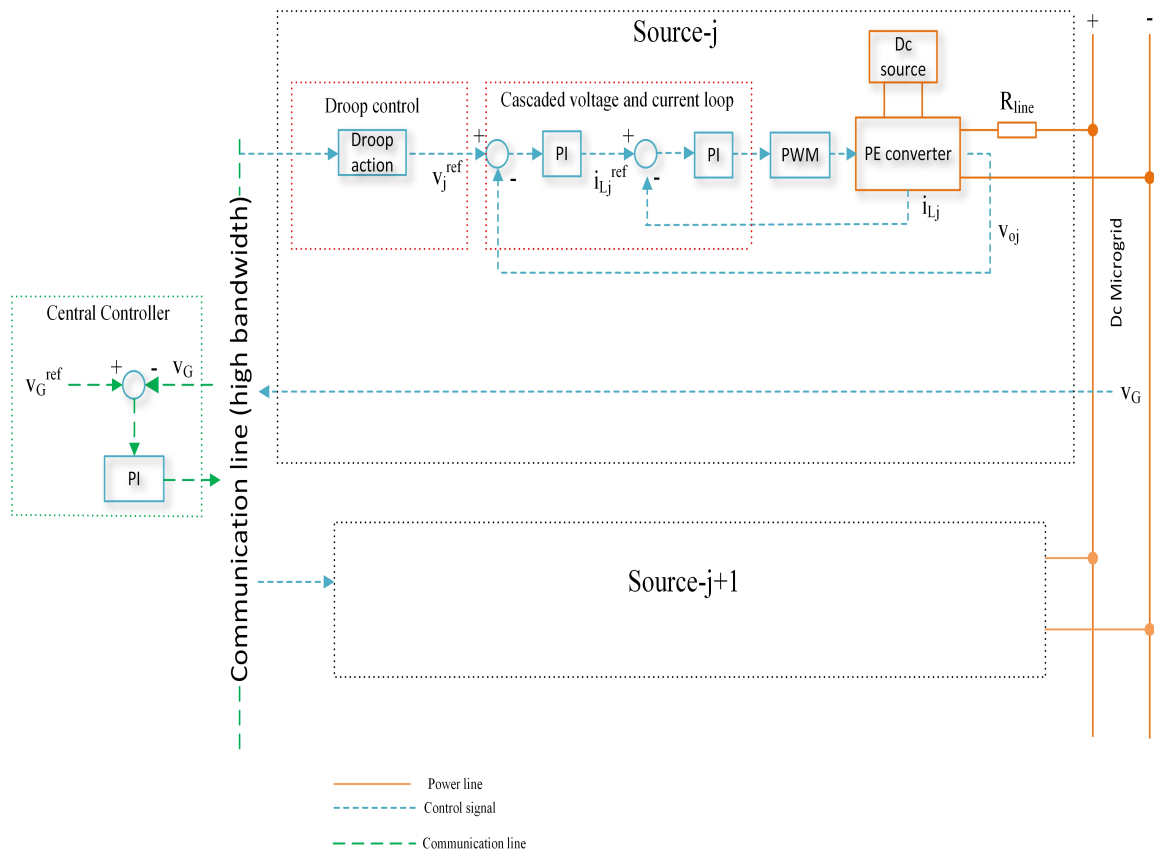


FIGURE 3.12: Centralized control

controller whose output is communicated to the primary controllers of each source as shown in the Fig. 3.12. However, if the single central controller fails, it will degrade the system performance and reliability. Hence, to use centralized control architecture for load sharing and voltage regulation objectives is not attractive.

3.3.2 Distributive Control

Disadvantages associated with the decentralized (droop control) and centralized control can be adjusted using distributive control which is an alternative solution to achieve efficient load sharing. In distributed control, as a substitute of single central controller, it is distributed in each source. A distributive control based on average current sharing (ACS) is shown in the Fig. 3.13. Each source in distributive scheme communicates to each other utilizing a common low bandwidth communication channel.

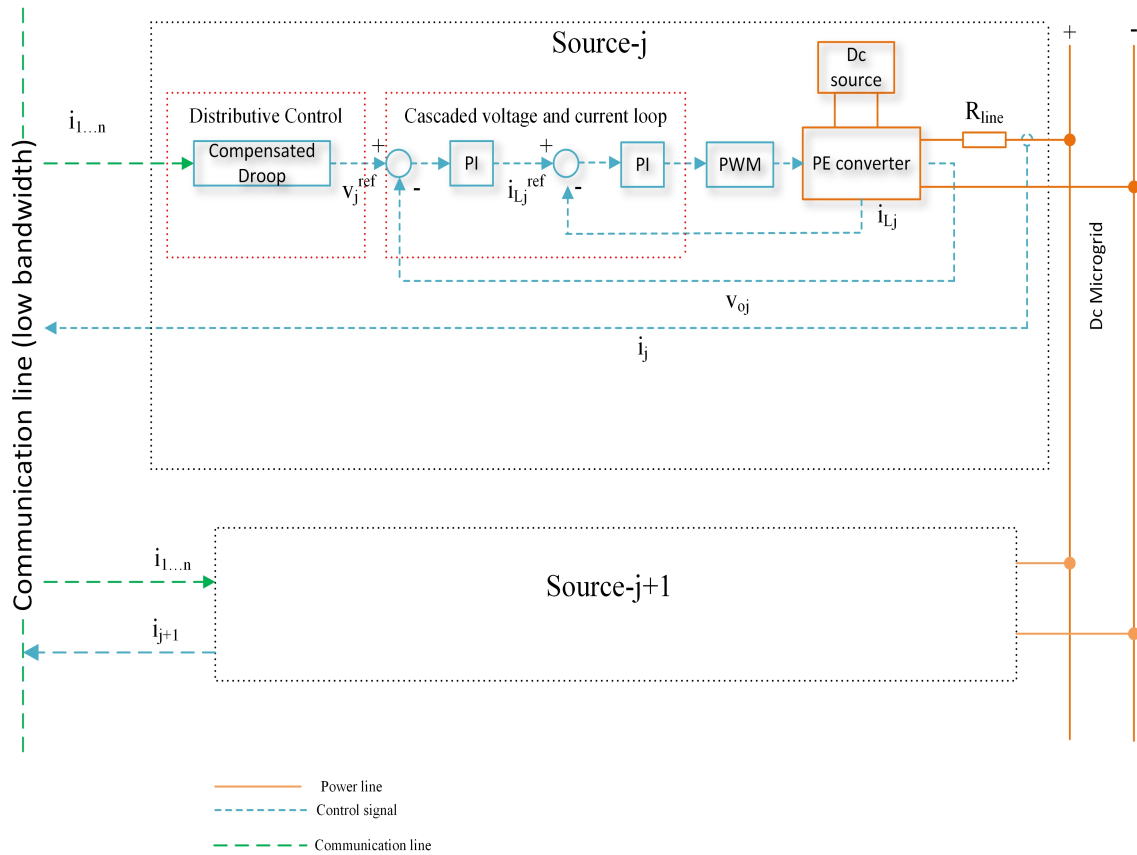


FIGURE 3.13: Distributive control

In [31], dc bus signaling (DBS) is proposed for distributed control in which dc voltage is used to communicate the decision about the operation of converters. In DBS, every entity in the system senses the dc voltage level for operation and decisions which limits the sources, loads and storage because dc bus voltage cannot be allocated unlimitedly. Also, some extreme situations like over-voltage/current and fully charged/under-charged battery are not deliberated. In [142], a current sharing bus is proposed and distributed in which average current is communicated among converters for operation. In dc microgrid, sources are displaced from each other over a region. Thus, current sharing bus need to be distributed over the region with the power lines. This may inject substantial noise which can degrade the system performance. In [143], a distributive secondary control using power line signaling (PLS) is presented. The major problem in PLS is that it is a slow communication. Further, electro-magnetic compatibility issues need to be addressed when using it with electronic devices.

TABLE 3.1: Summary of control architectures

| Control Scheme | Voltage regulation | Load sharing | Reliability |
|-----------------------|--------------------|--------------|-------------|
| Centralized | Precise | Good | Low |
| Decentralized (Droop) | Good | Inaccurate | High |
| Distributive | Good | Good | High |

A summary showing the comparison of the above-mentioned control schemes is presented in Table 3.1. The term precise signifies the regulation 2% while good means regulation 5%. Centralized scheme can achieve good load sharing and precise voltage regulation performance. But, it is not reliable due to the single central controller failure. Although, the reliability of decentralized scheme is high, but it shows inaccurate load sharing performance which is not acceptable for loads. Distributive control scheme ensures good load sharing and voltage regulation performance. Moreover, it shows better reliability compared to centralized control. Based on these facts, a distributive control utilizing low bandwidth controller area network (CAN) based communication is proposed for load sharing in dc microgrid application in this research work.

3.4 Summary

Proportional load sharing and precise voltage regulation are the key objectives to be achieved in dc microgrid. However, the problem in the parallel connected sources is that these objectives cannot be achieved simultaneously. To address the challenge, different control architectures are proposed in literature which can be categorized as passive and active type control. In this chapter, control architectures for load sharing in dc microgrids are reviewed with their limitations.

Droop based passive control is based on decentralized architecture which cannot achieve both objectives simultaneously due to voltage errors and load power variations. Decentralized control is communication less architecture in which PECs

operate on physical measured quantities. This architecture suffers stability and optimum operation due to lack of operational information and status of the other sources.

Centralized architecture is active type control, which collects system data using high bandwidth communication link, schedule the tasks based on collected information and directs control decisions. Centralized control can achieve good load sharing and precise voltage regulation performance. However, if single central controller fails, it will degrade system performance and reliability.

Distributive control architecture addresses the limitations of decentralized and centralized architectures. In this type, controller is distributed in each source. Main advantages achieved are high reliability, good load sharing and voltage regulation performance.

Chapter 4

Voltage Stability of DC Microgrid using Sliding Mode Control

4.1 Overview

Lack of complex architecture, easy integration and simple regulation are dc microgrid characteristics which may lead to false interpretation that dc microgrid stability concerns should be simpler than ac power systems [144]. DC microgrids are not exempted from the stability concerns [145, 146]. Stability issues in dc microgrid are of different nature which arise in ac grids. These concerns are naturally related with the PEC interfaces which are used to achieve different voltage levels in a microgrid. Different PECs are required for the integration of RESs, loads, and energy storing devices with dc microgrid. Therefore, dc microgrids have usually cascaded type distributed system architecture in which PECs act as interface elements among different subsystems with different voltage levels as shown in Fig. 1.1 of chapter 1.

Generally, control architecture is divided in centralized and decentralized control in a dc microgrid to provide consistent power to loads. In centralized control architecture, the controller collects system information using high bandwidth communication link, schedule the tasks based on the collected information and directs

control decisions [9, 10, 12]. However, single point failure will degrade the system performance and reliability. This constraint can be avoided in decentralized control [12, 16]. Significant benefits are relaxed scalability and lesser cost. In this type of architecture, PEC operates on locally measured quantities. In [32–36], droop control stability is reported for ac microgrids. Extensively used droop control in conventional ac power system inspires its use in dc microgrid [31, 38, 39, 41].

Classical controllers are being used to realize droop control for the stability of dc microgrid. Main reason to use these control techniques is due to their easy implementation of tuning method in industrial applications. These control techniques are based on PI type controllers. Regardless of the easiness in implementation of P controller, it suffers steady state error for the change in desired reference. Further, PI controlled converters suffer poor load sharing due to the integral action, where in most of the cases PI controllers do not attain stability [37, 41]. PI controller also exhibits slower transient response.

Moreover, the parameters of linear controllers are calculated using current specifications of the system [46, 47]. These parameters vary with load and sources apply to the system. Hence it becomes difficult to optimize controller parameters for different operating conditions. Linear controllers cannot ensure global stability of the desired equilibrium state. Hence to use these controllers for voltage stability is not feasible.

To address the aforementioned limitations, this chapter presents the voltage stability of dc microgrid based on decentralized control architecture using SM hysteresis control. Main advantages of are high robustness, fast dynamic response and good stability for large load variations. First part of this chapter highlights the theory and mathematical formulation of a system under SM. The minimum conditions for a system to show SM property are presented. In second part of this chapter, voltage stability of dc microgrid using SMC is presented. To analyze the stability and dynamic performance of the proposed scheme, a system model is derived, and its controllability and stability are verified. Modeled dynamics are graphically plotted and presented. Detailed simulations are carried out to show the effectiveness

of SM controller and results are compared with droop controller. The transient behavior on step load is also investigated and presented which shows the good performance of the proposed controller. A scaled down experimental setup of a source is also presented in this chapter.

4.2 Sliding Mode Control

The earliest form of published work on SM was introduced and successfully realized for dc generator control and ships-course control in early 1930s [72]. The development of SM theory and its applications were first initiated by Russian engineers as reported in literature [72], [147], [148]. The work by Russian outside Russia was subsequently transformed into English written documents by Itkis and Utkin [147]. Since then, SMC has gained a key interest from the researchers and control engineers around the world. The SMC is a type of nonlinear control which is primarily used to control VSSs [72], [147–150]. SMC is a state feedback time varying discontinuous control which switch the states from one state to another at a high frequency in the state space model. The objective is to direct the system dynamics to track exactly what is required.

The key advantage of the system design using SM controller is that it guarantees system stability for large load and line variations. Properties of the SM include insensitive to the matched disturbances and robustness against model uncertainties. It is robust control which shows fast dynamic response. Furthermore, the implementation of SM controller is comparatively easy compared with the other methods used for nonlinear controller design. These properties make SMC attractive for nonlinear systems and industrial applications e.g., furnace control, automotive control, electric motor drives, etc. [147].

This thesis is concerned with dc microgrid system in which each source consists of a particular class of VSSs known as PE converters. The objective of sections from 4.3 to 4.6 of this chapter is to present the basic theory and mathematical

overview of SMC which is required for the understanding of the study contained in subsequent sections of this chapters.

4.3 General Theory of Sliding Mode

To understand the basic theory of the SM, a system is considered in a three-dimensional space and a plane exists in this space. Further, a point O is considered on this plane which is called equilibrium point. The equilibrium point O is characterized as a stable attractor where, it is required that system trajectories when touches it, will settle down upon it. Next, it is considered that a system trajectory is randomly located in the defined space and is placed far away from the defined plane. If the system is left uncontrolled, its trajectory will move due to the natural behavior of the system. However, if a control action is applied, the system trajectory can be guided to a desired way. The direction of motion of the trajectory is dependent on the type of applied control action. A sequence of control actions might be required to direct the controlled trajectory towards the plane irrespective of the system initial conditions. When the trajectory reaches the plane, it will slide along the plan and ultimately, settle down on the equilibrium point O . A controller which do this is known as SMC. The plane which is required to guide the trajectory towards the equilibrium point is called as sliding manifold or sliding surface. To perform the task of SMC, fast switching among the different control actions are required.

Based on the terms defined above, more formal definition of SM can be established. If the given system is operated under SM, the feedback controlled trajectory S will be directed towards the sliding surface Ψ irrespective of the initial condition, and upon hitting the surface, it will switch at infinite frequency among the discrete control actions $U_1, U_2, \dots, etc.$, such that $S = \Psi = 0$, and ultimately, system trajectory will be directed, trapped and settles down on the equilibrium point O .

The systems trajectory under SMC is graphically represented in the Fig. 4.1 and 4.2. The whole operation of the SMC can be classified into two phases.

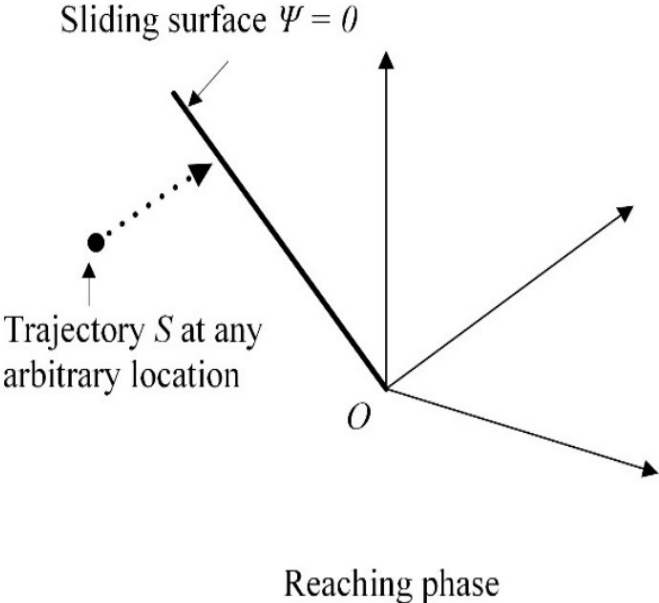


FIGURE 4.1: Reaching phase of SMC showing the system trajectory S moving towards the sliding surface irrespective of initial condition

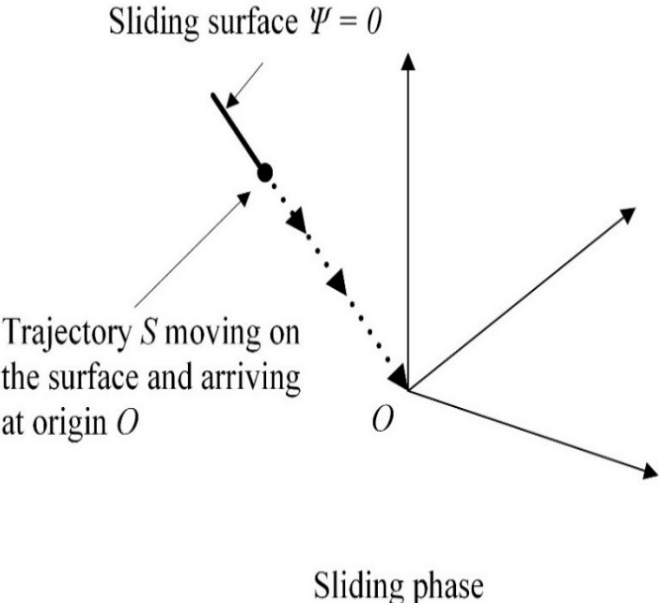


FIGURE 4.2: Sliding phase of SMC showing the system trajectory S moving on the sliding surface directed and settles at the origin O

4.3.1 Reaching Phase

Reaching phase is illustrated in Fig. 4.1. In this phase, the SM controller will force the system trajectory S towards the sliding surface Ψ irrespective of the initial condition. This phase is ensured through the agreement of hitting condition. Hitting condition guarantees that the systems trajectory under SM will always be directed towards the sliding surface irrespective of the initial condition [147].

4.3.2 Sliding Phase

Sliding phase is illustrated in Fig. 4.2. When the systems trajectory S hits the sliding surface, the system enters in the sliding phase control process. In this phase, the controller switches at infinite frequency among the series of control actions such that the systems trajectory is trapped on the sliding surface and guided towards the equilibrium point and ultimately, settles at the origin [147].

4.4 Sliding Motion Properties

In the sliding phase, the motion of the system trajectory on the sliding surface can be classified into two types which are discussed below.

4.4.1 Sliding Motion Through Ideal Control

The basic theory of SM in sliding phase is to direct system trajectory towards the desired equilibrium point employing the sliding surface as a reference track. This behavior is achieved by adopting the infinite gain for control actions such that the system trajectory remains trapped and follows the path along the sliding surface. This ideal behavior of the SMC is achievable only with the fundamental compliance that the switching frequency of the system is selected infinite. This behavior of the controller is called an ideal control which ensures ideal SM performance with

precise tracking, fast dynamic response and zero steady state regulation error. This type of SM motion is ideal for VSSs.

4.4.2 Practical Limits of Sliding Motion and Chattering Phenomena

The ideal SMC is so far based on the infinite switching frequency assumption. However, due to the practical limits of the real application, this ideal behavior is not possible. Practically, the sliding motion behavior slightly deviates from the ideal control condition due to the actual limitations of the switching devices such as switching time delays, slew rate, bandwidth and saturation limits. This behavior is known as chattering [72]. Therefore, these implementation requirements of the system limit the switching frequency inside a practical range which makes the controller a quasi SMC in close approximation to ideal SMC. This deteriorates the regulation performance and robustness of the system.

Fig. 4.3 shows the chattering behavior of the systems trajectory in sliding phase. The trajectory S oscillates at high frequency within the locality of sliding surface converging towards the origin. Further, upon reaching the trajectory S on the origin, it will be bounded near O in a periodically oscillating state unlike ideal SM as shown in Fig. 4.4. The consequence of this results in the steady state error of the controlled system. Note that the operation of reaching phase is not affected by chattering. Thus, Fig. 4.1 shows the operation of reaching phase in both ideal and practical condition.

4.5 Mathematical Formulation

A time dependent nonlinear switching system is considered to present the mathematical formulation of SM and is defined as:

$$\dot{x}(t) = a(x(t)) + b(x(t)) \cdot u(t) \quad (4.1)$$

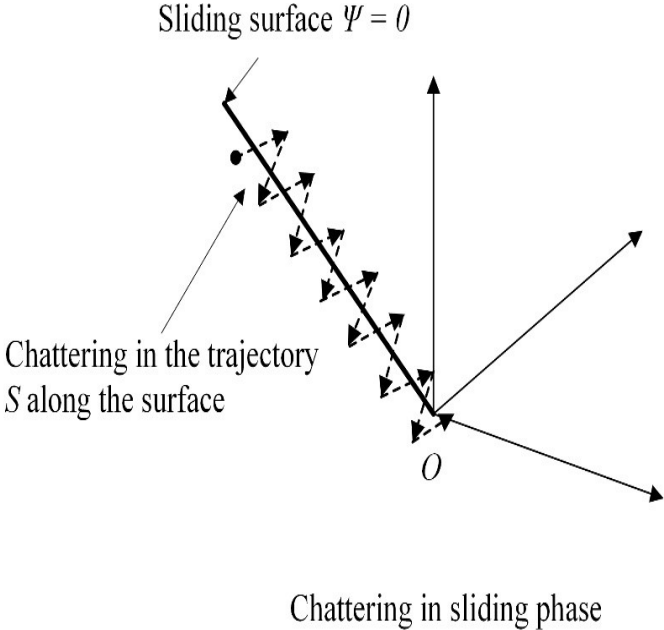


FIGURE 4.3: Practical SM with chattering in the system trajectory S moving along the sliding surface directed towards the origin O

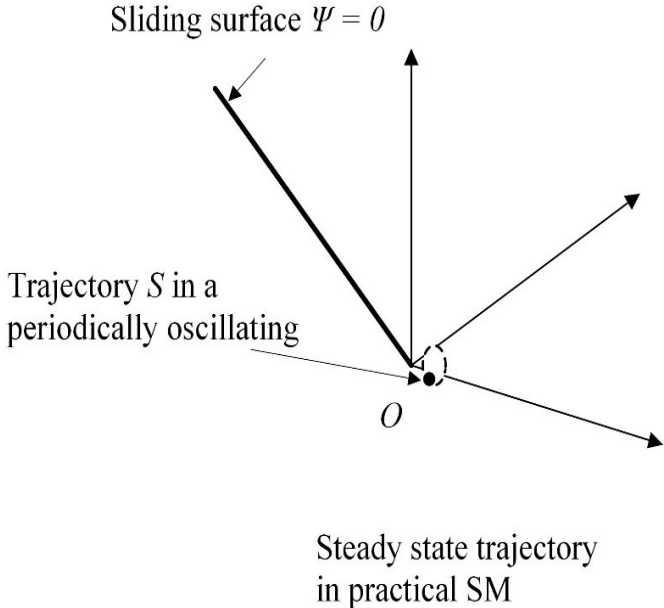


FIGURE 4.4: System trajectory S in steady state bounded in periodically oscillating state near the origin O

Where, $x(t)$ is a vector of state variable of space n -dimensions R^n , $a(\cdot)$ and $b(\cdot)$ are smooth vector in the same space. Whereas, $u(t)$ is a discontinuous control law defined as:

$$u(t) = \begin{cases} U^+ & \text{if } S(x, t) > 0 \\ U^- & \text{if } S(x, t) < 0 \end{cases} \quad (4.2)$$

Where, U^+ and U^- are scalar values respectively. Whereas, $S(x, t)$ represents instantaneous trajectory of the system which is function of state variables. Normally, $S(x, t)$ is selected as:

$$S(x, t) = \sum_{i=1}^m \alpha_i x_i(t) \quad (4.3)$$

Where, α represents the controller parameter and is known as sliding coefficient. There are three conditions which needs to be satisfied for a system to show SM property. These are hitting, existence and stability conditions which are defined below.

4.5.1 Hitting Condition

The goal of this condition is to guarantee that irrespective of the initial location, the control actions will force the system trajectory to approach and ultimately, reach inside the locality of sliding surface. This is graphically shown in Fig. 4.5. Suppose that the system with trajectory $S_i = S(t = 0)$ and initial state vector $x_i = x(t = 0)$ is positioned for away from the sliding surface as shown in the Fig. 4.5. The sufficient condition required to achieve hitting condition is to generate control action $u_i(t > 0)$ such that it will generate a state vector $x(t > 0)$ and trajectory $S(t = 0)$ which ensures the inequality given below.

$$S \frac{dS}{dt} < 0 \quad (\text{for } t > 0 \text{ and } |S| \geq \delta) \quad (4.4)$$

The (4.4) is defined based on the second theorem of Lyapunov stability [77, 78, 144, 145, 147] in which Lyapunov function is defined as:

$$V(S) = \frac{1}{2} S^2 \quad (4.5)$$

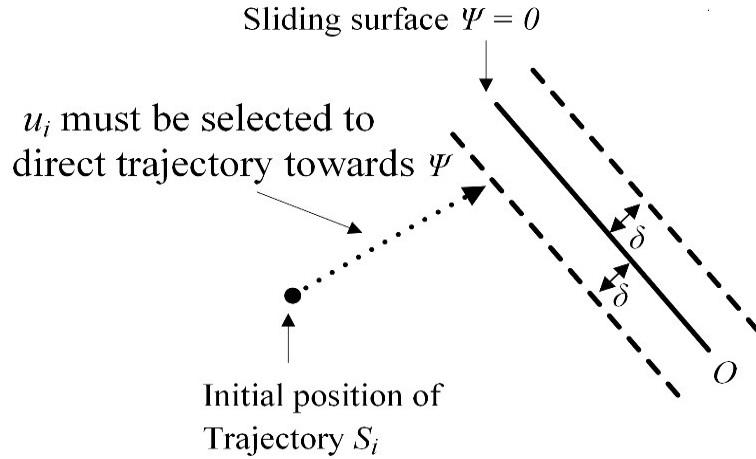


FIGURE 4.5: System trajectory S converging to the sliding surface upon satisfying the hitting condition

The inequality in (4.4) ensures that trajectory S at any position outside the locality of sliding surface will always be attracted and converged to the sliding surface $\Psi = 0$ and control action $u_i(t > 0)$ will support this convergence. Therefore, the fundamental design requirement of the SMC is to find the suitable control action as defined in (4.2) such that hitting condition is always satisfied.

4.5.2 Existence Condition

After satisfying the hitting condition, the system is then subjected to comply the existence condition. Existence condition ensures that upon reaching the system trajectory inside the locality of sliding surface $0 < |S| > \delta$ [144], it will remain trapped and still directed towards the sliding surface as shown in Fig. 4.6. The following condition must be fulfilled for the existence of the operation of the SM.

$$\lim_{s \rightarrow 0} S \frac{dS}{dt} < 0 \quad (4.6)$$

The condition in (4.6) can be divided into the following expression as:

$$\lim_{s \rightarrow 0^+} \frac{dS}{dt} < 0 \quad \text{and} \quad \lim_{s \rightarrow 0^-} \frac{dS}{dt} > 0 \quad (4.7)$$

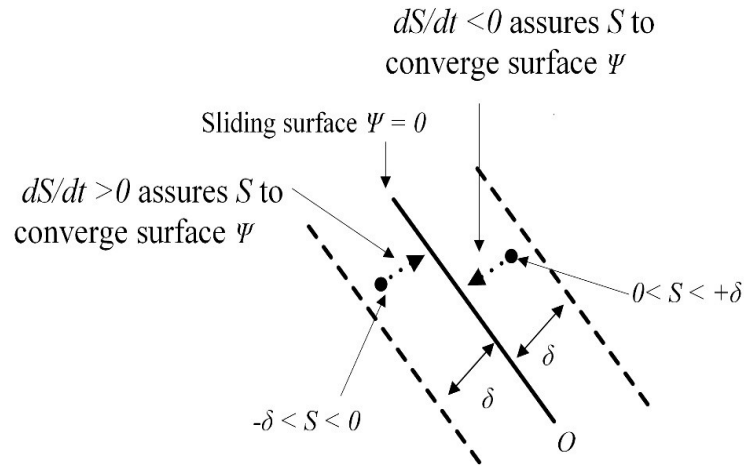


FIGURE 4.6: System trajectory S inside the locality $0 < |S| > \delta$ and converging to sliding surface upon satisfying the existence condition

It is reflected from (4.7) that the time derivative of the systems trajectory has opposite sign in the locality of sliding surface [72].

4.5.3 Stability Condition

After the Existence of the SM, the sliding coefficients and control actions must be complied with stability condition. This condition guarantees that under the operation in sliding phase, the system's trajectory will be directed and stay on the stable origin (equilibrium point). If this condition is not satisfied, the system will lead to an unstable behavior. Fig. 4.7(a) shows that system's moving trajectory stabilizing at the origin after satisfying stability condition. And Fig. 4.7(b) shows the unstable behavior when the moving trajectory passes the origin O .

Generally, the systems stability is guaranteed by ensuring that real part of the roots (eigen values) of the system matrix known as Jacobian matrix have negative values [147]. The following section presents the stability of the system with linear and nonlinear sliding surface.

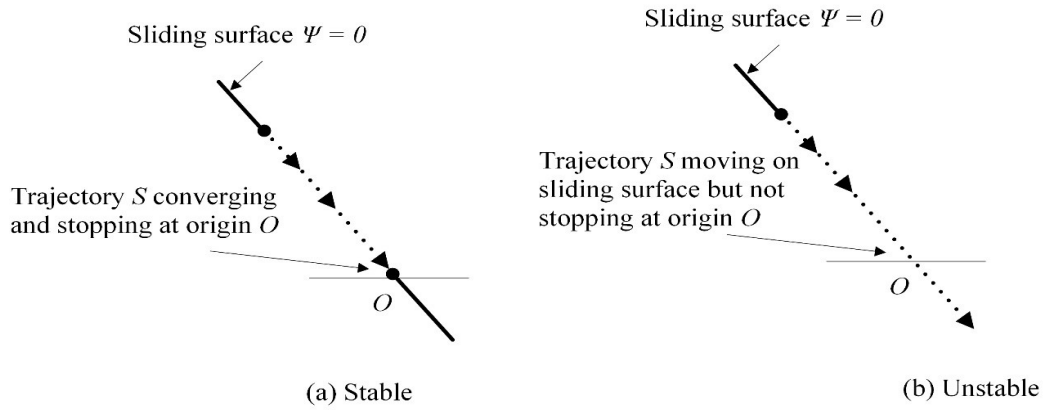


FIGURE 4.7: System trajectory S moving on sliding surface with stable and unstable behavior

4.5.3.1 Stability with Linear Sliding Surface

In this case, the system trajectory is selected as a linear combination of the weighted sliding coefficients of the state variables, time derivatives (or sub-derivatives) and/or integrals (or iterated-integrals) of the state variable as defined in (4.3). The equivalent sliding surface of such trajectory is primarily an equation of linear motion. Substituting $S = 0$ in (4.3), the motion equation can be expressed as:

$$\alpha_1 x_1(t) + \alpha_2 x_2(t) + \cdots + \alpha_m x_m(t) = 0 \quad (4.8)$$

Where, $x_{n=1,2,\dots,m}$ are state variables in phase canonical form [61]. Substituting $x_{n+1}(t) = dx_n/dt$ in (4.8) for phase canonical form and taking Laplace transform, it can be expressed as:

$$\alpha_1 X_1(s) + \alpha_2 s X_1(s) + \cdots + \alpha_m s^{m-1} X_1(s) = 0 \quad (4.9)$$

Where, $X_1(s)$ represents the Laplace transform of $x_1(t)$. After arranging and simplification, (4.9) can be expressed as:

$$\alpha_m s^{m-1} + \cdots + \alpha_3 s^2 + \alpha_2 s + \alpha_1 = 0 \quad (4.10)$$

The polynomial in (4.10) is linear with $(m - 1)^{th}$ order and is used to prove the stability of a system under SM. Now for the stability, apply the criteria of Routh Hurwitz stability condition which states that the real part of all the roots of this polynomial have negative values [72].

4.5.3.2 Stability with Nonlinear Sliding Surface

Equivalent control method is used to prove the stability of a system with nonlinear motion under SM [133, 134]. In this method, ideal sliding dynamics are derived first and then stability analysis is performed on the equilibrium point.

- Ideal Sliding Dynamics

Substituting $u(t)$ by $u_{eq}(t)$ in (4.1), it can be expressed as:

$$\dot{x}(t) = a(x(t)) + b(x(t)) \cdot u_{eq} \quad (4.11)$$

Where, $u_{eq}(t)$ is continuous control law which is known as equivalent control. The $u_{eq}(t)$ can be determined by putting $dS(t)/dt = 0$ as defined in equivalent control method [151, 152]. The $u_{eq}(t)$ can be expressed as:

$$u_{eq}(t) = f\left(\sum_{i=1}^m \alpha_i \dot{x}_i(t) = 0\right) \quad (4.12)$$

Where, $f(\dot{S}(t) = 0)$ is a function of system trajectory (where $S(t)$ is a function of sliding coefficients and state variables as defined in (4.3)). Substituting $u_{eq}(t)$ from (4.12) into (4.11) gives as:

$$\dot{x}(t) = a(x(t)) + b(x(t)) \cdot f\left(\sum_{i=1}^m \alpha_i \dot{x}_i(t) = 0\right) \quad (4.13)$$

The (4.13) denotes the ideal sliding dynamics which shows that it doesn't depend on the control signal.

- Stability on Equilibrium Point

Assume that a stable point exists on the sliding surface and ideal sliding dynamics of a system under SM ultimately settles on this point. Then, the system state equation defined in (4.13) can be solved by putting $\dot{x}(t) = 0$ to give the operating point $(x_{1(ss)}, x_{2(ss)}, \dots, x_{m(ss)})$ in steady state condition.

Furthermore, the stability can also be ensured through the proper selection of the stable sliding coefficients to achieve the required dynamic behavior of the system under SM [153]. Thus, the sliding coefficients are designed to achieve the desired system response which inherently satisfies the stability condition.

4.6 Implementation types of SM controller

The SM controller can be implemented through three types known as relay and signum, hysteresis and equivalent control function. These types are presented below.

4.6.1 Relay and Signum Function

The conventional implementation of the SM controller is directly based on the definition of the control law defined in (4.2) and (4.3). The (4.3) deals with the computation of instantaneous system trajectory $S(t)$ which can be realized through digital or analog components and (4.2) is a discontinuous control function which can be easily realized through relay. SM controller through relay function is shown in the Fig. 4.8.

In applications where controller comprises only on positive or negative control decisions, the control law through relay operation can be expressed by signum function as:

$$u(t) = \text{sign}(S(x, t)) \quad (4.14)$$

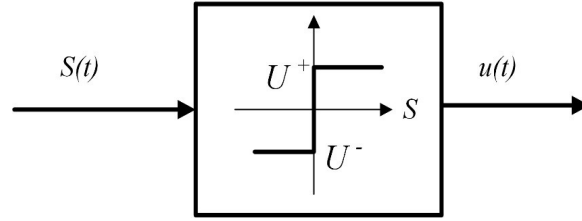


FIGURE 4.8: Relay function using SMC

Where, $sgn(\cdot)$ represents the signum function which is defined as:

$$u(t) = \begin{cases} U^+ = 1 & \text{if } S(x, t) > 0 \\ 0 & \text{if } S(x, t) = 0 \\ U^- = -1 & \text{if } S(x, t) < 0 \end{cases} \quad (4.15)$$

In applications where controller contains digital logic, the control law in (4.15) is replaced by the following:

$$u(t) = \begin{cases} 1 & \text{if } S(x, t) > 0 \\ 0 & \text{if } S(x, t) \leq 0 \end{cases} \quad (4.16)$$

The implementation of the SM controller through relay is simple and straightforward. However, implementing directly (4.15) or (4.16) results in undesirable chattering effect in the system trajectory due to the practical switching constraints as presented earlier. Further, it produces high switching noise which is not suitable for many applications. Thus, to restrict the operating frequency range of the system hysteresis function can be used and discussed below.

4.6.2 Hysteresis Function

The hysteresis implementation is commonly used to control the chattering effect in the operation of the SM controller and is accomplished through redefining control law as:

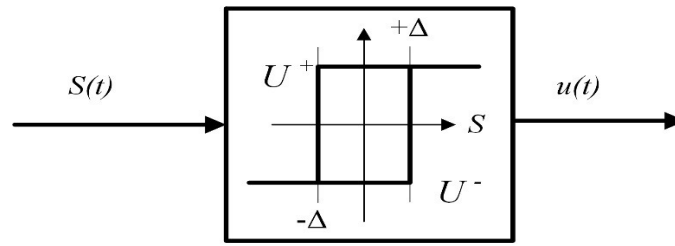
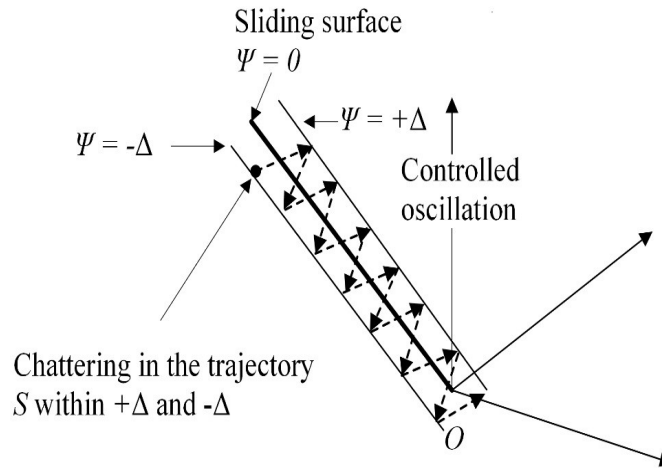


FIGURE 4.9: Hysteresis function using SMC

FIGURE 4.10: Chattering in trajectory S through hysteresis function

$$u(t) = \begin{cases} U^+ = 1 & \text{if } S(x, t) > \Delta \\ U^- = -1 & \text{if } S(x, t) < -\Delta \\ \text{Previous state} & \text{if Otherwise} \end{cases} \quad (4.17)$$

Where, Δ is a small arbitrary quantity. The hysteresis band $\Delta \leq S \leq -\Delta$ defined in (4.17) solves the high switching frequency problem by delaying the control actions as shown in Fig. 4.9. In this way, the trajectory in sliding phase will move in close locality of $\pm\Delta$ of the sliding surface as shown in the Fig. 4.10. Therefore, introducing hysteresis band, the switching frequency and chattering effect can be controlled by Δ .

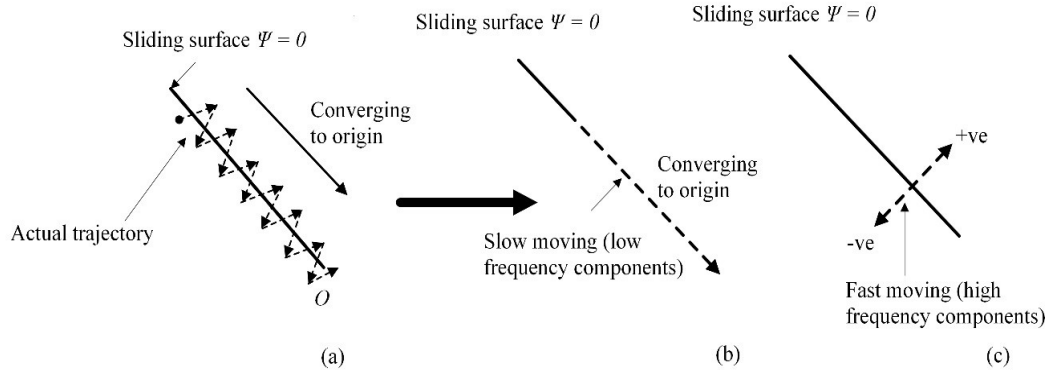


FIGURE 4.11: Low and high frequency components of trajectory in sliding phase

4.6.3 Equivalent Control Function

In ideal SM operation, the system is switched at infinite frequency to move the trajectory exactly on sliding surface. As presented earlier, the ideal SM is not possible due to the limitations of the practical switching devices which results in chattering produced in the sliding motion. In the motion of the trajectory, two components can be recognized as low and high frequency components as shown in the Fig. 4.11. The slow moving components move along the sliding surface whereas fast moving components oscillate between positive and negative direction as shown in Fig. 4.11(b) and (c). The slow and fast components can be related by following relations:

$$U^- < u_{low}(t) < U^+ \quad (4.18)$$

$$u_{high}(t) = \begin{cases} U^+ - u_{low}(t) & \text{if } S(x, t) > 0 \\ U^- - u_{low}(t) & \text{if } S(x, t) < 0 \end{cases} \quad (4.19)$$

Control law is then given by:

$$u(t) = u_{low}(t) + u_{high}(t) \quad (4.20)$$

Practically, fast moving components can be easily filtered using low pass filter.

Therefore, the system motion is completely determined by slow moving components of the trajectory. Thus, $u_{low}(t)$ will move the system almost equivalent to the ideal SM and is known as equivalent control $u_{eq}(t)$.

The $u_{eq}(t)$ can be derived by putting $\dot{S} = 0$ based on the property of invariance [76] as expressed in (4.12). The resulting equivalent dynamics is expressed in (4.13). Therefore, the implementation through equivalent control will derive the system with ideal sliding dynamics without chattering.

4.7 DC Microgrid Architecture

A general dc microgrid connecting different sources and loads is presented in Fig. 1.1 of chapter 1. All nodes contain a local source and load. Sources can be categorized as ac and dc sources. AC sources are nonrenewable generator, wind and ac grid. These sources require ac to dc converter to integrate with dc microgrid. PV, fuel cell and energy storage batteries are dc sources. These sources require dc to dc converter to connect with dc microgrid. A node structure is shown in Fig. 4.12. Each PEC contains a local voltage controller which maintains its output voltage equal to its reference value. It is also responsible for damping out high frequency oscillations. For steady state operation, total demanded power should be less than the total available power from the sources. The dc microgrid control objectives include voltage regulation and proportional load sharing. Droop controllers are used as local controllers to achieve these objectives. These controllers operate with voltage controllers in cascaded connection as shown in Fig. 4.12. Droop control can be easily designed using proportional controller in a similar way like a dc source which has a series resistance. But it shows steady state error for load variations. Furthermore, droop is realized through PI controllers which show poor load sharing performance. These controllers do not achieve global stability and exhibits slower transient response. The parameters of these controllers are calculated on the bases of physically measured values of the system. Thus, it becomes difficult to optimize control parameters for different operating conditions.

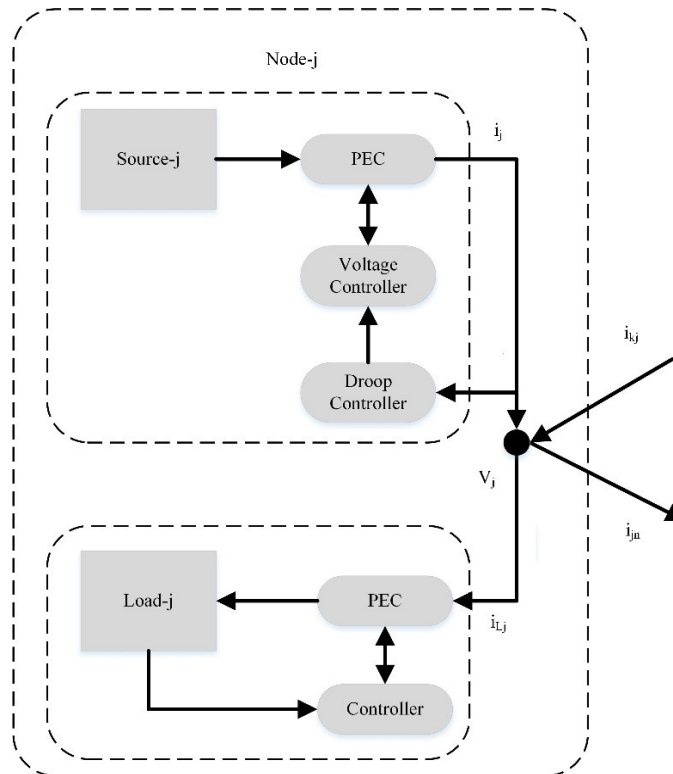


FIGURE 4.12: Structure of a node

Hence, to use linear controllers for voltage stability of dc microgrid is not suitable. Due to these reasons, a nonlinear SMC is analyzed and proposed for dc microgrid application in this chapter.

Most of the loads are electronics, VFDs and lighting. These loads operate at different voltage level. So, PECs are required to integrate these loads with dc microgrid as shown in Fig. 4.12. PEC regulates the output voltage to supply demanded power. These loads are estimated to use constant power and termed as constant power loads (CPLs). The increased uses of CPLs make its study not important but also practical. Currently, CPLs are used in many applications such as in telecom switches, base stations and data center servers. There are different interconnections structures available to connect nodes through distribution cables. Some popular structures are circular (loop) and radial type as discussed in [38, 41]. However, many others are possible. Practical systems are complex in nature and hence, radial and circular types are not suitable to represent these systems. Therefore, a generic interconnection structure is presented in this chapter. The structure presented can be applied to any interconnection structure.

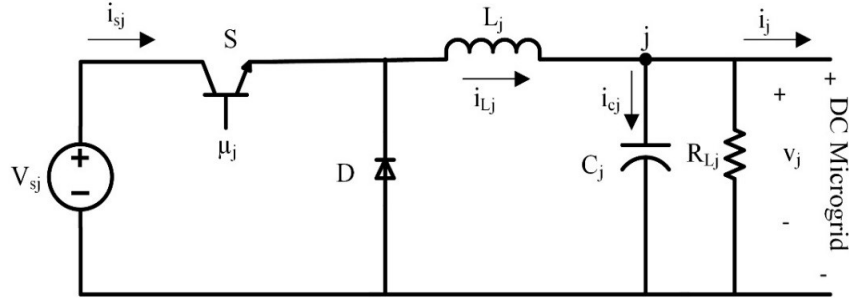


FIGURE 4.13: Model of source-j with dc microgrid

4.8 Modeling of DC Microgrid

An equivalent model of a source-j which is connected with dc microgrid through dc to dc converter is shown in Fig. 4.13. Source is modeled by voltage source V_{sj} with current i_{sj} . Regulating node voltages of dc microgrid is an error tracking problem. Therefore, to derive the system dynamics, state variables selected are voltage error x_1 and the rate of change of voltage error (voltage error dynamics) x_2 respectively. Voltage error at node-j in Fig. 4.13 can be expressed as:

$$x_1 = e_{vj} = V_{refj} - \beta_j v_j \quad (4.21a)$$

Where, e_{vj} , V_{refj} , v_j and β_j are voltage error, reference voltage, output voltage and sensing ratio of PEC at node-j respectively. After differentiating (4.21a), rate of change of voltage error at node-j can be expressed as:

$$x_2 = \frac{dx_1}{dt} = 0 - \beta_j \frac{dv_j}{dt} \quad (4.21b)$$

Capacitor current i_{cj} of PEC at node-j is defined as:

$$i_{cj} = C_j \frac{dv_j}{dt} \quad (4.21c)$$

Substituting dv_j/dt from (4.21c) into (4.21b), it can be expressed as:

$$x_2 = -\beta_j \frac{i_{cj}}{C_j} \quad (4.21d)$$

Where, C_j is capacitance of PEC at node-j. The (4.21a) and (4.21d) are state equations of the system. To achieve efficient regulation in dc microgrid, x_1 and x_2 should approach to zero.

4.8.1 Interconnection Structure

Interconnection structure of dc microgrid shown in Fig. 1.1 can be expressed through Kirchhoffs Current Law (KCL) and Kirchhoffs Voltage Law (KVL). In matrix form, applied KVL can be expressed as:

$$V_b = MV \quad (4.22)$$

Where, V_b is column vector of branch/cable voltages of $m \times 1$ dimension, V is column vector of node voltages of $n \times 1$ dimension and M is incidence matrix of $m \times n$ dimension respectively. Whereas, n represent nodes and m represent connecting branches/cables respectively. In matrix form, KCL applied at the node of PEC is given as:

$$i - i_L - i_c = M^T i_b \quad (4.23)$$

Where, i , i_L and i_c are column vector of inductor currents, load currents and capacitor currents of $n \times 1$ dimension respectively. Whereas, i_b is a column vector of branch currents of $m \times 1$ dimension and $()^T$ is transpose of a matrix.

4.8.2 System Dynamic Equations

To determine the system dynamics, differentiating (4.21a) can be expressed by the following differential equation as:

$$\dot{x}_1 = \frac{dx_1}{dt} = -\beta_j \frac{dv_j}{dt} = x_2 \quad (4.24a)$$

After differentiating (4.21d), it can be expressed in matrix form by the following differential equation as:

$$\dot{x}_2 = (-C^{-1}\beta) \frac{di_c}{dt} \quad (4.24b)$$

Substituting i_c from (4.23) into (4.24b), after simplification, it can be expressed as:

$$\dot{x}_2 = (-C^{-1}\beta) \frac{d(i - i_L - M^T i_b)}{dt} \quad (4.24c)$$

Substituting column vector of inductor currents $i = L^{-1} \int (v_i u - V) dt$, load currents $i_L = R_L^{-1} V$ and branch currents $i_b = R_b^{-1} V_b$ into (4.24c), after simplification, it can be expressed in matrix form as:

$$\dot{x}_2 = -L^{-1} C^{-1} x_1 - (R_L^{-1} C^{-1} + R_b^{-1} C^{-1} M^T M) x_2 - L^{-1} C^{-1} \beta v_i u + L^{-1} C^{-1} V_{ref} \quad (4.24d)$$

From (4.24a) and (4.24d), the system dynamics can be expressed in state-space form as:

$$\begin{aligned} \begin{bmatrix} \dot{x}_1 \\ \dot{x}_2 \end{bmatrix} &= \begin{bmatrix} 0 & 1 \\ -L^{-1} C^{-1} & -(R_L^{-1} C^{-1} + R_b^{-1} C^{-1} M^T M) \end{bmatrix} \begin{bmatrix} x_1 \\ x_2 \end{bmatrix} \\ &+ \begin{bmatrix} 0 \\ -L^{-1} C^{-1} \beta v_i \end{bmatrix} u + \begin{bmatrix} 0 \\ L^{-1} C^{-1} \end{bmatrix} V_{ref} \end{aligned} \quad (4.24e)$$

Where, x_1 and x_2 are column vectors of voltage errors and rate of change of voltage errors of $n \times 1$ dimension respectively. Whereas, L , C , and R_L are diagonal matrices of inductance, capacitance, sensing ratio and load resistance with $n \times n$ dimension, R_b is diagonal matrix of branch resistance of $m \times m$ dimension, v_i is instantaneous input voltage and u is the control law with $n \times 1$ dimension respectively.

Control law u defines the switching state of the PEC switch. It can be expressed as:

$$u = \begin{cases} 1 & \text{if Switch is 'ON'} \\ 0 & \text{if Switch is 'OFF'} \end{cases} \quad (4.24f)$$

Linearized dynamics of dc microgrid system given in (4.24e) can be expressed as:

$$\dot{x} = Ax + Bu \quad (4.25)$$

Where, A represents the system matrix of state variables and B represents the system input matrix respectively. From (4.24e), the matrices A and B can be expressed as:

$$A = \begin{bmatrix} 0 & 1 \\ -L^{-1}C^{-1} & -(R_L^{-1}C^{-1} + R_b^{-1}C^{-1}M^T M) \end{bmatrix} \quad (4.25a)$$

$$B = \begin{bmatrix} 0 \\ -L^{-1}C^{-1}\beta v_i \end{bmatrix} \quad (4.25b)$$

4.9 Stability Analysis

System dynamics in (4.25) are linear differential equations which are used to analyze that all the states of the system are controllable. Furthermore, stability of the modeled system is analyzed through eigen values of system matrix A .

4.9.1 Controllability

A system is said to be completely controllable if, for all initial times and states, there exist some input function which moves the state vector to any final state at some finite time. A necessary and sufficient condition for a system is said to be controllable if its controllability matrix R has full rank (i.e. $rank(R) = p$) [154].

$$R = [B \quad AB \quad A^2B \cdots A^{p-1}B] \quad (4.26)$$

Where, p is number of linearly independent rows/columns. Controllability of the presented system model of dc microgrid in (4.25) is verified using MATLAB and it is completely controllable.

4.9.2 Eigen values

Eigen values of system matrix A are values of λ which satisfy the following equation.

$$|A - I\lambda| = 0 \quad (4.27)$$

Where, I is the identity matrix. If the determinant of above equation is opened, it gives a characteristic polynomial of n^{th} degree which can be expressed as [154]:

$$|A - I\lambda| = -\lambda^n + c_{n-1}\lambda^{n-1} + \cdots + c_1\lambda + c_0 = \Delta(\lambda) \quad (4.28)$$

The roots of the above characteristic polynomial are eigen values λ_i . For a two-source dc microgrid system with parameters given in table 4.1, 4.2 and 4.3 presented in section 4.11, the eigen values are determined and given below:

$$\lambda_1 = (-2.3457)10^3$$

$$\lambda_2 = (-0.0391 + 1.5807i)10^3$$

$$\lambda_3 = (-0.0391 - 1.5807i)10^3$$

$$\lambda_4 = (-1.0658)10^3$$

The above eigen values are real and complex. Real part of these values is negative which shows that the modeled system in (4.25) is stable.

4.10 Voltage Stability Through Sliding Mode Control

The objective of system under SM is to direct system dynamics to follow exactly what is desired as presented in the first part of this chapter. Following design conditions need to be satisfied for the stable operation of the modeled dc microgrid system.

4.10.1 System Design using Sliding Mode Controller

SM controller requires a switching law which defines the control actions to derive the system dynamics to follow the desired path. In SM voltage control, the switching law u is based on the definition of sliding surface.

4.10.1.1 Sliding Surface Design

Sliding surface S for state parameters x_1 and x_2 of the modeled dc microgrid is defined as:

$$S = \alpha x_1 + x_2 = Jx \quad (4.29)$$

Where, $J = [\alpha, \quad 1]$, $x = [x_1, x_2]$ and α is sliding coefficient (control parameter) of $n \times 1$ dimension which is to be designed. This sliding surface ($n \times 1$ dimension) is used as a boundary condition to divide the phase plan into two regions. First is named as reaching phase and second as sliding phase. In the reaching phase,

controller will take decisions to direct the system trajectories to converge on the sliding surface irrespective of initial condition. When the system trajectories reach within the locality of sliding surface, it enters in the sliding phase mode. Here, controller will take decision to maintain the system trajectories within the locality of sliding surface and eventually system reaches the origin as desired. In this state, the system is said to be stable (i.e., $x_1 = 0$ and $x_2 = 0$).

4.10.1.2 Control Law

Control law u which adopts the switching states is defined as:

$$u = \frac{1}{2}(1 + \text{sign}(S)) = \begin{cases} U^+ & \text{when } S > 0 \\ U^- & \text{when } S < 0 \end{cases} \quad (4.30)$$

Where, u is of $n \times 1$ dimension. The task of control law is to decide the state of U^+/U^- by selecting proper value of α such that it obeys hitting, existence and stability conditions for all operating conditions of system.

4.10.1.3 Hitting Condition

To design hitting condition of the modeled dc microgrid system, the state variable x_1 is sufficient to consider which plays predominant role in the configuration of S in reaching phase. Apparently, the value of S is positive if the sensed voltage is lower than the desired reference voltage and the action required is to turn-on the switch of the dc to dc converter so that the energy is transferred to the inductor. Conversely, the value of S is negative if the sensed voltage is higher than the desired reference voltage and the action required is to turn-off the switch of the dc to dc converter. The resulting control function which formulate the bases of hitting condition is given as:

$$u = \begin{cases} 1 = ON & \text{when } S > 0 \\ 0 = OFF & \text{when } S < 0 \end{cases} \quad (4.31)$$

Above hitting condition is the requirement that the system trajectories will eventually reach the sliding surface S .

4.10.1.4 Existence Condition

For the switching states U^+/U^- defined in hitting condition, it cannot be ensured that the system trajectories will remain within the locality of sliding surface. To ensure system trajectories remain on sliding surface, the existence condition which is the requirement for asymptotic stability must be obeyed [72, 77]. According to the Lyapunov's second method [72], the existence condition is defined as:

$$\lim_{S \rightarrow 0} S \cdot \dot{S} < 0 \quad (4.32)$$

After differentiating (4.29), \dot{S} is given as:

$$\dot{S} = \alpha \dot{x}_1 + \dot{x}_2 = J\dot{x} \quad (4.33)$$

Substituting the \dot{x}_1 and \dot{x}_2 from (4.24e) into (4.33), the result can be expressed as:

$$\begin{aligned} \dot{S} &= \alpha x_2 - L^{-1}C^{-1}x_1 - (R_L^{-1}C^{-1} + R_b^{-1}C^{-1}M^T M)x_2 \\ &\quad - L^{-1}C^{-1}\beta v_i u + L^{-1}C^{-1}V_{ref} = J\dot{x} \end{aligned} \quad (4.34)$$

After substituting \dot{S} in (4.32), it becomes as:

$$\dot{s} = \begin{cases} J\dot{x} & \text{for } 0 < S > q \\ J\dot{x} & \text{for } -q < S < 0 \end{cases} \quad (4.35)$$

Where, q is a random small positive value. The existence condition in (4.32) can be arranged as:

$$\begin{aligned} \xi_1 &= (\alpha - (R_L^{-1}C^{-1} + R_b^{-1}C^{-1}M^T M))x_2 - L^{-1}C^{-1}x_1 \\ &\quad + L^{-1}C^{-1}(V_{ref} - \beta v_i) < 0 \end{aligned} \quad (4.36a)$$

$$\begin{aligned} \xi_2 = (\alpha - (R_L^{-1}C^{-1} + R_b^{-1}C^{-1}M^T M))x_2 - L^{-1}C^{-1}x_1 \\ + L^{-1}C^{-1}V_{ref} > 0 \end{aligned} \quad (4.36b)$$

where,

$$\xi = \begin{cases} \xi_1 = J\dot{x} & \text{for } 0 < S > q \\ \xi_2 = J\dot{x} & \text{for } -q < S < 0 \end{cases} \quad (4.36c)$$

For the existence of the SM operation, the sliding coefficient must be selected to obey the inequalities expressed in (4.36a) and (4.36b). The operating condition of source-j shown in Fig. 4.13 (dc to dc buck converter) is $0 \leq v_j \leq v_i$ and the region in which the trajectories of the system will be bounded is $V_{ref} - \beta v_i < x_1 < V_{ref}$.

4.10.1.5 Stability Condition

The stability condition of SM is to ensure that system trajectories will always be directed towards the stable equilibrium point during sliding phase. The sliding coefficient and control action must obey this condition. For the presented model of dc microgrid, motion equation can be obtained by putting $S = 0$ as:

$$S = \alpha x_1 + x_2 = 0 \quad (4.37)$$

Substituting $x_2 = \dot{x}_1$ from (4.24a) into (4.37), it becomes as:

$$\alpha x_1 + \dot{x}_1 = 0 \quad (4.38)$$

This is first order linear differential equation and its solution can be written as:

$$x_1(t) = x_1(t_0)e^{-\alpha(t-t_0)} \quad (4.39)$$

Where, $x_1(t_0)$ is voltage error at time t_0 . It is clear from equation (4.39) that α controls the system dynamic response and it is selected by applying Hurwitz stability condition [61]. Hence to control the system dynamic response, it is sufficient to select α as:

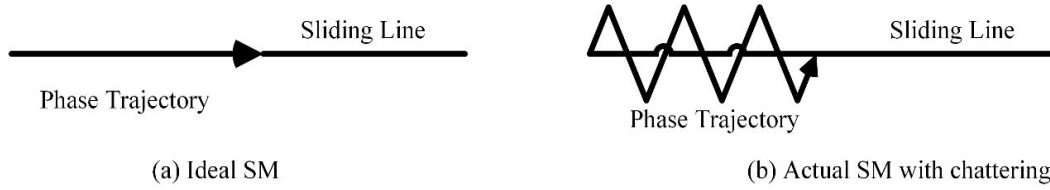


FIGURE 4.14: Phase trajectories for (a) ideal SM; (b) actual SM with chattering

$$\alpha = \frac{1}{\tau} = \frac{1}{R_L C} \quad (4.40)$$

Where, τ is time constant of the system response. The value of α can be increased and reduced for fast and slow dynamic response, if the existence condition is met. While, α must be selected a positive value for system stability. For negative α , system trajectories will move away from the equilibrium point in phase plane.

4.10.1.6 Sliding Mode Hysteresis Control

In ideal SM, the dc to dc converter will be switched at infinite frequency when the system trajectories enter in the sliding phase as shown in Fig. 4.14(a). But the actual switch will experience some switching time delay and switching imperfections. Due to this ideal SM is not possible. It will initiate a specific dynamic behavior in the locality of sliding surface which is recognized as chattering as shown in Fig. 4.14(b). If the produced chattering is not controlled, the system will start fluctuating at a high frequency. This behavior of the system is not desired because it will produce high switching losses. Furthermore, in the presence of chattering the exact switching frequency cannot be predicted. Hence, the component selection and system design will be difficult. To solve the aforementioned issues, a hysteresis band is introduced in the switching law and redefined as:

$$u = \begin{cases} 1 = \text{"ON"} & \text{when } S < -k \\ 0 = \text{"OFF"} & \text{when } S > k \\ \text{Unchanged} & \text{Otherwise} \end{cases} \quad (4.41)$$

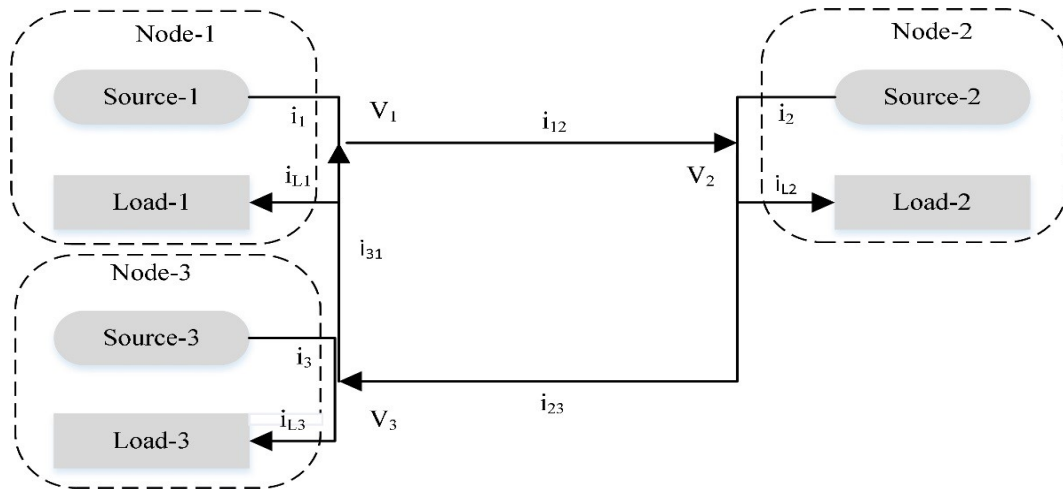


FIGURE 4.15: Three-source dc microgrid

Where, k is small positive quantity. This hysteresis band is commonly used to improve the effect of chattering in SMC. In this method, the switch of dc to dc converter will turn-on when $S < -k$ and turn-off when $S > k$. In the band $k \leq S \leq -k$, the state of the converter remains unchanged and it will maintain its previous state. Therefore, introducing band $k \leq S \leq -k$, the exact value of the switching frequency can be measured and controlled by varying the values of k .

4.11 Simulation Results and Discussion

A three-source dc microgrid system as shown in Fig. 4.15 is simulated using MATLAB/Simulink. Each source consists of a voltage controlled dc to dc converter. The parameters used for dc to dc converter are given in Table 4.1.

4.11.1 Results using Droop Control

The detail of nodes and connecting cables is given in Table 4.2 and 4.3. respectively. Each source using droop control is shown in Fig. 4.16.

To observe the steady state node voltages, a three-source dc microgrid as shown in Fig. 4.15 is simulated and shown in Fig. 4.17. Source 1, 2 and 3 are simulated with

TABLE 4.1: DC to dc converter parameters

| Parameters | Values |
|---------------------|--------------|
| Desired voltage | 400 V |
| Rated power | 100 kW |
| Switching frequency | 10 kHz |
| Inductor L | 100 μH |
| Capacitor C | 4000 μF |

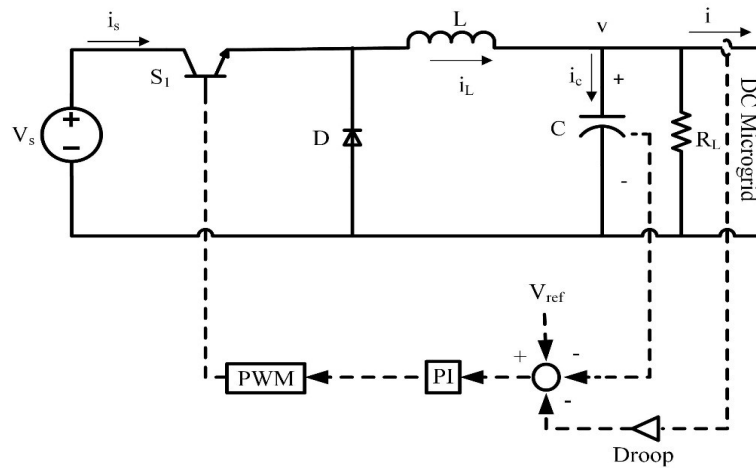


FIGURE 4.16: Voltage controlled dc to dc buck converter using droop control

TABLE 4.2: Node parameters of dc microgrid

| Parameters | Node-1 | Node-2 | Node-3 |
|-------------------------|---------------|--------------|--------------|
| Desired nominal voltage | 400 V | 400 V | 400 V |
| Source rated power | 60 kW | 80 kW | 110 kW |
| Load rated power | 40 kW | 50 kW | 75 kW |
| Droop gains | 0.04 Ω | 0.4 Ω | 1.9 Ω |
| Voltage deviation | $\leq 5\%$ | $\leq 5\%$ | $\leq 5\%$ |

TABLE 4.3: Connecting line parameters of dc microgrid

| Parameters | Branch-12, Branch-23, Branch-31 |
|------------------------|--------------------------------------|
| Current rating | 200 A |
| Cable type | 1-Conductor Al-PVC185mm ² |
| Resistance (per meter) | 0.152 m Ω |
| Cable length | 1000 meters |

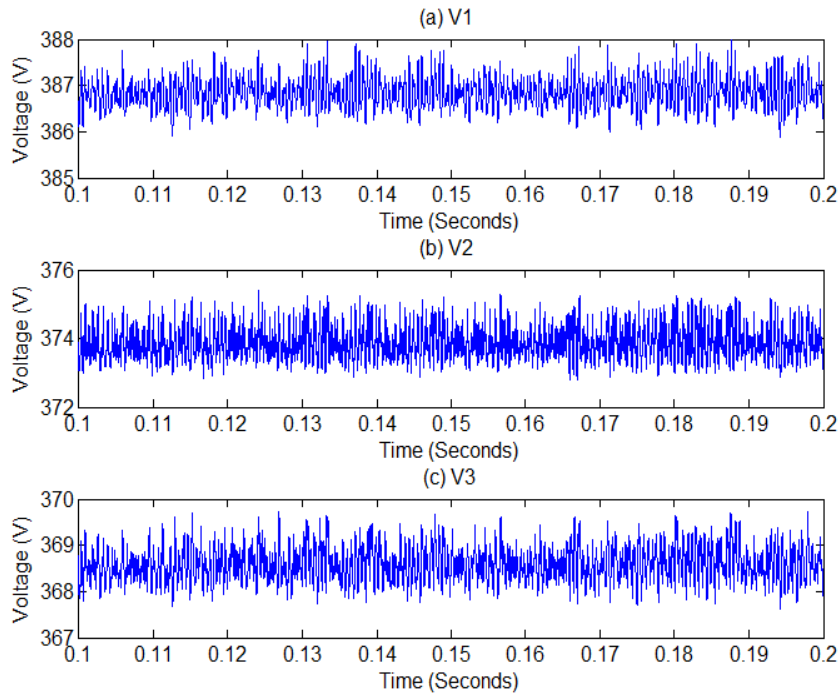
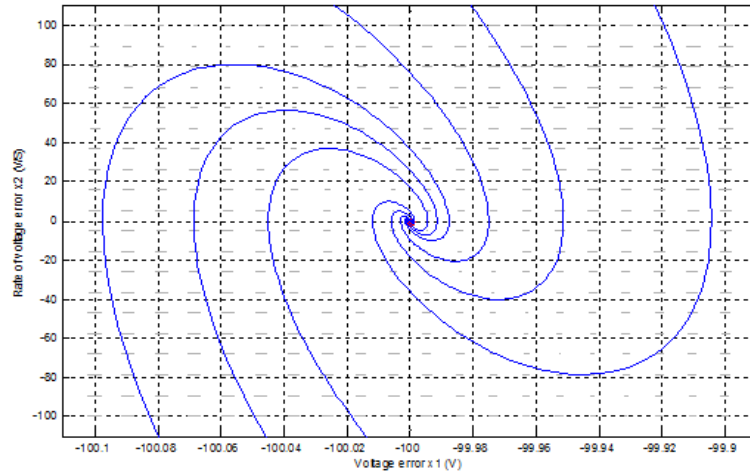
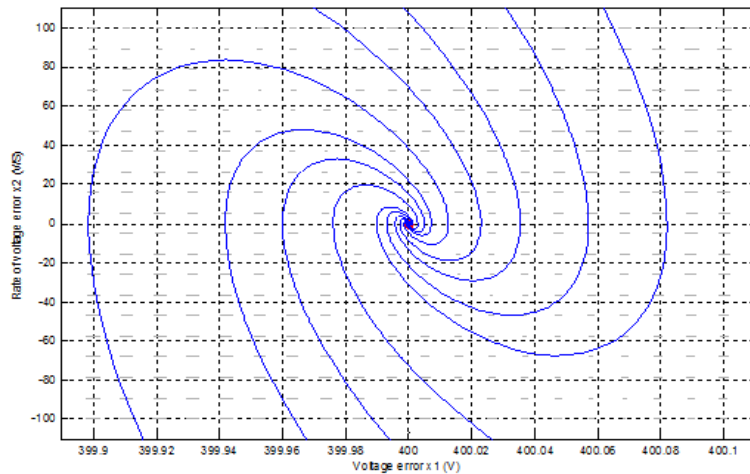


FIGURE 4.17: Node voltages using droop control in (a) with droop 0.04Ω (b) with droop 0.4Ω and (c) with droop 1.9Ω

droop gains 0.04Ω , 0.4Ω and 1.9Ω respectively. The voltage deviations observed at node 1, 2 and 3 are 3.25%, 6.25% and 7.86% respectively. This shows that good voltage regulation is ensured with small droop values. For large droop values, poor voltage regulation is observed which is not acceptable to loads. Hence droop controlled dc microgrid involves voltage regulation tradeoff.

4.11.2 Results using Sliding Mode Control

The dynamics of dc microgrid system modeled in (4.24e) are graphical presented in phase plane plot with $u = 1$ and $u = 0$, as shown in Fig. 4.18 and 4.19 respectively. Fig. 4.18 shows that phase trajectories with $u = 1$ which are converged to the equilibrium point $(x_1 = V_{ref} - \beta v_i, x_2 = 0)$ for any starting condition after some finite time. Similarly, Fig. 4.19 with $u = 0$ converged to the equilibrium point $(x_1 = V_{ref}, x_2 = 0)$ as presented in (4.36).

FIGURE 4.18: Phase trajectories with $u = 1$ FIGURE 4.19: Phase trajectories with $u = 0$

Each source using SM hysteresis control is shown in Fig. 4.20 . To observe the steady state node voltages, dc microgrid shown in Fig. 4.15 is simulated using hysteresis modulation based SMC and is shown in Fig. 4.21. The voltage deviation observed is 0.125% under the nominal operating conditions which is significantly improved from droop controlled dc microgrid. This shows good steady state performance of the system using SMC.

Fig. 4.22 shows graph of average node voltage of source 1 against hysteresis band k for load resistance of 2 and 6 Ω . For small values of k i.e., high switching frequency, voltage deviation is small and regulation is more accurate. For large k i.e., low switching frequency (increased chattering), voltage deviation is increased. Hence, small k ensures tight voltage regulation. To validate robustness of SMC, average

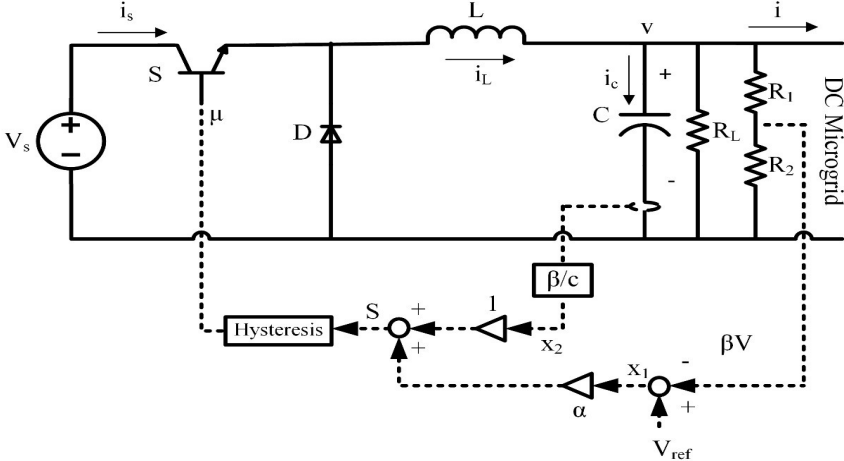


FIGURE 4.20: Voltage controlled dc to dc buck converter using SM hysteresis control

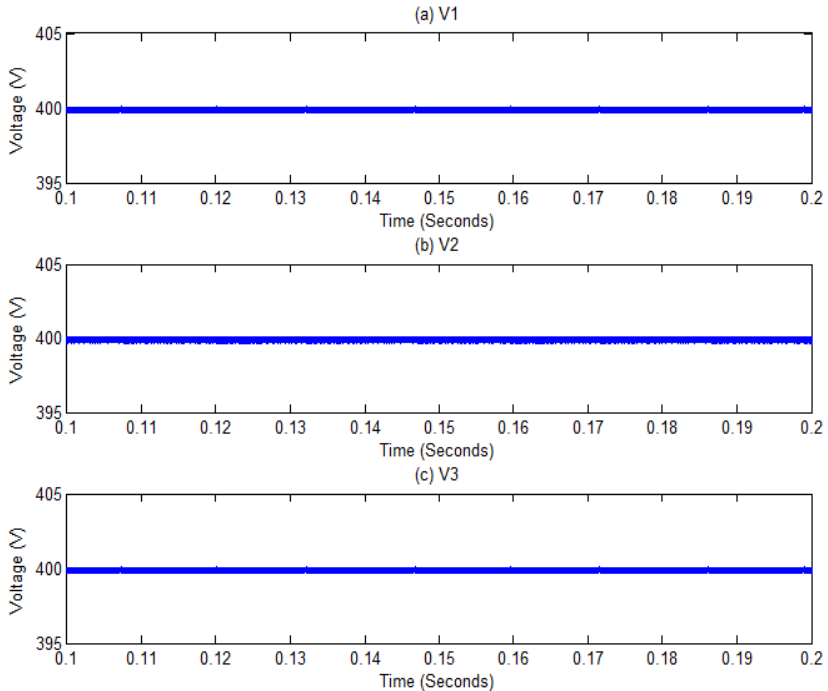
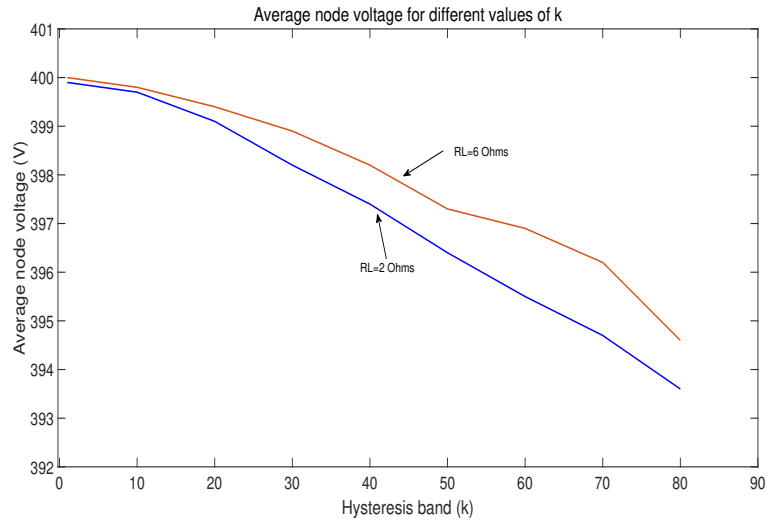
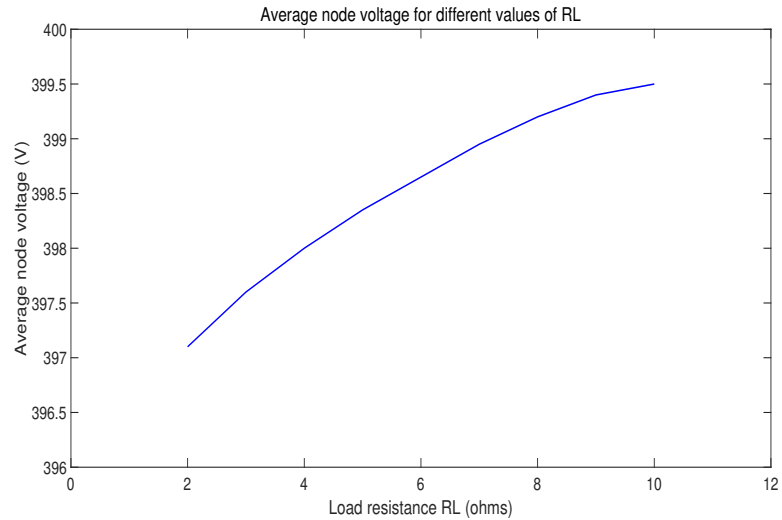


FIGURE 4.21: Node voltages using hysteresis modulation based SMC

FIGURE 4.22: Average node voltage for different values of k FIGURE 4.23: Average node voltage for different values of R_L

node voltage is plotted for load resistance in range $2\Omega \leq R_L \leq 10\Omega$ and shown in Fig. 4.23. It concludes that voltage regulation is robust with only a $2.9V$ (0.725%) deviation for entire range i.e., voltage regulation $\frac{dv}{dR_L}$ averages at $0.29 \frac{V}{\Omega}$.

To see the effect of source power variation on node voltages, Per Unit (p.u.) power at source 1 and 2 are varied as shown in Fig. 4.24. Fig. 4.25 shows node voltages with the variation in source power. SMC shows the satisfactory behavior of the node voltages with the variation in source power. This confirms the stability of SMC.

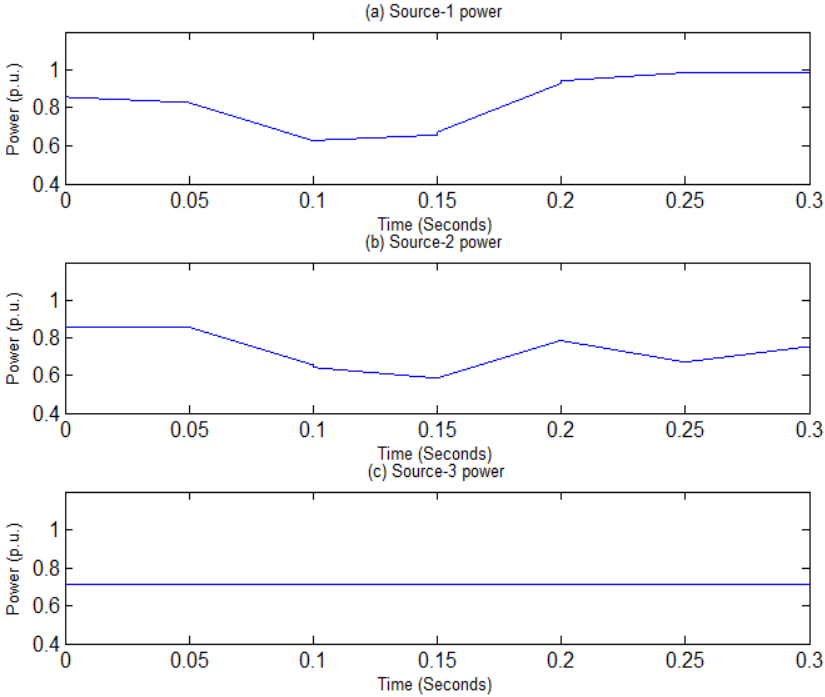


FIGURE 4.24: Source power variations applied to dc microgrid

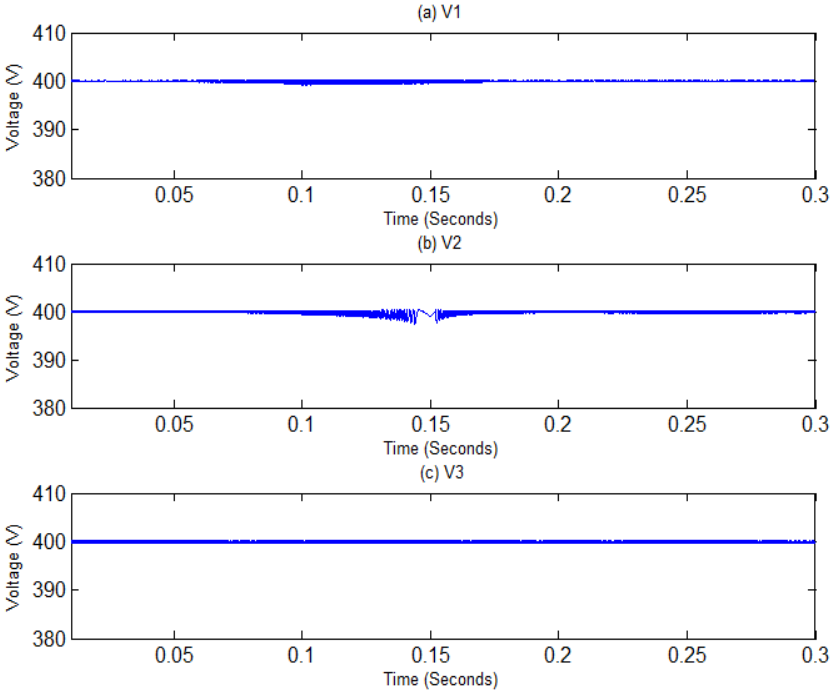


FIGURE 4.25: Node voltages with the variation in source power

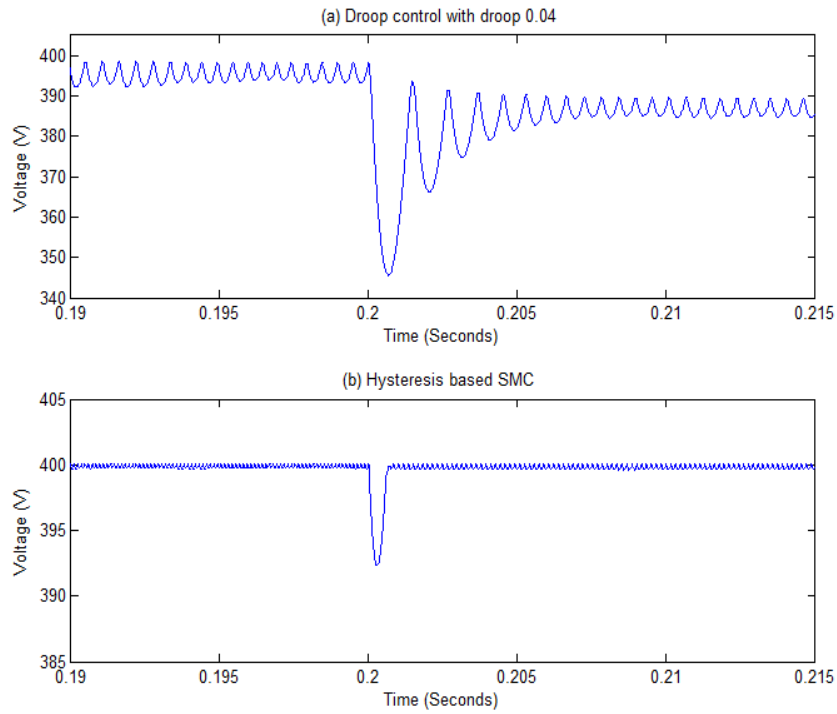


FIGURE 4.26: Transient response when a step load is applied to dc to dc converter at $0.2s$

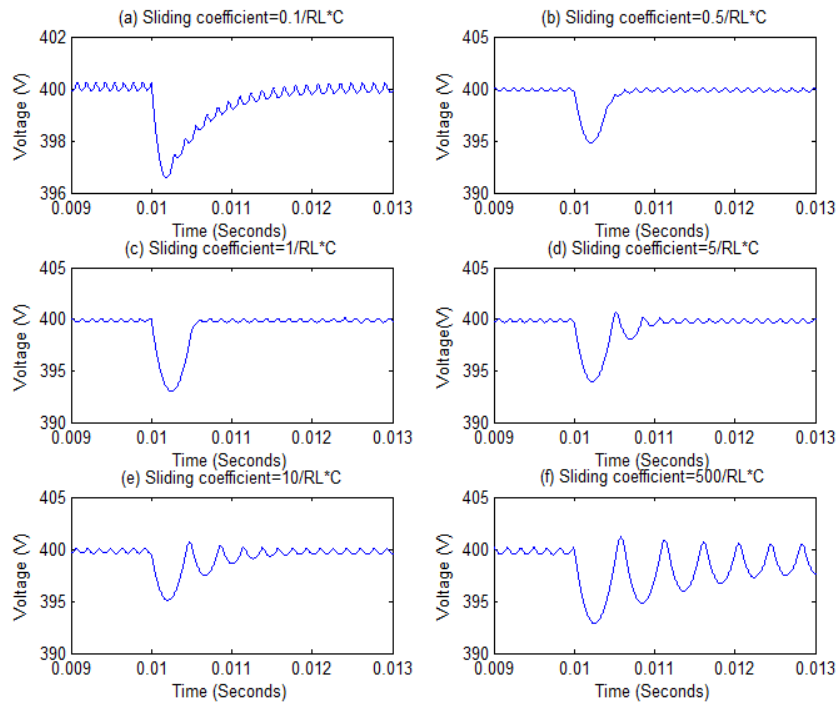


FIGURE 4.27: Output voltage when step load is changed from $R_L = 6.4\Omega$ to $R_L = 1.6\Omega$ with different values of α

TABLE 4.4: Dynamic behavior with different values of α

| Sliding Coefficient α | Output Voltage Ripple | Settling Time |
|------------------------------------|------------------------------------|---------------|
| $\alpha = \frac{0.1}{R_{L(nom)}C}$ | 0.4V (0.1% of desired voltage) | 2ms |
| $\alpha = \frac{0.5}{R_{L(nom)}C}$ | 0.39V (0.0975% of desired voltage) | 0.75ms |
| $\alpha = \frac{1}{R_{L(nom)}C}$ | 0.39V (0.098% of desired voltage) | 0.5ms |
| $\alpha = \frac{5}{R_{L(nom)}C}$ | 0.48V (0.12% of desired voltage) | 1ms |
| $\alpha = \frac{10}{R_{L(nom)}C}$ | 0.48V (0.14% of desired voltage) | 2ms |
| $\alpha = \frac{100}{R_{L(nom)}C}$ | 1.85V (0.46% of desired voltage) | 5ms |

To observe and compare the transient response using droop control and hysteresis based SMC, a step change in load is applied to the dc to dc buck converter which is operating at nominal load. Fig. 4.26 shows that a step load of 250 ampere is applied at 0.2s. The transient settling time observed in droop controlled converter is 10ms. Whereas, the settling time in hysteresis based SMC is 0.5ms which is significantly lower than the droop controlled. In droop controlled converter, voltage dip of 50V is observed after step change at 0.2s. Whereas in hysteresis based SMC, voltage dip of 8V is observed which is significantly lower value than the droop control. This verifies the better transient response of the SMC. Further, the dynamic behavior of the dc to dc converter with different sliding coefficient is also investigated. Fig. 4.27(a) to Fig. 4.27(f) show the output voltage when the load resistance is altered from $R_L = 6.4\Omega$ to $R_L = 1.6\Omega$ with sliding coefficients: (a) $\alpha = \frac{0.1}{R_L C}$; (b) $\alpha = \frac{0.5}{R_L C}$; (c) $\alpha = \frac{1}{R_L C}$; (d) $\alpha = \frac{5}{R_L C}$; (e) $\alpha = \frac{10}{R_L C}$; and (f) $\alpha = \frac{500}{R_L C}$, respectively. The results of settling time and output voltage ripple are summarized in Table 4.4.

It can be observed that as α is increased up to $\frac{1}{R_L C}$, the dynamic response is improved with smaller settling time. The settling time increases as α is increased beyond $\frac{1}{R_L C}$. The response is in good agreement with the presented theory. The fast-dynamic response is achieved at $\alpha = \frac{1}{R_L C}$. However, if α is increased too high, the system will become unstable.

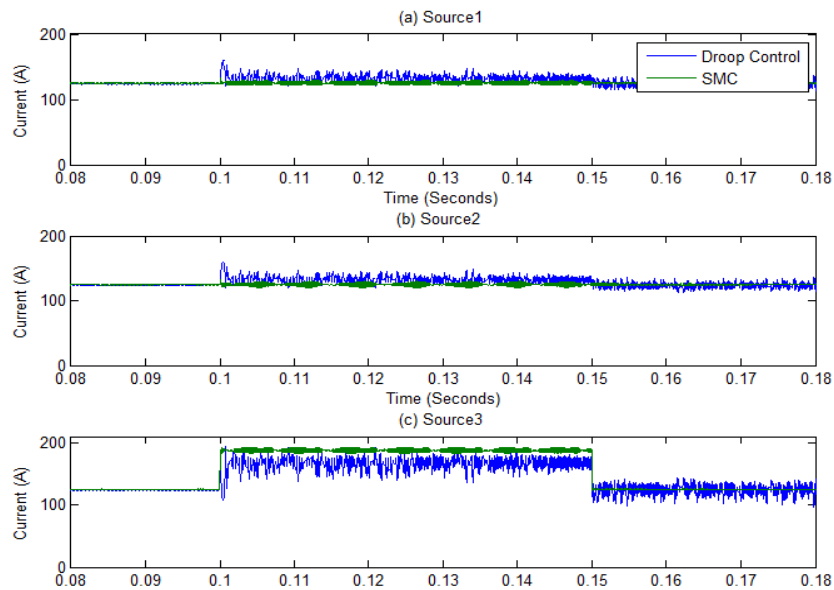


FIGURE 4.28: Source currents for step change in power of load-3

To view the source currents of dc microgrid at a step load, load power at node-3 is changed from $50kW$ to $75kW$ at $0.1s$ and $75kW$ to $50kW$ at $0.15s$. Source currents using droop control and hysteresis based SMC are shown in Fig. 4.28. Overshoot and oscillations are observed in source currents using droop control which are significantly small in SMC. This confirms the stability of SMC over droop control. It is further observed that current sharing error among three sources is 13%. There are different schemes presented in literature for load sharing. The modeling and analysis presented in this paper is also valid for these schemes.

A dc microgrid with eight sources as shown in Fig. 4.29 is simulated to validate the performance of proposed SM controller for more sources. The specifications are given in Table 4.5. Fig. 4.30 and 4.31 show that observed voltage deviations at each node is less than 1%. This validate the performance of SMC for more sources in a dc microgrid.

TABLE 4.5: Node parameters of dc microgrid with eight sources

| Nodes | Desired voltage | Load power | Connecting lines |
|--------|-----------------|------------|---------------------------|
| Node-1 | 400 V | 10 kW | $R_{line12} = 1.5m\Omega$ |
| Node-2 | 400 V | 20 kW | $R_{line23} = 4.5m\Omega$ |
| Node-3 | 400 V | 30 kW | $R_{line36} = 6m\Omega$ |
| Node-4 | 400 V | 40 kW | $R_{line14} = 3m\Omega$ |
| Node-5 | 400 V | 50 kW | $R_{line45} = 7.5m\Omega$ |
| Node-6 | 400 V | 60 kW | $R_{line67} = 10m\Omega$ |
| Node-7 | 400 V | 70 kW | $R_{line78} = 11m\Omega$ |
| Node-8 | 400 V | 80 kW | $R_{line58} = 9m\Omega$ |

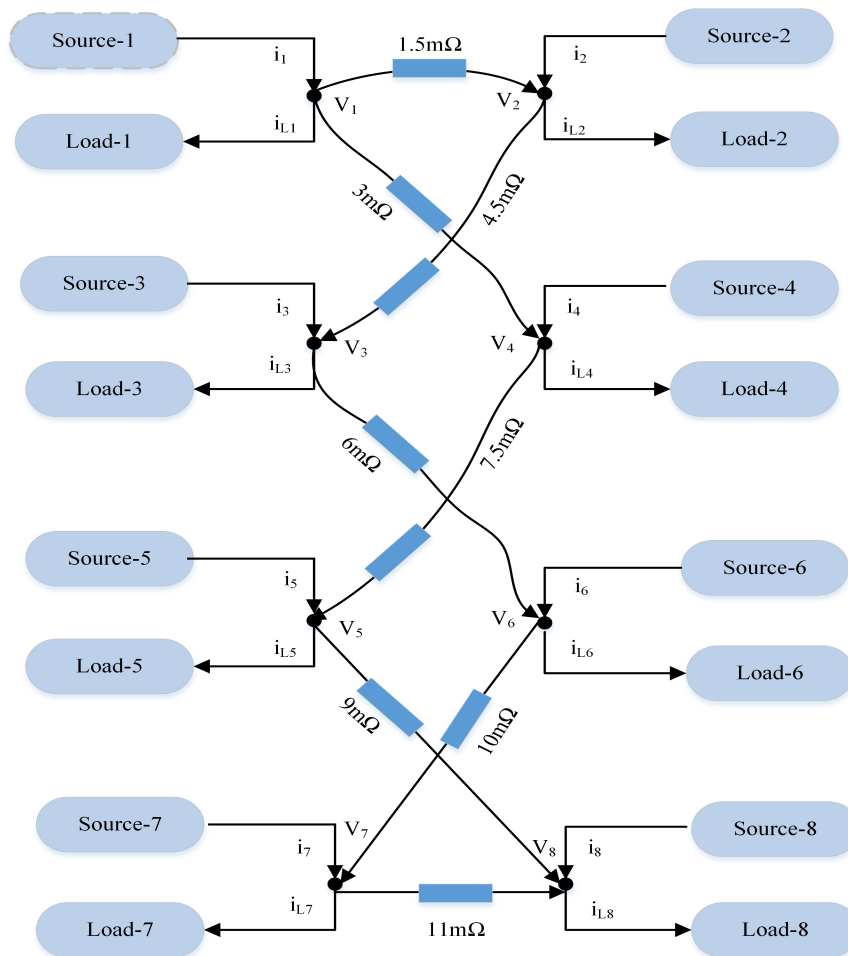


FIGURE 4.29: A dc microgrid with eight sources

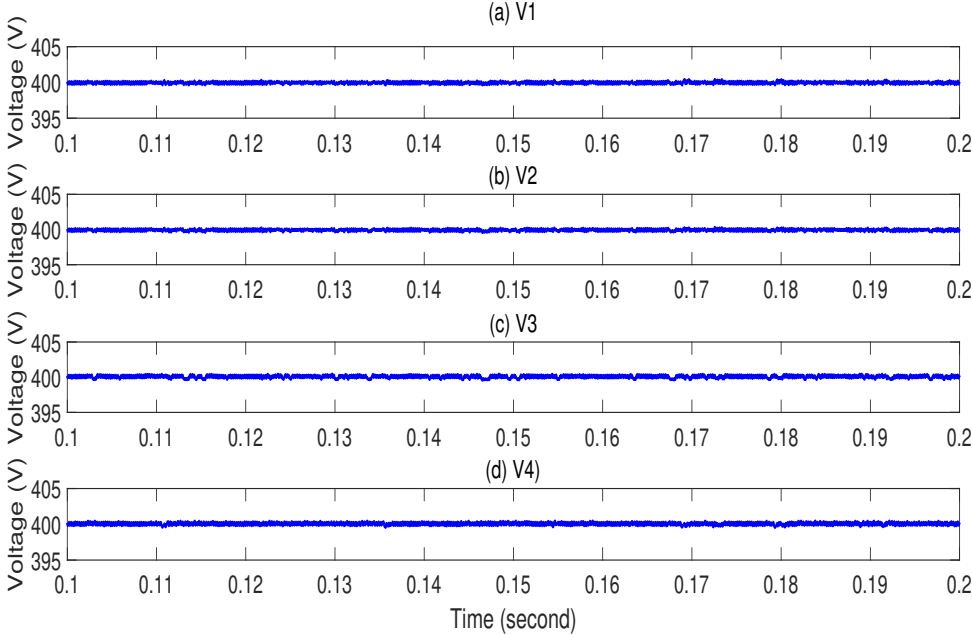


FIGURE 4.30: Node voltages V1, V2, V3 and V4

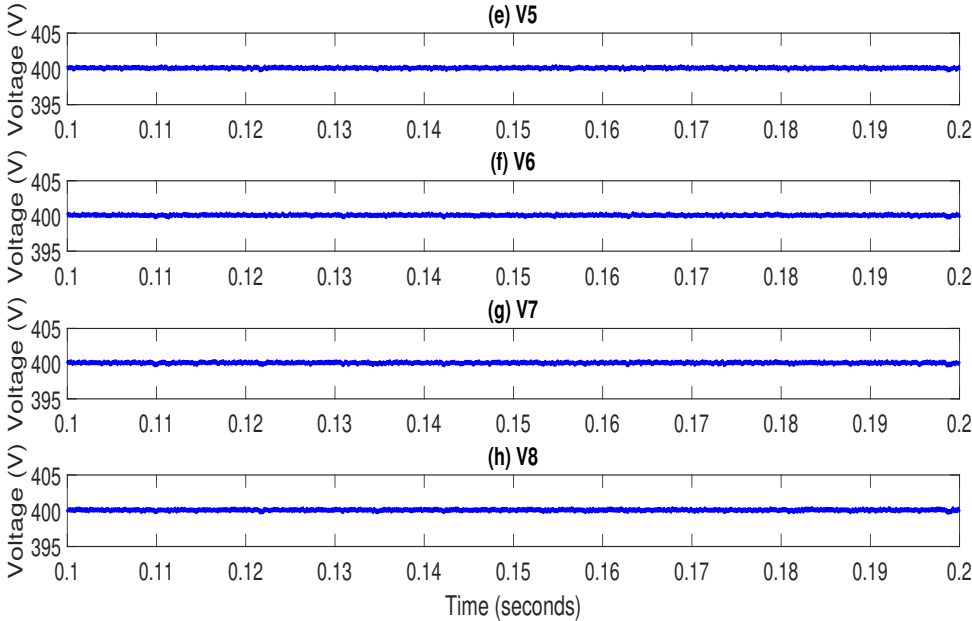


FIGURE 4.31: Node voltages V5, V6, V7 and V8

TABLE 4.6: Parameters of experimental setup

| Parameters | Values |
|-----------------------|-----------------|
| Desired voltage | 12V |
| Switching frequency | 10kHz |
| Inductor L | 150 μ H |
| Capacitor C | 1000 μ F |
| Connecting resistance | 0.0181 Ω |
| Load powers | 10, 15W |

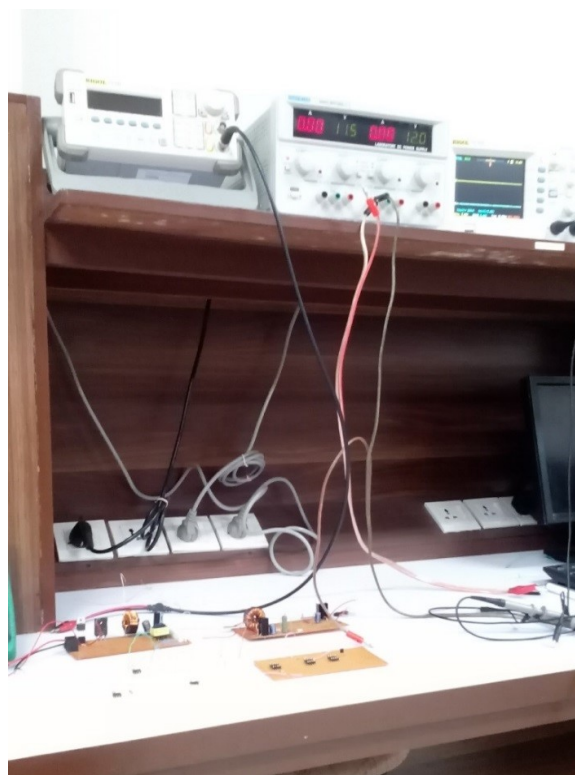


FIGURE 4.32: Small scale experimental setup

4.12 Experimental Setup

A small scale experimental setup of two source dc microgrid is established to observe the steady state behavior of SM hysteresis controller and is shown in Fig. 4.32. Parameters of this system are shown in Table 4.6.

4.12.1 Hardware Design Procedure

The calculation of hardware components for practical realization of small scale dc microgrid is presented in this section. Each source is voltage controlled dc to dc converter in a dc microgrid. Fig. 4.33 shows schematic diagram of each source with dc to dc buck converter using hysteresis based SMC. In SM, controller contains circuits of a differential amplifier U_V , a voltage follower U_i , a difference amplifier U_D and a Schmitt Trigger U_S with non-inverting configuration. A voltage divider circuit is used for feedback sensing of output voltage. Furthermore, a current sensor with low resistance is employed in series with filter capacitor to sense capacitor current i_C .

- Voltage Divider Circuit (β)

Setting $V_{ref} = 3.3V$, β can be calculated as:

$$\beta = \frac{V_{ref}}{V_d} = \frac{3.3}{1.2} = 0.275 \quad (4.42)$$

Where, V_d is desired voltage. For R_1 and R_2 , it can be expressed as:

$$R_2 = \frac{\beta}{1 - \beta} R_1 \quad (5.43)$$

Selecting $R_1 = 270\Omega$, the value of R_2 is 330Ω .

- Differential Amplifier Gain (U_V)

In the sliding surface design, continuous assessment of the state variables x_1 and x_2 is required in SM operation. Since, $x_2 = \dot{x}_1$, it is difficult to realize the time derivative of state variable using analogue components. Therefore, the sliding surface in (4.29) needs to be redefined to address this problem. Substituting (4.21a), (4.21d) and (4.40) into (4.29), the sliding surface can be expressed as:

$$S = K_{P1}(V_{ref} - \beta v) + K_{P2}i_c \quad (4.44)$$

Where, $K_{p1} = \frac{1}{R_L C}$ and $K_{p2} = -\frac{\beta}{C}$.

In (4.44), $V_{ref} - \beta v$ and i_C are feedback variables which are amplified by K_{p1} and K_{p2} . From a practical view point, the output capacitance of the converter is usually in the range of microfarads (μF) and its inverse will be significantly large value than β and R_L . This will increase overall gains K_{p1} and K_{p2} too high that feedback signal can enter in to saturation region. Hence, (4.44) may provide unreliable signal which will become difficult for practical implementation. To address aforementioned problem, the sliding surface is redefined as:

$$S = \frac{C}{\beta} \alpha x_1 + \frac{C}{\beta} x_2 = Qx \quad (4.45)$$

Where, $Q = [\frac{C}{\beta} \alpha \quad \frac{C}{\beta}]$ and $x = [x_1 \quad x_2]$. Substituting (4.21a), (4.21d) and (4.40) into (4.45), sliding surface can be expressed as:

$$S = \frac{1}{\beta R_L} (V_{ref} - \beta v) + i_c \quad (4.46)$$

The sliding surface in (4.46) shows that S becomes independent of capacitance C which will significantly reduce the amplification gain of feedback signal. The gain required in (4.46) is $\frac{1}{\beta R_L}$. Setting $R_L = R_{L(nom)}$, then R_{V1} and R_{V2} are related as:

$$R_{V1} = (\beta R_{L(nom)}) R_{V2} \quad (4.47)$$

Selecting $R_{V2} = 20k\Omega$, we get R_{V1} as $30k\Omega$. All resistors R_{DIF} in difference amplifier shown in Fig 4.33 are set to $10k\Omega$.

- Hysteresis Band (k)

The value of k in hysteresis band as defined in (4.41) is selected based on the criteria reported in [42] and is given as:

$$k = \frac{V_d(1 - \frac{V_d}{V_i})}{2f_s L} \quad (4.48)$$

Where, f_s is switching frequency of converter. For converter parameters in Table 4.6, the calculated value of k is $2V(Hz^{-1})H^{-1}$.

- Schmitt Trigger (U_S)

Non-inverting Schmitt Trigger U_S configuration is expressed as:

$$2k = \frac{R_{ST1}}{R_{ST2}}(V_{cc}^+ - V_{cc}^-) \quad (4.49)$$

Where, V_{cc}^+ and V_{cc}^- are positive and negative voltage supplies. Selecting $R_{ST1} = 1k\Omega$, we get R_{ST2} as $6k\Omega$.

Fig. 4.34 shows the steady state node voltages of two-source dc microgrid. Voltage ripple of $0.5V$ is observed at node voltages. Voltage deviation observed is 2.5% which is comparatively high from simulated results due to the tolerance involved in the practical components, but it is less than 5%. This confirms the satisfactory performance of system. Fig. 4.35 shows control law u which is used to operate switch of dc to dc converter.

4.12.2 Practical Issues in Sliding Mode Implementation

- In SM, selecting a state variable is serious because having more variables leads to more sensing and computations which increase the complexity of the design.
- Choosing derivative and integral of state variables involve noise sensitivity and need to be indirectly controlled; e.g., $(\frac{dV_c}{dt})$ alternatively can be obtained by sensing capacitor current.
- Chattering produced is a big problem in SM. It produces excessive switching losses and limits the selection of switching device.
- Limitations of the analog components e.g., slew rate; saturation limits and bandwidth should be considered for the proper operation of the control.

4.13 Summary

First part of this chapter highlights theory and mathematical formulation of SMC. Minimum conditions for a system to show SM property are presented. In the second part of this chapter, voltage stability of dc microgrid using SMC is presented. Stability of the dc microgrid is key challenge in the presence of various distributed sources. Droop controllers are being used for stability of dc microgrids. Droop controllers suffer stability due to error in nominal voltages and load variations. Additionally, these controllers are realized through PI controllers which cannot ensure global stability of the desired equilibrium point. Moreover, it is difficult to optimize the controller parameters for different line and load variations. Hence, to use PI controllers for stability of dc microgrid is not feasible. Therefore, SMC is proposed for stability and better dynamic response in dc microgrid application.

To analyze stability and dynamic performance, mathematical model of a dc microgrid is derived. Controllability and stability conditions of modeled system are verified. Hitting, existence and stability conditions are verified using SMC. Modeled dynamics of system are graphically plotted which shows that system trajectories converge to equilibrium point. Detailed simulations of a three source microgrid are carried out to show the effectiveness of SM controller and results are compared with droop controller. In steady state condition, voltage regulation of 3.25%, 6.25% and 7.86% are observed with droop gains of 0.04Ω , 0.4Ω and 1.9Ω respectively. This shows that good voltage regulation is ensured with small droop values. For large droop values, poor voltage regulation is observed which is not acceptable to loads. Whereas, using SMC, voltage regulation observed is 0.125% which is significantly improved from droop controlled dc microgrid. This shows good steady state performance using SMC. The effect of transient on a step load is also investigated and observed settling time in droop control is $10ms$. While, the observed settling time in SMC is $0.5ms$ which is significantly lower than droop control. This confirms the transient performance of the proposed controller. Additionally, dynamic behavior of dc to dc converter with different sliding coefficients

is also investigated and results are presented. Moreover, a small scale practical setup is developed and results are presented in this chapter.

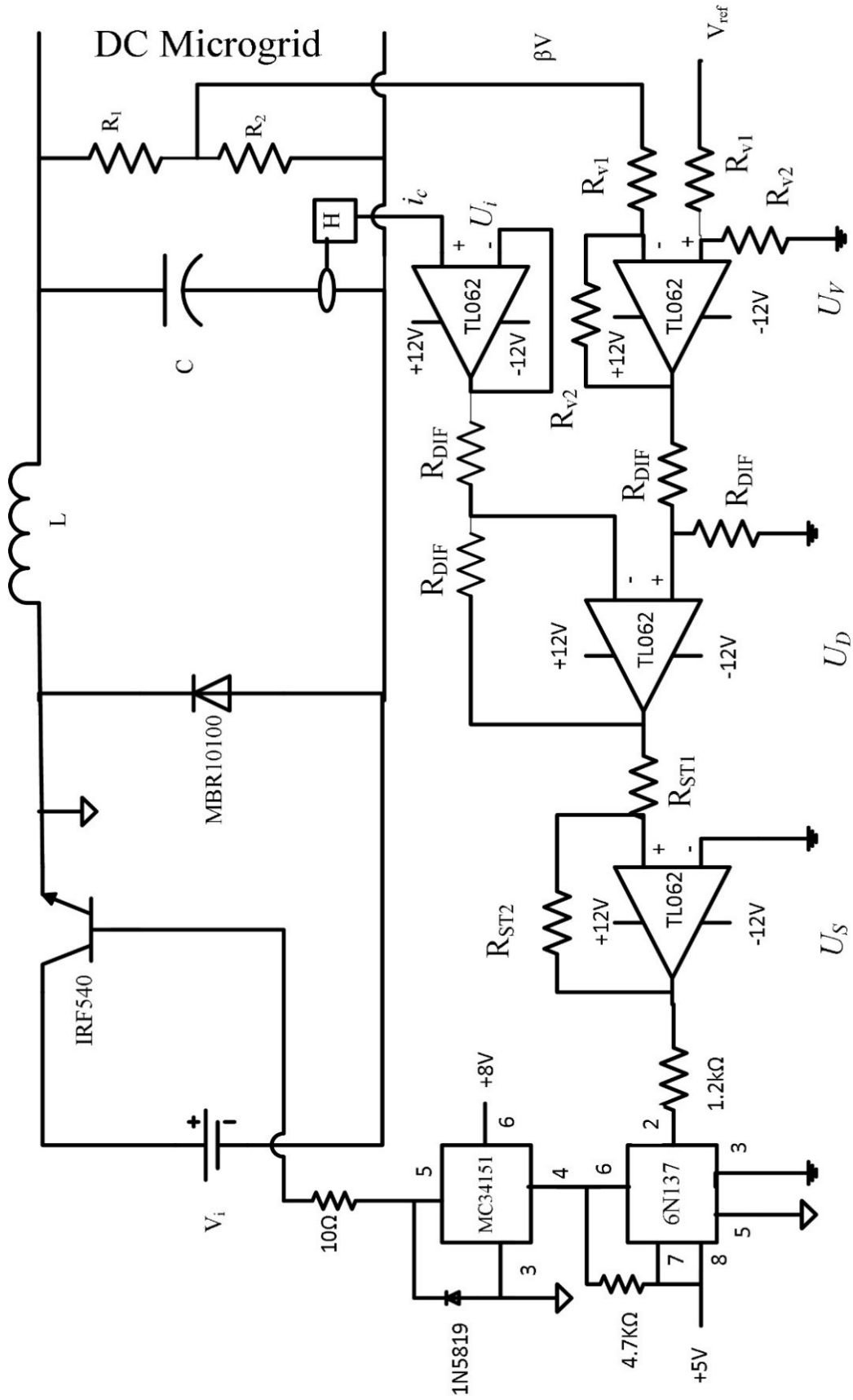


FIGURE 4.33: Voltage controlled dc to dc buck converter using hysteresis based SMC

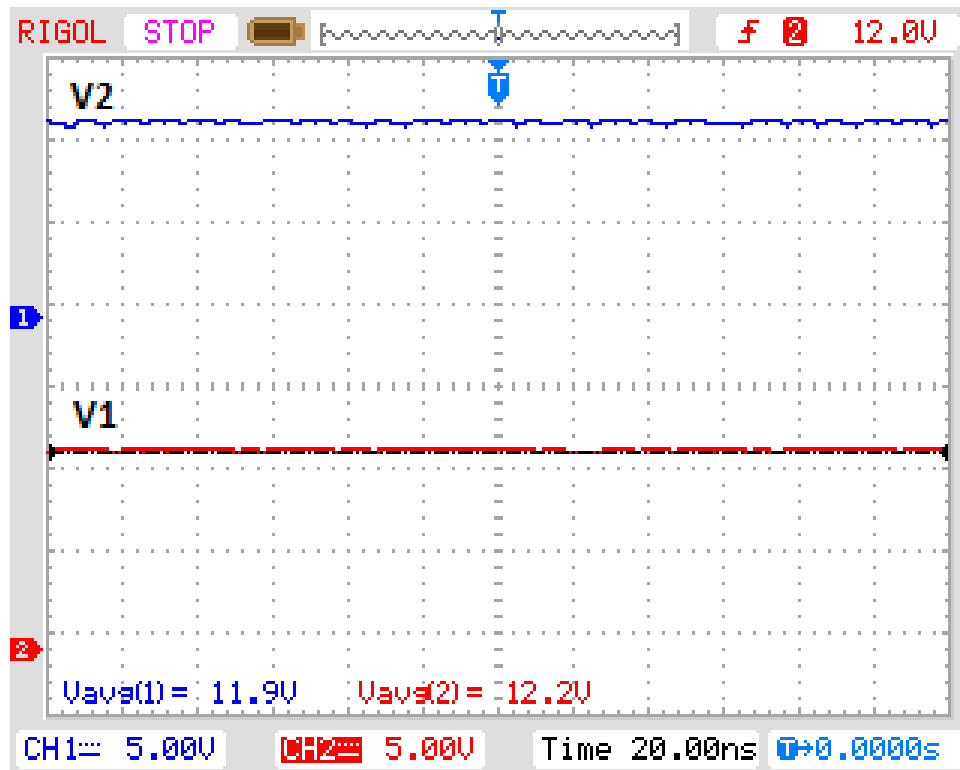


FIGURE 4.34: Experimental results: node voltages. Voltages: 10V/div, x-axis: 20ns/div

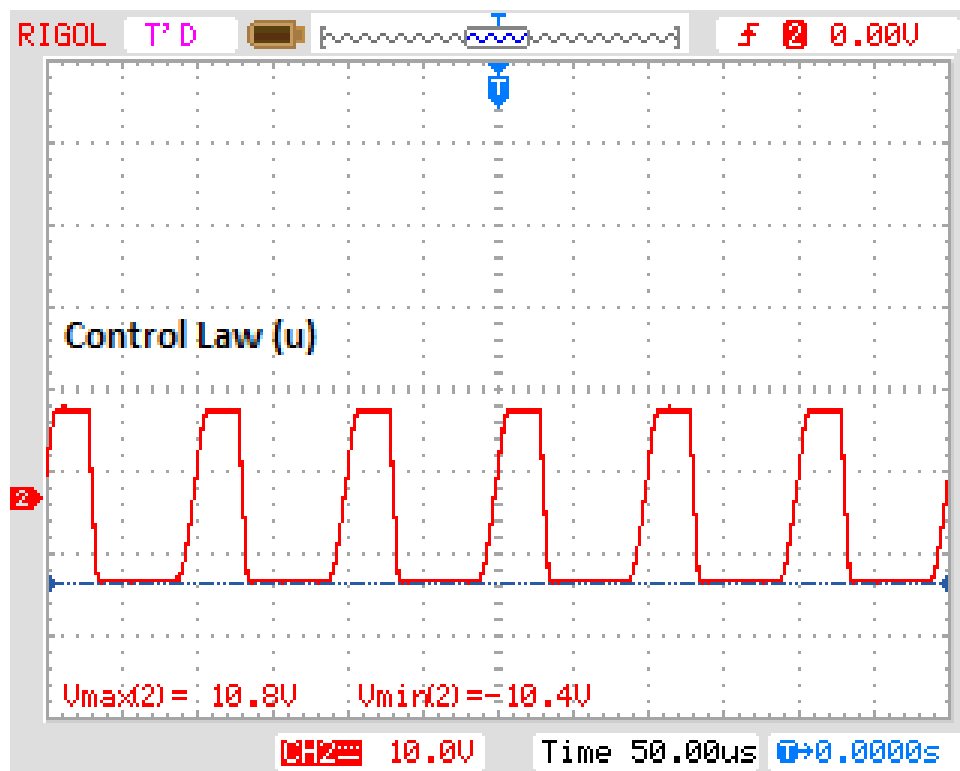


FIGURE 4.35: Experimental results: control law u . Voltages: 10V/div, x-axis: 50us/div

Chapter 5

Proportional Load Sharing using Sliding Mode Control

5.1 Overview

Distributed sources can be connected to the dc microgrid through power PECs in parallel configuration. It is required to find efficient control to coordinate among various sources, loads and energy storage. The key objectives of the parallel connected converter are: first objective is the stability of the dc microgrid as electronic loads are very sensitive to voltage deviation and second objective is load sharing among various sources [10], [146], [155, 156]. However, it is the nature of sources that only one unit can establish the voltage level in a paralleling system. The reason is that the output resistances of power sources are extremely low. Thus, even a small difference in the output voltage between the paralleled sources will cause the one that is a few mili volt higher to share all current. The lower the output voltage of the module, the more severe this problem is [20].

To address the aforementioned challenges as presented in chapter 3, decentralized control architecture is not effective to achieve these objectives simultaneously due to the voltage error and load power variation. Centralized control architecture can achieve these objectives using high bandwidth communication link. However, it

loses reliability due to the single point failure. Additionally, these controllers are realized through PI controllers which cannot ensure load sharing and stability in all operating conditions.

To address limitations, a distributed architecture using SM controller utilizing low bandwidth communication is proposed for dc microgrid in this chapter. Main advantages are high reliability, proportional load sharing and precise voltage regulation. Further, SM controller show high robustness, fast dynamic response and good stability for large load variations. To analyze the stability and dynamic performance, system model is developed and its transversality, reachability and equivalent control conditions are verified. Furthermore, the dynamic behavior of the modeled system is investigated for underdamped and critically damped response. Detailed simulations are carried out to show the effectiveness of the proposed controller.

5.1.1 Proposed Distributive Control Architecture

Disadvantages associated with the decentralized and centralized control can be adjusted using distributed control which is an alternative solution to achieve efficient load sharing. In distributed control, as a substitute of single central controller it is distributed among every PEC. Proposed distributive architecture for a source- j is shown in Fig. 5.1. To alleviate the deviation created by droop action, the voltage relationship of compensated droop action is given as

$$v_j^{ref} = v_j^o + \Delta v_j - i_j R_{dj} \quad (5.1)$$

Where, Δv_j is voltage shift which depends on the source current and v_j^o is no load voltage. As the source current increases, Δv_j should increase to compensate the effect created by $i_j R_{dj}$ and hence, making the reference voltage close to the source voltage. To find Δv_j , each source communicates its supplied current with the other utilizing controller area network (CAN) as a low bandwidth communication as shown in Fig. 5.1. Based on the communicated currents, the controller of each

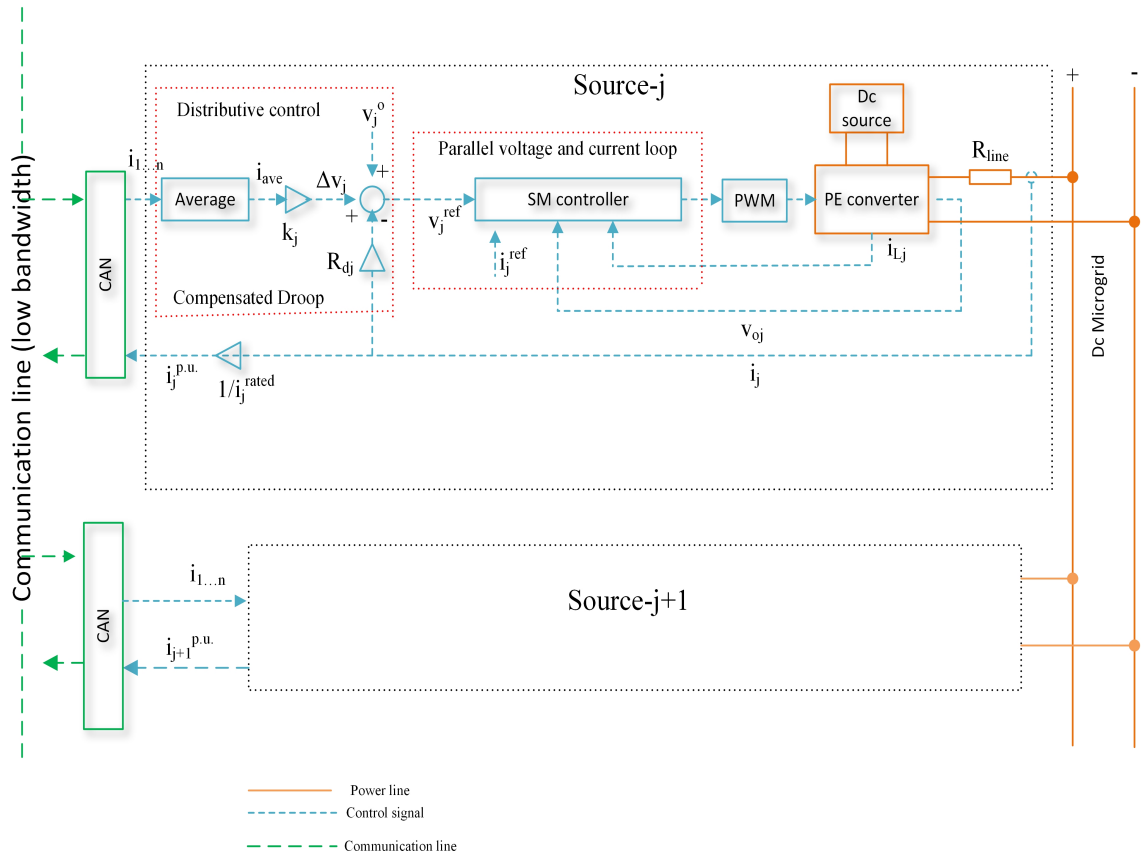


FIGURE 5.1: Distributive control architecture

source determines the average supplied current as

$$i_{ave}^{pu} = \frac{\sum_{m=1}^n i_j^{pu}}{n} \quad (5.2)$$

Where, i_j^{pu} is $p.u.$ current of source- j and n is number of sources. Based on the information communicated to each source, the voltage shift Δv_j is determined using average current i_{ave}^{pu} as

$$\Delta v_j = k_j i_j^{rated} i_{ave}^{pu} \quad (5.2a)$$

Where, k_j and i_j^{rated} are shift gain and rated current of source- j respectively. In the architecture shown in Fig. 5.1, since the $p.u.$ current of each source is shared. Hence, the data transmitted over communication link by each source is of maximum 2 byte and total data transmitted is $2n$ bytes. Data read by each source is $2(n-1)$ bytes. Hence, the technique used for communication has to manage small

data, thus a low speed communication is feasible. So, CAN based communication is proposed for dc microgrid in this chapter.

5.2 Sliding Mode Control

Each source in dc microgrid consists of PEC. Linear controllers (*PI*, *PID*, lead-lag etc.) are being used to control PECs for load sharing objective in dc microgrids. These controllers require linearized model of the system which makes them difficult to show good power sharing performance and stability in all operating conditions. So, SM controller is alternatively proposed in [157–160] ensures stability in all operating conditions. Hence, in this paper, SM controller technique is proposed for proportional load sharing and stability of dc microgrid.

5.2.1 Modeling

A generalized dc microgrid architecture is presented in Fig. 1.1 of chapter 1. An equivalent model of one source with dc microgrid through dc to dc converter is shown in Fig. 5.2. Source is modeled as voltage source v_s with current i_s , whereas, dc bus of microgrid is modeled through capacitor C and its associated connecting line current i_{dc} . Source and dc microgrid are interfaced through dc to dc PEC.

The differential equations describing system dynamics of a one source as modeled in Fig. 5.2 are expressed in (5.3) and (5.4).

$$\frac{di}{dt} = \frac{-v_{dc} + uv_s}{L} \quad (5.3)$$

Where, $v_{dc} = v_{line} + v_G$

$$\frac{dv_{dc}}{dt} = \frac{i - i_{dc}}{C} \quad (5.4)$$

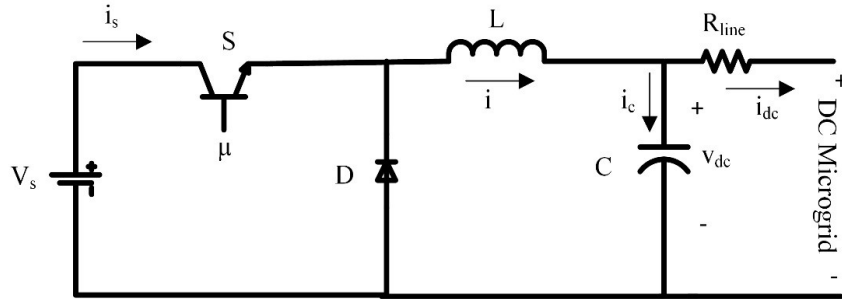


FIGURE 5.2: Equivalent model of one source with dc microgrid

Where, i , v_{dc} , v_{line} , v_G , i_{dc} , L and C are inductor current, bus voltage (capacitor voltage), connecting line voltage, grid voltage, line current, inductance and capacitance respectively. Whereas, u defines the switching state of the transistor switch which can be expressed as:

$$u = \begin{cases} 1 & \text{Switch is "ON"} \\ 0 & \text{Switch is "OFF"} \end{cases} \quad (5.5)$$

5.2.2 Sliding Mode Controller Analysis

In SM, most of the controllers include error of one or multiple states of the system in the sliding surface (e.g. inductor current or capacitor voltage) [161, 162]. Furthermore, some controllers include error and both the time derivative and integral of the error in the sliding surface to stabilize the system [158]. In this case, sliding surface can be represented as second order differential equation for which extensive mathematical analysis is required to guarantee system stability. Another surface is defined in [163] for the improvement in the steady state error and settling time which includes voltage error and square of capacitor current of the system.

This thesis proposes SM controller which is designed to achieve both proportional load sharing and dynamic stability of dc microgrid. The sliding surface is selected to ensure load sharing and precise voltage regulation. Thus, it is formed using the bus voltage error, current error and integral of the bus voltage error. In this

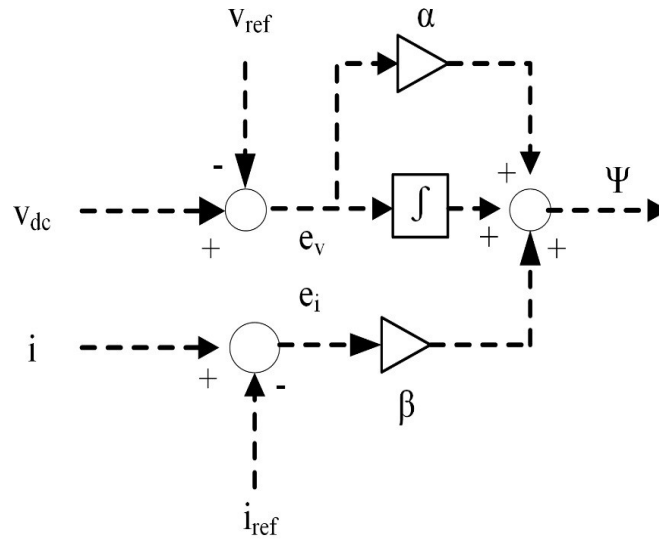


FIGURE 5.3: Block diagram of SM controller

way, the SM controller can detect and minimize the voltage and current errors. Further, the integral action is included to reduce steady state voltage error. The proposed sliding surface Ψ is given in (5.6).

$$\Psi = \alpha e_v + \beta e_i + \int e_v dt \quad (5.6)$$

Where, $e_v = v_{dc} - v_{dc}^{ref}$ and $e_i = i - i^{ref}$ respectively. Whereas, e_v , e_i , v_{dc}^{ref} and i^{ref} are voltage error, current error, reference bus voltage and reference inductor current respectively. While, α and β are parameters of the sliding surface. Fig. 5.3 shows the block diagram of SM control system.

The derivative of the sliding surface is used to ensure the existence of SM which is expressed as:

$$\frac{d\Psi}{dt} = \alpha \frac{dv_{dc}}{dt} + \beta \frac{di}{dt} + e_v \quad (5.7)$$

Substituting (5.3) and (5.4) into (5.7) leads to (5.8) as:

$$\frac{d\Psi}{dt} = \frac{\alpha}{C}(i - i_{dc}) - \frac{\beta}{L}(v_{dc} - uv_s) + e_v \quad (5.8)$$

For the existence of SM, the conditions described in (5.9) needs to be fulfilled [72] which describes that in steady state condition: $v_{dc} = v_{dc}^{ref}$ and $i = i^{ref}$. Hence, voltage and current achieves the desired reference.

$$\Psi = 0 \quad \text{and} \quad \frac{d\Psi}{dt} = 0 \quad (5.9)$$

To ensure the existence of SM i.e., guaranteeing (5.9), the transversality, reachability and equivalent control conditions must be guaranteed.

5.2.2.1 Transversality Condition

The transversality condition describes the system controllability. Thus, this condition must be satisfied to allow that the system dynamics are affected by SM controller [72]. It ensures that the control variable is present in the derivative of sliding surface. It can be expressed as:

$$\frac{d}{du} \frac{d\Psi}{dt} \neq 0 \quad (5.10)$$

Substituting (5.8) into (5.10) results in:

$$\frac{d}{du} \left(\frac{d\Psi}{dt} \right) = \frac{\beta}{L} (v_s) \neq 0 \quad (5.11)$$

Equation (5.11) depends on the value of β . Section 5.2.3 determines that the value of β must be positive value to guarantee stable system behavior. Moreover, v_s and L are positive quantities. Hence, (5.10) will be fulfilled and transversality condition of the modeled dc microgrid system is satisfied.

5.2.2.2 Reachability Condition

The reachability condition describes the systems ability to reach the sliding surface. Thus, reachability condition ensures that the system will always be directed towards the sliding manifold. Mathematically, it is described in (5.12).

$$\lim_{\Psi \rightarrow 0^-} \left. \frac{d\Psi}{dt} \right|_{u=1} > 0 \quad \text{and} \quad \lim_{\Psi \rightarrow 0^+} \left. \frac{d\Psi}{dt} \right|_{u=0} < 0 \quad (5.12)$$

Substituting (5.8) into (5.12), it can be expressed as:

$$\frac{\alpha}{C}(i - i_{dc}) + \frac{\beta}{L}(v_s - v_{dc}) + e_v > 0 \quad (5.13a)$$

$$-\frac{\alpha}{C}(i_{dc} - i) - \frac{\beta}{L}v_{dc} + e_v < 0 \quad (5.13b)$$

The conditions in (5.13a) and (5.13b) must be fulfilled to guarantee that the SM will exist, and the system will be derived to the desired operating condition.

5.2.2.3 Equivalent Control Condition

Equivalent control condition defines the local stability of the system and enables that system will remain trapped inside the sliding surface [72, 150]. Mathematically, equivalent control condition can be expressed as:

$$\left. \frac{d\Psi}{dt} \right|_{u=u_{eq}} = 0 \quad \longrightarrow \quad 0 < u_{eq} < 1 \quad (5.14)$$

Substituting $u = u_{eq}$ in (5.8) and equating to zero results in the following expression:

$$u_{eq} = \frac{v_{dc}}{v_s} - \frac{\alpha}{\beta} \left(\frac{L}{C} \right) \left(\frac{i - i_{dc}}{v_s} \right) - \frac{L}{\beta v_s} e_v \quad (6.15)$$

Fulfilling reachability condition also verifies the equivalent control condition.

5.2.3 Sliding Mode Dynamics

The inequalities in (5.13a) and (5.13b) generally describe the existence of SM. These inequalities do not give information about the selection of the sliding parameters α and β . This section deals with the selection of sliding parameters based on desired dynamic behavior. Thus, the stability of the system is fulfilled. For this purpose, closed loop dynamics in time domain of the system are achieved by

putting sliding surface $\Psi = 0$ in (5.6). The dynamics are given in (5.16).

$$e_i = -\frac{\alpha}{\beta}e_v - \frac{1}{\beta} \int e_v dt \quad (5.16)$$

The closed loop dynamics in Laplace domain are given in (5.17).

$$\frac{e_i(s)}{e_v(s)} = -\frac{1 + \alpha s}{\beta s} \quad (5.17)$$

Formerly, the voltage dynamics of dc bus defined in (5.4) is imposed by (5.17). Further, to find complete closed loop dynamics of the system, (5.4) can be expressed in Laplace domain as:

$$C s v_{dc}(s) = i(s) - i_{dc}(s) \quad (5.18)$$

Finally, combining (5.17) and (5.18), complete closed loop dynamics of the dc bus voltage can be expressed as:

$$v_{dc}(s) = -\frac{\beta s}{C\beta s^2 + \alpha s + 1} i_{dc}(s) + \frac{1 + \alpha s}{C\beta s^2 + \alpha s + 1} v_{dc}^{ref}(s) + \frac{\beta s}{C\beta s^2 + \alpha s + 1} i^{ref}(s) \quad (5.19)$$

It is shown in (5.19) that closed loop dynamics depends on the perturbation introduced by dc bus current and the reference. Since, the reference is a constant value and dc bus current depends on the source and load power requirements, (5.19) can be expressed as (5.20) which is used to design sliding parameters α and β of the SM controller.

$$\frac{v_{dc}(s)}{i_{dc}(s)} = -\frac{s}{Cs^2 + \frac{\alpha}{\beta}s + \frac{1}{\beta}} \quad (5.20)$$

Finally, it is established in (5.20) that both the sliding parameters α and β must be positive value to ensure stable SM dynamics, otherwise the system will show unstable behavior.

5.2.4 Design of Sliding Mode Dynamic Behavior

The dynamics shown in (5.20) demonstrate that SM controller will compensate any perturbation produced in bus current i_{dc} (i.e., $\lim_{\Psi \rightarrow \infty} \frac{v_{dc}(s)}{i_{dc}(s)} = 0$). However, large undershoots and overshoots in bus voltage can turn-off or destroy the load. Therefore, the dynamics of the bus voltage should be controlled. The characteristic polynomial in the denominator of (5.20) shows that it is second order system of the form given in (5.21).

$$s^2 + 2\zeta\omega_0s + \omega_0^2 = 0 \quad (5.21)$$

Where, ζ and ω_0 are damping ratio and undamped natural frequency respectively. Comparing the left-hand side of (5.21) with the denominator of (5.20), ζ and ω_0 can be written as:

$$\omega_0 = \sqrt{\frac{1}{\beta C}} \quad (5.22)$$

$$\zeta = \frac{\alpha}{2} \sqrt{\frac{1}{\beta C}} \quad (5.23)$$

ζ and ω_0 can control the response of the system. Two types of the responses are considered in this paper: underdamped and critically damped response. The characteristics of these are discussed below.

- Underdamped Response

In this type, controller enables the system response to reach faster the desired voltage. But this faster response is achieved at the expense of oscillation around the desired voltage. The loads which are sensitive to voltage drops but not sensitive to oscillations are suitable to be controlled using underdamped response, e.g., microprocessors [164].

- Critically Damped Response

In this type, controller enables the system response to avoid oscillations. But the response will experience a longer delay in reaching the desired voltage level.

The loads which are sensitive to oscillation but show tolerance to voltage drops are suitable to be controlled through critically damped response, e.g., variable frequency drive motors [165]. An overdamped response is not considered in this paper because it does not achieve any improvement over the critically damped response.

5.2.4.1 Underdamped Response

The underdamped time domain response of the system presented in (5.20) is given in (5.24) for the values of α and β that will lead to an underdamped response. The condition to guarantee the underdamped response is given in (5.25).

$$v_{dc}(t) = \frac{-\Delta i_{dc}}{c(\sqrt{(\frac{\alpha}{2\beta C})^2 - (\frac{1}{\beta C})})} e^{-(\frac{\alpha}{2\beta C}t)} \sin(\sqrt{(\frac{\alpha}{2\beta C})^2 - (\frac{1}{\beta C})}) \quad (5.24)$$

$$\frac{\alpha^2}{4C} < \beta \quad (5.25)$$

Where, Δi_{dc} represents the step change in dc bus current. Percentage overshoot for underdamped response is given in (5.26).

$$\%OS = 100e^{(-\frac{\zeta\pi}{\sqrt{1-\zeta^2}})} \quad (5.26)$$

Conversely, damping ratio ζ for a specific overshoot percentage is given in (5.27).

$$\zeta = \sqrt{\frac{\ln(\frac{\%OS}{100})}{\pi^2 + (\ln(\frac{\%OS}{100}))^2}} \quad (5.27)$$

The settling time T_s of underdamped response is given in (5.28).

$$T_s = \frac{\ln(\text{tolerance fraction})}{\zeta\omega_0} \quad (5.28)$$

Equations (5.26) to (5.28) can be used to design SM controller for desired response of a system. Finally, the constraints in (5.13a) and (5.13b) must be satisfied for

the existence of SM operation. Moreover, selected values of α and β must satisfy the constraint in (5.25) which is the condition for underdamped response.

5.2.4.2 Critically Damped Response

Critically damped time domain response is given in (5.29) while ensuring that the values of α and β will leads to the critically damped response. The condition for this response is given in (5.30).

$$v_{dc}(t) = \frac{-\Delta i_{dc}}{C}(t)e^{-\left(\frac{\alpha}{2\beta C}t\right)} \quad (5.29)$$

$$\beta = \frac{\alpha^2}{4C} \quad (5.30)$$

Finally, the constraints defined in (5.13a) and (5.13b) must be satisfied for the existence of SM. Further, (5.30) must be satisfied for the critically damped response.

5.2.5 Sliding Mode Hysteresis Control

In ideal situation, the SM controller will switch the dc to dc converter at infinite frequency with system trajectories moving along sliding surface when the system enters in SM operation. This condition is shown in Fig. 5.4(a). However, the practical switch of the dc to dc converter will experience some switching imperfections and time delays. This will produce a dynamic behavior in the locality of sliding surface which is identified as chattering and is shown in Fig. 5.4(b) [72, 150].

If the chattering produced in the sliding surface is left uncontrolled, the converter will start self-oscillating at a high frequency. This behavior of the converter is not desirable due to the high switching losses. Further, the exact switching frequency in the produced chattering cannot be predicted. Therefore, the converter design and component selection will turn out to be difficult. To solve these issues, the

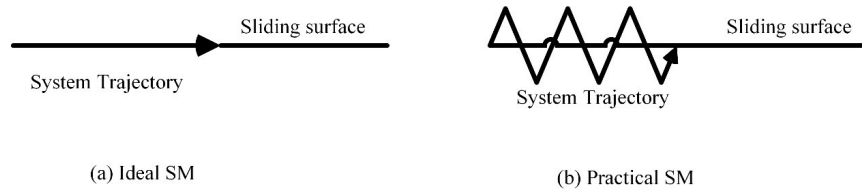


FIGURE 5.4: System trajectory during SM operation

control law u is redefined as:

$$u = \begin{cases} 0 = \text{"OFF"} & \text{when } \Psi > k \\ 1 = \text{"ON"} & \text{when } \Psi < -k \\ \text{Unchanged} & \text{otherwise} \end{cases} \quad (5.31)$$

Where, k is positive number. Usually in SMC, a hysteresis band is introduced to tackle the chattering problem. With this alteration, the converter switch will turn-on when $\Psi < -k$ and turn-off when $\Psi > k$. In the region $-k \leq \Psi \leq k$, the converter switch remains unchanged and maintains its former state. Therefore, introducing a region $-k \leq \Psi \leq k$ in which no switching occurs, the switching frequency can be controlled by varying the magnitude of k .

5.3 Simulation Results and Discussion

To examine the load sharing performance among parallel connected sources, a dc microgrid with two sources connected in parallel configuration to the load through connecting lines is proposed and shown in Fig. 5.5. This type of configuration can be easily extendable for more sources and microgrids in parallel configuration. This type of system is attractive for remote areas where national grid cannot be easily extendable due to the high cost associated with the installation of new transmission lines. Thus, a two-source dc microgrid system for load sharing is simulated using MATLAB/Simulink. Each source consists of dc to dc converter. The parameters of dc to dc converter are selected to support maximum voltage and current levels equal to 50V and 10A, respectively. Therefore, the converter

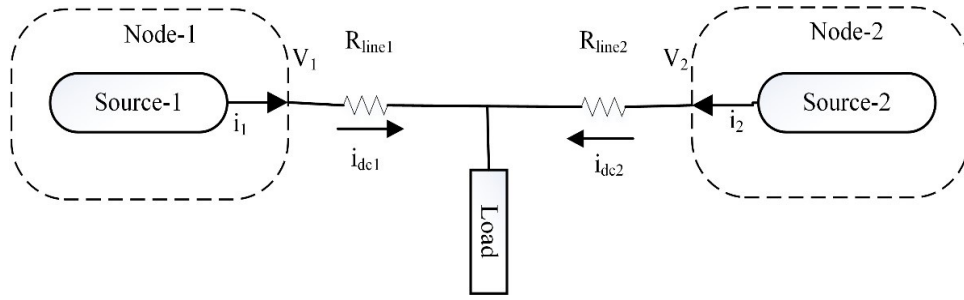


FIGURE 5.5: A two-source dc microgrid

TABLE 5.1: DC to dc converter parameters

| Parameters | Values |
|---------------------|-------------|
| Desired voltage | 48V |
| Switching frequency | 10kHz |
| Inductor L | $100\mu H$ |
| Capacitor C | $4000\mu F$ |

TABLE 5.2: Node parameters of dc microgrid

| Parameters | Node-1 and Node-2 |
|--------------------------------|-------------------|
| Desired voltage | 48V |
| Source rated power | 250W and 500W |
| Load resistance | 6Ω |
| Voltage and current regulation | $\leq 5\%$ |

supports a maximum power of 500W. The parameters for dc to dc converter are given in Table 5.1.

5.3.1 Results Using Droop Control

The detail of nodes and connecting lines is given in Table 5.2 and Table 5.3 respectively. Each source using droop control is shown in Fig. 5.6.

A two-source dc microgrid shown in Fig. 5.5 is simulated using droop control. To observe the steady state behavior, load is drawing rated current and steady state is reached. For equal load sharing, source 1 and 2 are simulated for same power

TABLE 5.3: Connecting cable parameters of dc microgrid

| Parameters | Branch-12 | Branch-21 |
|------------------|---------------|-------------|
| Current rating | 20A | 20A |
| Cable resistance | 205m Ω | 2m Ω |

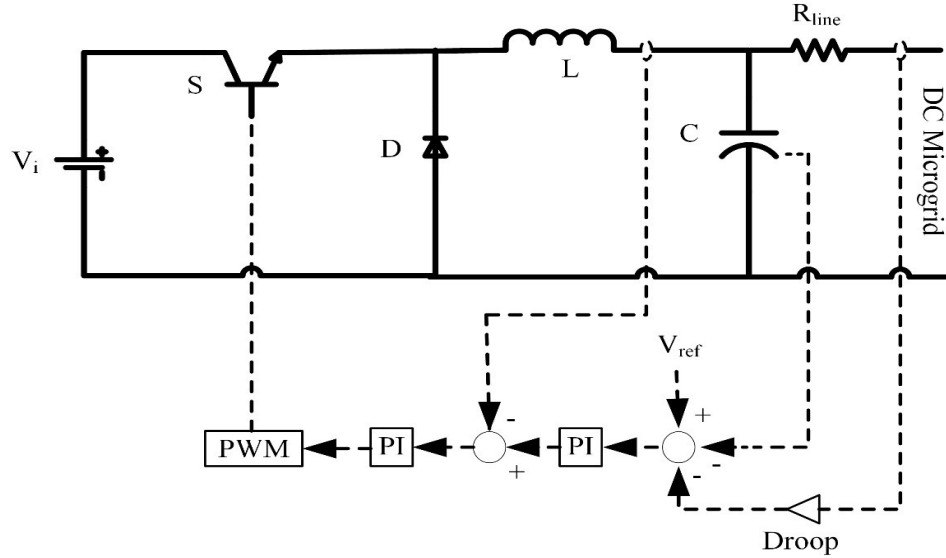


FIGURE 5.6: DC to dc buck converter using droop control

rating. Thus, droop gain $R_{d1} = R_{d2} = 0.2\Omega$ are selected for equal load sharing. Node voltage and current by each source is shown in Fig. 5.7. For droop gain 0.2Ω , the steady state current supplied by source 1 and source 2 are 2.9 and 4.9A respectively as shown in Fig. 5.7. Since, for equal load sharing, the desired current to be supplied by each source is 4A. The maximum deviation observed in supplied current is 27.5%. Steady state node voltages at source 1 and 2 are 47.4 and 46.8V respectively. The deviation observed in node voltages at no load and full load is 2.5%. These results show that small droop gains assure decent voltage regulation, but load sharing performance is not acceptable. For large droop gain 1.9Ω , current supplied by source 1 and 2 are 3.8 and 4.2A respectively. The observed deviation in supplied currents is 5% which is acceptable and lower value from the earlier case. But, the deviation in node voltages has increased to 16% which is not acceptable for the loads.

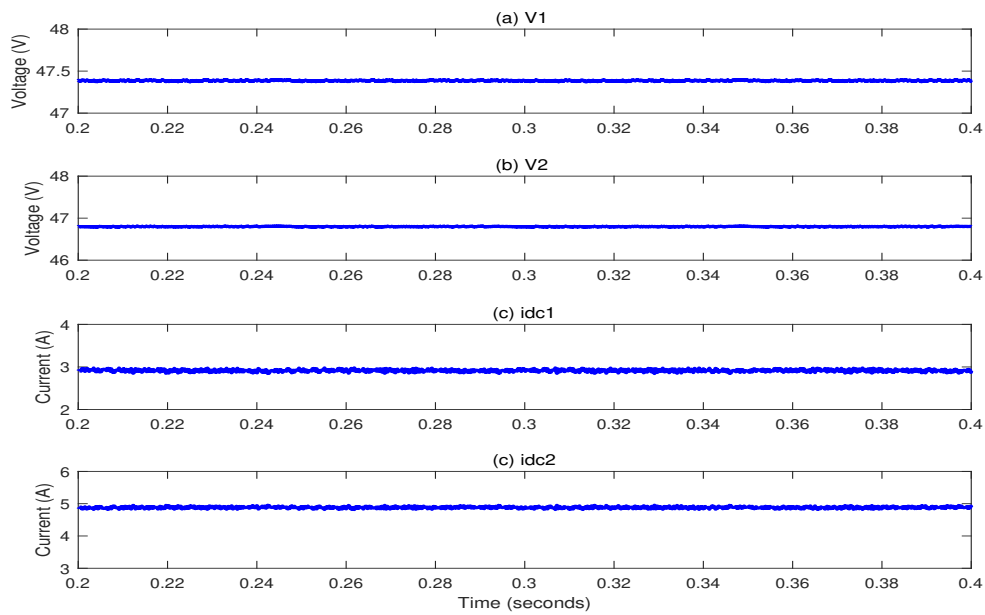


FIGURE 5.7: Node voltages and source currents with droop gain 0.2Ω

5.3.2 Results using Sliding Mode Control

Fig. 5.8 shows each source with distributed architecture using SM controller. The *p.u.* value of current of each source is communicated to the other sources at every $10ms$. The total communication delay is around $0.1ms$.

To observe the steady state behavior with distributed architecture using SM controller, two-source dc microgrid shown in Fig. 5.5 is simulated and results are shown in Fig. 5.9. Current supplied by source 1 and 2 are 3.91 and $3.92A$ respectively. The observed deviation in supplied currents is 2.08% which is a significant low value compared to the droop controlled dc microgrid. Further, the node voltages at source 1 and 2 are 47.78 and $47V$ respectively. The deviation observed in node voltages is 2.25% . This confirms the steady state load sharing and voltage regulation performance of the proposed distributed SM controller. Further, Fig. 5.10 shows that source 1 is sharing 25% and source 2 is sharing 75% of the rated load current. The current deviation observed in this case is 4.1% which shows the effectiveness of the proposed architecture using SM controller. In addition, simulations are carried out to see the effects of varying resistances of connecting lines and results are summarized in Table 5.4. Each column represents the fixed

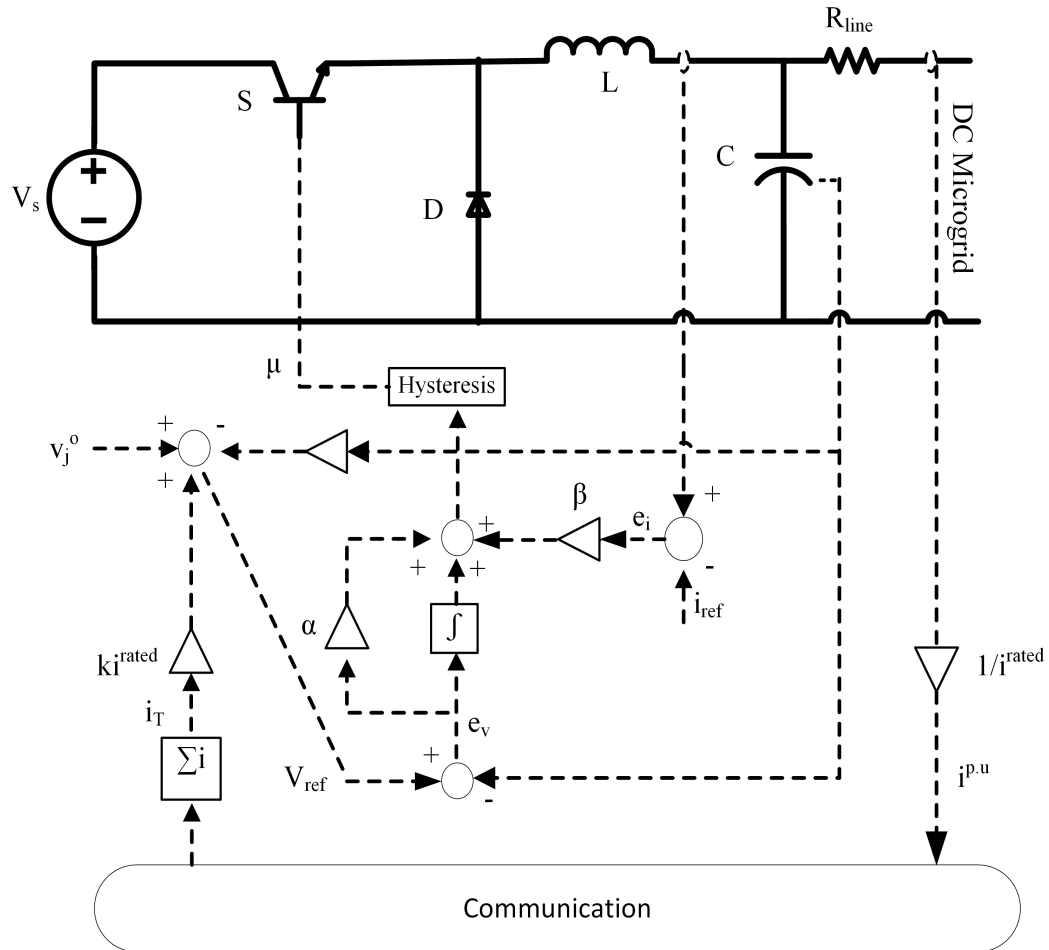


FIGURE 5.8: DC to dc buck converter with distributed architecture using SM controller

value of resistance R_{line1} of connecting line of source 1 and each row represents the fixed value of resistance R_{line2} of connecting line of source 2. Each entity in Table 5.4 represents the voltage and current sharing deviations. It can be observed that load sharing between sources is not significantly affected by varying the resistances of connecting lines.

To observe the transient condition, a step load of 3Ω is applied at $0.5s$ when system is operating in steady state at rated load and is shown in Fig. 5.11. At the instant when step change in load is applied, node voltages drops shortly as shown in Fig. 5.11. However, within $25ms$, node voltages of source 1 and 2 settle down to 49.29 and $46.83V$ respectively. This corresponds to voltage deviation of 2.68% . Current supplied are 11.96 and $11.45A$ respectively. The deviation in supplied currents is 4.5% . This shows the performance of SM controller on a step

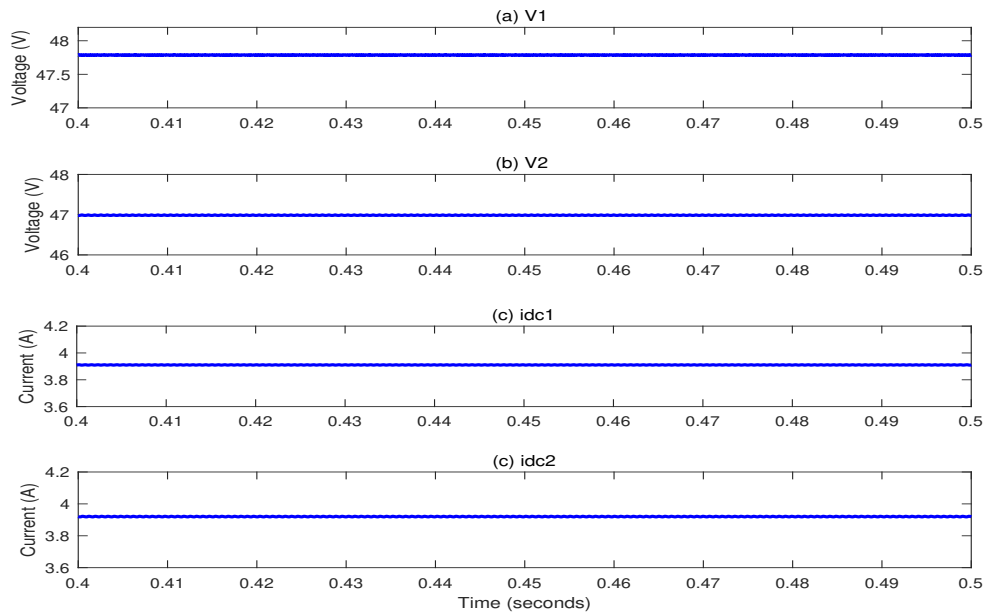


FIGURE 5.9: Node voltages and source currents with distributed architecture using SM controller

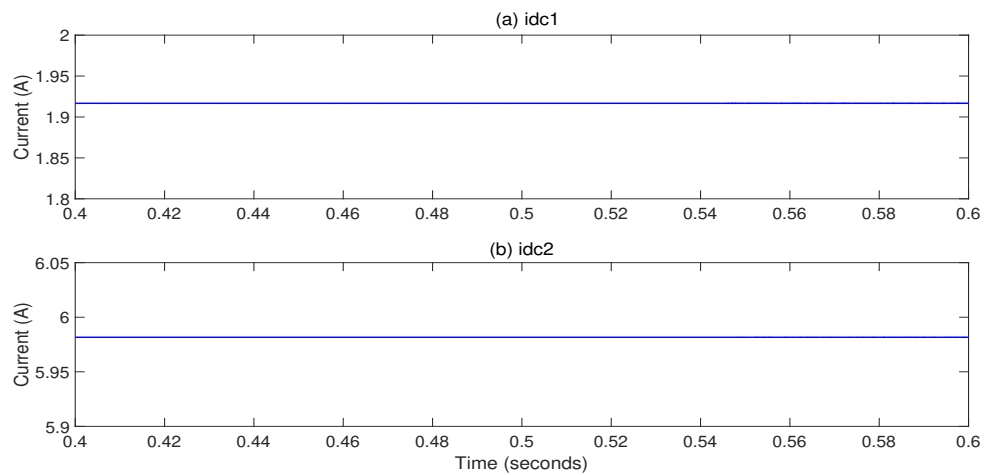
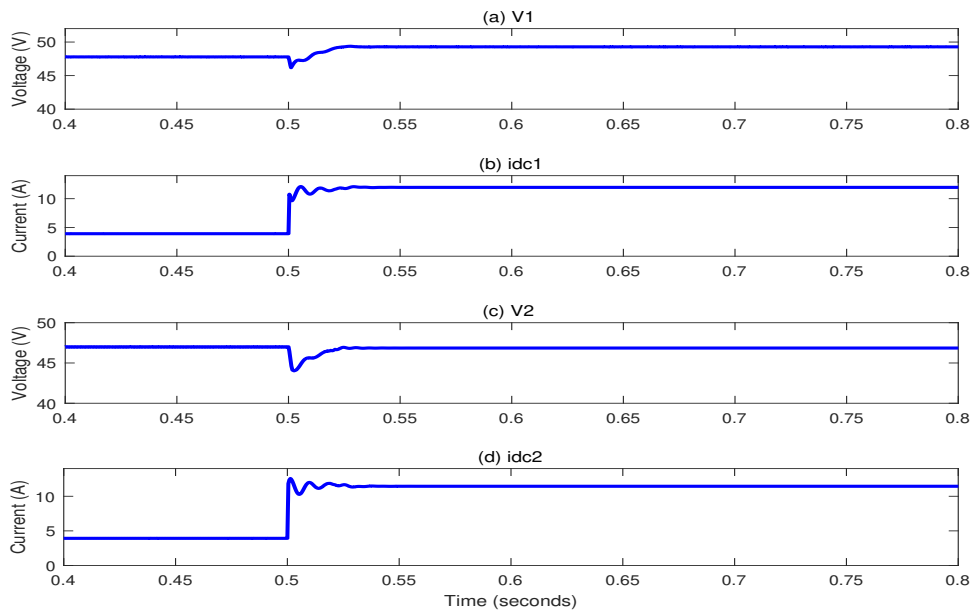


FIGURE 5.10: Source 1 with 25% and source 2 with 75% load sharing of the rated load

TABLE 5.4: Voltage regulation and current deviation for different Connecting cable resistance

| | $R_{line1} = 0.5 \times 205m\Omega$ | $R_{line1} = 1 \times 205m\Omega$ | $R_{line1} = 2 \times 205m\Omega$ |
|-----------------------------------|-------------------------------------|-----------------------------------|-----------------------------------|
| $R_{line2} = 0.5 \times 2m\Omega$ | (1.92%, 1.9%) | (2.05%, 2.24%) | (2.26%, 2.52%) |
| $R_{line2} = 1 \times 2m\Omega$ | (1.95%, 1.925%) | (2.08%, 2.25%) | (2.27%, 1.875%) |
| $R_{line2} = 2 \times 2m\Omega$ | (1.99%, 1.95%) | (2.12%, 2.75%) | (2.27%, 1.925%) |

FIGURE 5.11: Transient response when a step load of 3Ω is applied at 0.5 seconds

load. Furthermore, the dynamic behavior of a node voltage is investigated for underdamped and critically damped response. The sliding parameters α and β are selected positive according to the conditions defined in (6.25) and (6.30). Fig. 5.12 shows a node voltage when the load resistance is changed from 6Ω to 3Ω at 0.5s with sliding parameters that show underdamped and critically damped response. The results of settling time are summarized in Table 5.5. It can be observed that as value of ζ is increased from 0.1 to 0.6, the underdamped response is improved with smaller settling time. This response is in good agreement with the presented

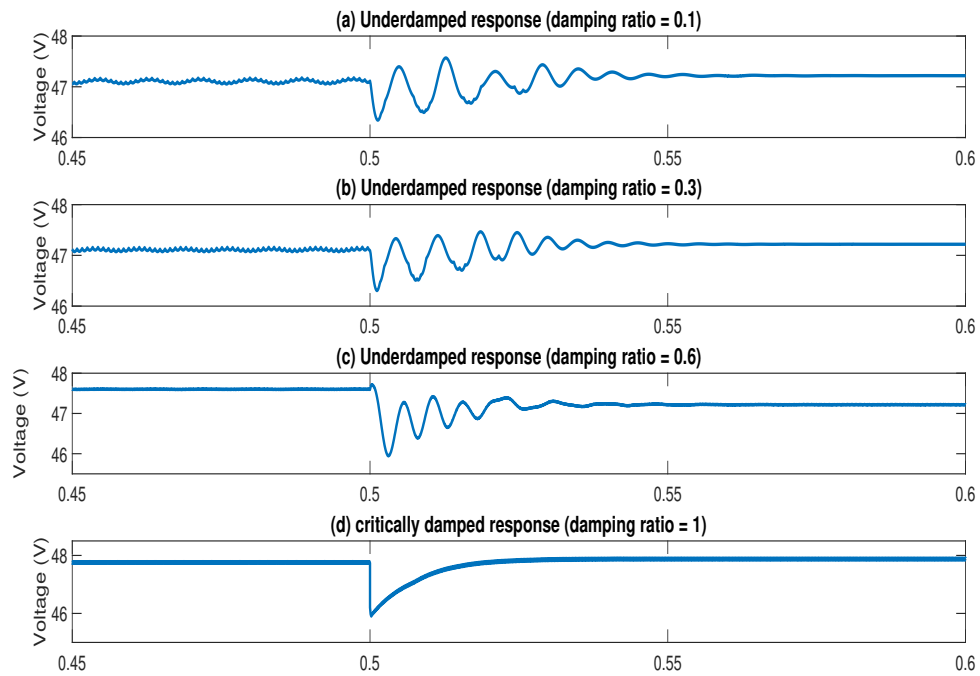


FIGURE 5.12: Voltage response of a source when load resistance is changed from 6 to 3Ω at 0.5 seconds

TABLE 5.5: Voltage dynamic behavior for different values of ζ

| Damping ratio ζ | Sliding parameters (α, β) | Settling time | Response type |
|--------------------------|---|---------------|-------------------|
| $\zeta = 0.1$ | (0.28, 100) | 50ms | Under-damped |
| $\zeta = 0.3$ | (0.85, 100) | 40ms | Under-damped |
| $\zeta = 0.6$ | (1.7, 100) | 30ms | Under-damped |
| $\zeta = 1$ | (2.85, 100) | 20ms | Critically damped |

theory. Additionally, for $\zeta = 1$, the response is critically damped with further improved settling time. These results show the good dynamic performance of the SM controller with distributed architecture.

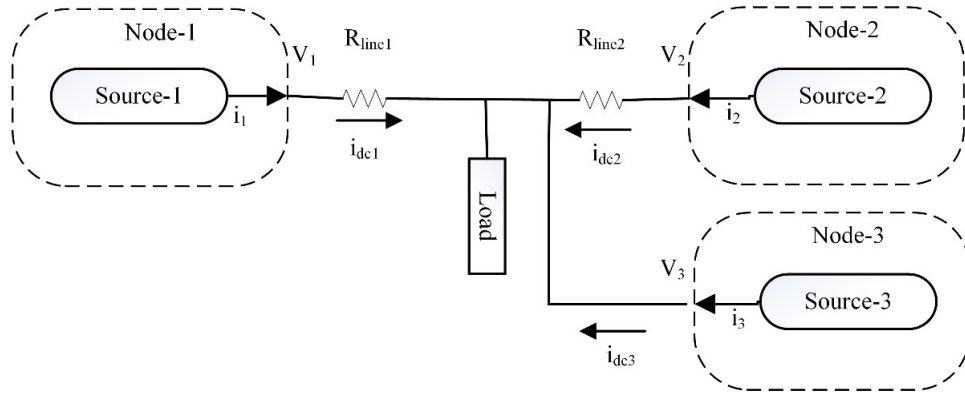


FIGURE 5.13: A three-source dc microgrid

5.3.3 Fail Safe Performance of Distributed Control Architecture

A significant improvement in the distributed architecture is that it provides high reliability. To prove this claim, a three-source dc microgrid shown in Fig. 5.13 is simulated for fault condition and shown in Fig. 5.14. The parameters of each source are same as given in Table 5.1. Source 1 and 2 are connected to load through connecting line resistances. But source 3 is directly connected to load. At steady state, voltage across the load is 47.04V. Three sources are supplying 3.915, 3.91 and 3.93A respectively. The maximum deviation observed in supplied currents is 2.25%. If one source becomes faulty, the capacity of the other two source is enough to satisfy the load. Failure of source 2 is simulated by removing its power supply at 0.5s. Under this fault, voltage across load and supplied currents by sources are shown in Fig. 5.14. After this fault, system reaches steady state in about 25ms. Voltage across load is maintained at 47.35V. The supplied current by source 1 and 3 are 5.91 and 5.93A respectively. This corresponds 1.5% deviation in supplied current. This confirms the performance of the distributed architecture using SM controller during source failure condition.

5.3.4 Performance Validation for More Sources

A dc microgrid with eight sources sharing a load as shown in Fig. 5.15 is simulated to validate the performance of proposed SM controller for more sources. The values

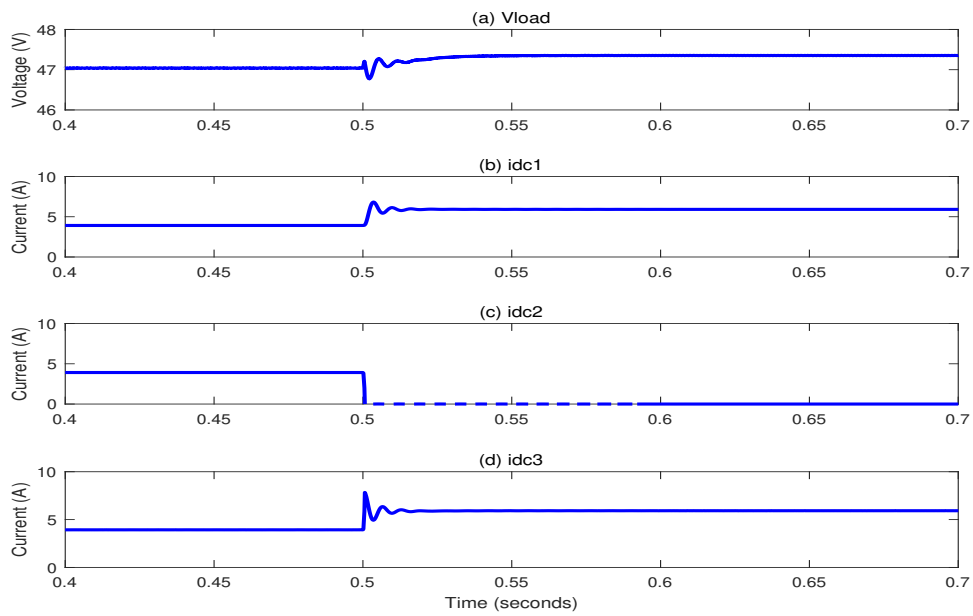


FIGURE 5.14: Transient response during fault on source 2 at 0.5 seconds

TABLE 5.6: Current deviation for eight sources in a dc microgrid

| Sources | Desired current | Observed value | Current deviation |
|----------|-----------------|----------------|-------------------|
| Source-1 | 4 A | 3.93 A | 1.75% |
| Source-2 | 4 A | 3.94 A | 2.33% |
| Source-3 | 3 A | 2.93 A | 2.33% |
| Source-4 | 5 A | 4.93 A | 1.4% |
| Source-5 | 6 A | 5.94 A | 1.16% |
| Source-6 | 3 A | 2.94 A | 2.33% |
| Source-7 | 3 A | 2.93 A | 2.33% |
| Source-8 | 4 A | 3.94 A | 1.75% |

of connecting lines are shown in Fig. 5.15. Fig. 5.16 and 5.17 show the voltages across load and current shared by each source. Results of current deviations are summarized in Table 5.6. The maximum observed current deviation is 2.33%. This validates load sharing performance of SMC for more sources in a dc microgrid.

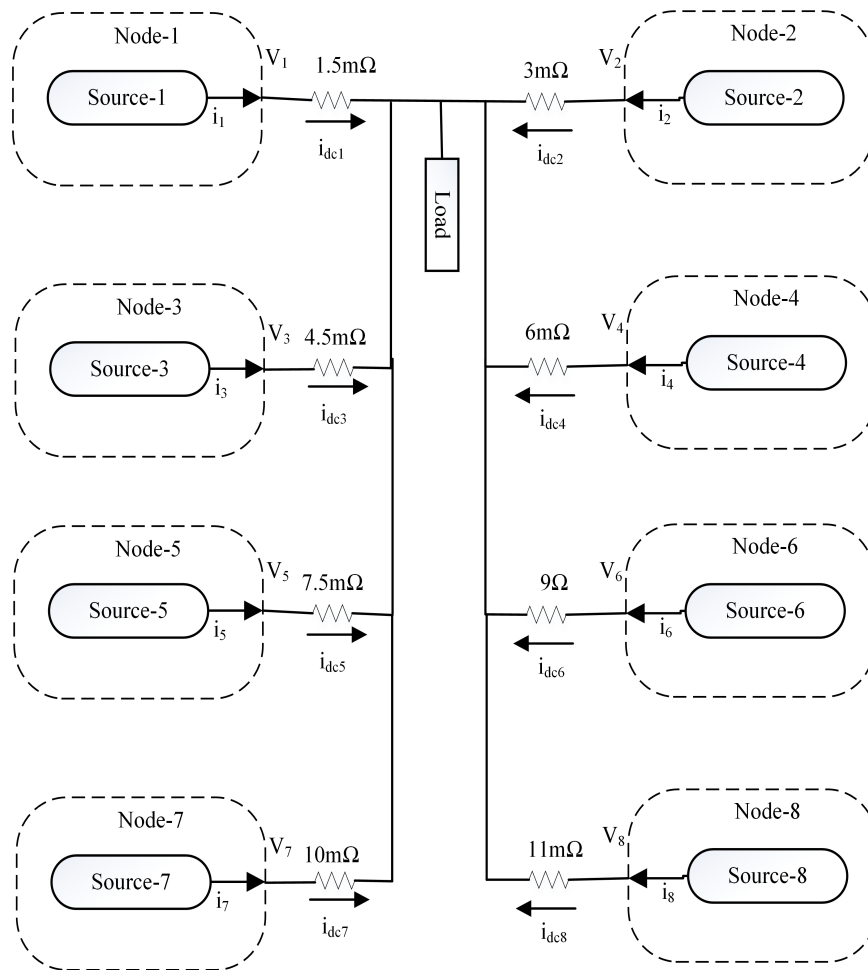


FIGURE 5.15: A dc microgrid with eight sources sharing a load

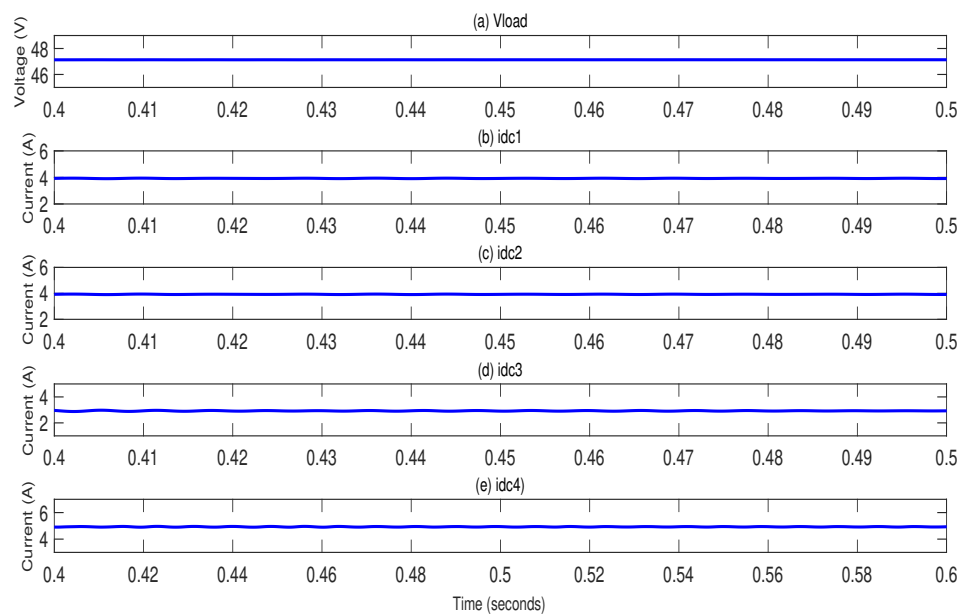


FIGURE 5.16: Load voltages and current shared by source 1, 2, 3 and 4

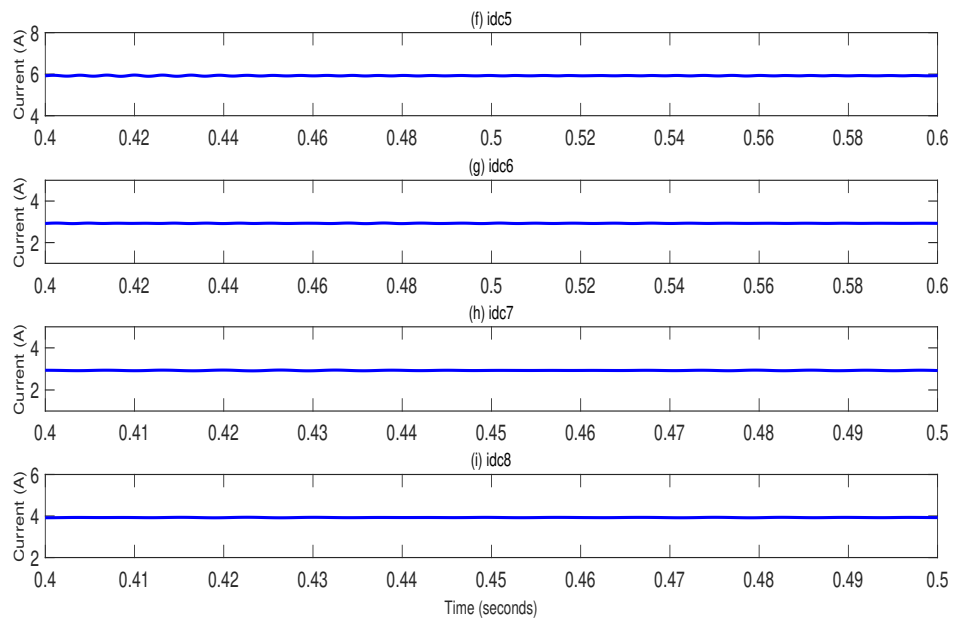


FIGURE 5.17: Current shared by source 5, 6, 7 and 8

5.4 Summary

Distributive control architecture using SM controller utilizing low bandwidth CAN based communication is proposed in this chapter. Main advantages achieved are high reliability, good load sharing and voltage regulation performance. To analyze the stability and dynamic performance, system model is developed, and SM transversality, reachability and equivalent control conditions are verified. Additionally, stability of sliding coefficients is verified. Furthermore, dynamic behavior of the modeled system is investigated for underdamped and critically damped response.

A two source dc microgrid sharing a load is simulated and results are presented for droop and distributive control. For equal load sharing between two sources with droop gain 0.2Ω , maximum deviations observed in supplied currents and node voltages are 27.5% and 2.5% respectively. With large droop gain 1.9Ω , observed deviations are 5% and 16% respectively. This shows that current deviation with large droop value is acceptable and lower from small droop value. But, deviation in node voltages has increased to 16% which is not acceptable for loads. The observed

deviations in supplied currents and node voltages with distributed architecture using SMC are 2.08% and 2.25% respectively which are significantly lower values compared to droop control. This confirms the steady state load sharing and voltage regulation performance of the proposed scheme. A step load is applied to see the effect of transient and observed settling time is 25ms. Further, dynamic behavior is presented for underdamped and critically damped response and results show the performance of proposed controller. Moreover, a three-source dc microgrid is simulated to show the fail-safe performance of distributive architecture under faulty condition. The presented results showed that if one source fails, the other two sources share load power. This confirms the reliable performance of distributed architecture during source failure.

Chapter 6

Conclusion and Future Work

A brief conclusion of thesis is outlined in this Chapter. Moreover, some future research recommendations are suggested for researchers interested to work in the area of dc microgrids.

6.1 Conclusion

Engineering foundations of ac electrical DSs were planned above hundred years ago, and it is still dominating. However, the debate between ac and dc DS has started again due to the depleting threat, high prices and ecological fear of burning fossil fuels. Further, PE devices have become abundant today due to their capabilities for precise process control and energy savings benefits. This inspired that generating power close to the end user reduces power losses associated in transmitting and hence, increases system efficiency. The unique property of the microgrids is that they can work in islanded mode under faulty grid conditions which increases the reliability of power supply. This motivates that microgrid is an effective way of power generation and consumption. In near future, DS may consist of some interconnected microgrids with local generation, storage and consumption of power.

Solar, wind and fuel cell technologies are playing an important role in electric power generation among various RESs. Most of these sources are inherently designed for dc or they are dc friendly. On the load side, most of electronics, domestic and industrial loads convert ac to dc before consuming it. AC to dc rectifiers are nonlinear loads which derate transformers and cause damage to other devices due to produced harmonics. Moreover, batteries are operated on dc. Therefore, a conversion stage is required to interconnect these sources, loads and batteries with ac microgrid. The losses associated with conversions decrease overall system efficiency. Hence, efficiency can be improved if the RESs, loads and batteries are directly powered by dc.

Due to these reasons, dc microgrids are becoming popular in the residential complexes, data centers and shipyard systems. It is expected that the efficiency of dc distribution will be 10 – 22% high than ac distribution. Further, reactive power compensation and frequency synchronization circuits are not required in dc which are prominent in ac power. Due to these advantages, dc is better suited for microgrid system. Different voltage standards have been proposed in literature for dc microgrid based on operational requirement of the systems. Voltage levels e.g., 380-400, 120, 325, 230V are suitable for domestic installations and data centers. Other voltage level could be ± 230 , ± 170 , $\pm 110V$ which can be preferred for protection measures. As all loads convert 220V ac into dc which is about 300V, this is best suited standard for domestic and industrial loads.

Stability of dc microgrid is a key challenge in the presence of various distributed sources. Droop controllers are being used for stability of dc microgrids. Droop controllers suffers stability due to error in nominal voltages and load variations. Additionally, these are realized through PI controllers which cannot ensure global stability of the desired equilibrium point. Further, they exhibit slower transient response. Moreover, parameters of these controllers are calculated using current specifications of the system. Control parameters vary with load and source conditions of the system. Therefore, it becomes difficult to optimize controller parameters for different operating conditions. Hence, to use PI controllers for stability of dc microgrid is not feasible. Therefore, SMC technique is proposed for stability

and better dynamic response in dc microgrid application. To analyze stability and dynamic performance, mathematical model of a dc microgrid is derived. Controllability and stability of the modeled system are verified. Hitting, existence and stability conditions are guaranteed using SMC. Modeled dynamics of the system are graphically plotted which show that system trajectories converge to the equilibrium point. Detailed simulations of a three source microgrid are carried out to show the effectiveness of SM controller and results are compared with droop controller. In steady state condition, voltage regulation of 3.25%, 6.25% and 7.86% are observed with droop gains of 0.04Ω , 0.4Ω and 1.9Ω respectively. This shows that good voltage regulation is ensured with small droop values. For large droop values, poor voltage regulation is observed which is not acceptable to loads. Whereas, using SMC, voltage regulation observed is 0.125% which is significantly improved from droop controlled dc microgrid. This shows the good steady state performance of the system using SMC. The effect of transient on a step load is also investigated and observed settling time in droop control is $10ms$. While, the observed settling time in SMC is $1ms$ which is significantly lower than droop control. This confirms the good performance of the proposed controller. Additionally, the dynamic behavior of a source with different sliding coefficients is also investigated and results are presented. Moreover, a small scale practical setup is developed, and results are presented.

Proportional load sharing and precise voltage regulation are the key objectives to be achieved in dc microgrid. However, the problem in the parallel connected sources is that these objectives cannot be achieved simultaneously. To address the challenge, different control architectures are proposed in literature which can be categorized as centralized and decentralized control. In centralized control, single central controller collects system data using high bandwidth communication link, schedule the tasks based on the collected information and directs control decisions. Centralized control can achieve good load sharing and voltage regulation ($< 5\%$) performance. However, if single point failure exists, it will degrade system performance and reliability. Additionally, these controllers are realized through PI controllers which cannot ensure load sharing and stability in all operating

conditions. Single point failure problem can be avoided in decentralized control. In this type of control architecture, PE converters operate on physical measured quantities. But, the improvement is achieved at the cost of partial stability and losing optimum operation due to the lack of operational information and status of the other converters. To address limitations, a distributive architecture using SM controller utilizing low bandwidth CAN based communication is proposed in this thesis. Main advantage achieved are high reliability, good load sharing and voltage regulation ($< 5\%$) performance. To analyze stability and dynamic performance, system model is developed, and SM conditions are verified. Furthermore, the dynamic behavior of the modeled system is investigated for underdamped and critically damped response. A dc microgrid consists of two source is simulated and results of load sharing are presented for droop and distributive control. For equal power sharing between two sources with droop gain 0.2Ω , the maximum deviations observed in supplied currents and node voltages are 27.5% and 2.5% respectively. With large droop gain 1.9Ω , observed deviations are 5% and 16% respectively. This shows that the current deviation with large droop value is acceptable and lower from small droop value. But, the deviation in node voltages has increased to 16% which is not acceptable for loads. Whereas, with distributed architecture using SMC, observed deviations in supplied currents and node voltages are 2.08% and 2.25% respectively which are significantly lower than droop control. This confirms the steady state load sharing and voltage regulation performance of the proposed distributed SM controller. The effect of transient on a step load is also simulated and observed settling time is $25ms$. Additionally, the dynamic behavior of voltage at a node is presented for underdamped and critically damped response. Presented results showed the performance of critically damped response which settles in $20ms$. Furthermore, a three source dc microgrid is simulated to show the fail safe performance of distributive architecture during a source failure condition. The presented results showed that if one source fails, the other two sources share load power and system reaches in steady state within $25ms$. This confirms the reliable performance of distributed architecture during source failure.

6.2 Future Recommendations

The research work presented in this thesis focuses on the proportional load sharing and stability of dc microgrid. Following are some recommendation for researchers who want to work in this area.

- The SMC technique based on hysteresis controller is proposed in this research work. Hysteresis function suffers from the frequency variation problem. This is not desired because it will oversize the filter requirement and complicates the EMI suppression. The operation of converters at fixed frequency is preferred. Therefore, PWM based on an equivalent control function can be investigated for fixed frequency operation of converters.
- The stability of dc microgrid due to the cascaded PECs architecture is not explored in this work. This can be explored and its effects can be analyzed using SM controller.
- The impacts due to faults and surges are not examined in this work. In future, these can be explored and a protection scheme can be worked for reliable operation under faults.
- Demand response is an old idea, but it is attracting attention due to the extensive applications of smart meters and wireless communication. Applying demand response in dc microgrid system will help to optimally consume generated power and reduce the peak demand hours by defining schedule for the energy requirements. This idea can be applied to manage the end user demands in dc microgrid system.
- Future work can also focus on economic dispatch of dc microgrid and scheduling of energy tariff which is communicated to the end user based on the energy cost of the dc microgrid.

Bibliography

- [1] L. Meng, Q. Shafiee, G. F. Trecate, H. Karimi, D. Fulwani, X. Lu, and J. M. Guerrero, “Review on control of dc microgrids and multiple microgrid clusters,” *IEEE Journal of Emerging and Selected Topics in Power Electronics*, vol. 5, no. 3, pp. 928–948, 2017.
- [2] X. Li, L. Guo, S. Zhang, C. Wang, Y. W. Li, A. Chen, and Y. Feng, “Observer-based dc voltage droop and current feed-forward control of a dc microgrid,” *IEEE Transactions on Smart Grid*, 2017.
- [3] Q. Sun, B. Huang, D. Li, D. Ma, and Y. Zhang, “Optimal placement of energy storage devices in microgrids via structure preserving energy function,” *IEEE Transactions on Industrial Informatics*, vol. 12, no. 3, pp. 1166–1179, 2016.
- [4] B. Nordman, R. Brown, and C. Marnay, “Low-voltage dc: Prospects and opportunities for energy efficiency,” *Lawrence Berkeley National Laboratory*, 2007.
- [5] A. Khorsandi, M. Ashourloo, H. Mokhtari, and R. Iravani, “Automatic droop control for a low voltage dc microgrid,” *IET Generation, Transmission & Distribution*, vol. 10, no. 1, pp. 41–47, 2016.
- [6] W.-J. Ma, J. Wang, X. Lu, and V. Gupta, “Optimal operation mode selection for a dc microgrid,” *IEEE Transactions on Smart Grid*, vol. 7, no. 6, pp. 2624–2632, 2016.
- [7] A. Esmaeli, “Stability analysis and control of microgrids by sliding mode control (retraction of vol 78, pg 22, 2016),” 2017.

-
- [8] S. ali Moayedi and A. Davoudi, "Distributed tertiary control of dc microgrid clusters," *IEEE Trans. on Power Electron.*, vol. 31, no. 2, pp. 1717–1733, 2015.
- [9] C. Jin, P. Wang, J. Xiao, Y. Tang, and F. H. Choo, "Implementation of hierarchical control in dc microgrids," *IEEE transactions on industrial electronics*, vol. 61, no. 8, pp. 4032–4042, 2014.
- [10] S. Anand, B. G. Fernandes, and J. Guerrero, "Distributed control to ensure proportional load sharing and improve voltage regulation in low-voltage dc microgrids," *IEEE Transactions on Power Electronics*, vol. 28, no. 4, pp. 1900–1913, 2013.
- [11] X. Liu, P. Wang, and P. C. Loh, "A hybrid ac/dc microgrid and its coordination control," *IEEE Transactions on Smart Grid*, vol. 2, no. 2, pp. 278–286, 2011.
- [12] J. M. Guerrero, "Hierarchical control of droop-controlled ac and dc microgrids: a general approach toward standardization," *IEEE Trans. on Ind. Electron.*, vol. 58, no. 1, pp. 158–172, 2011.
- [13] H. Kakigano, Y. Miura, and T. Ise, "Low-voltage bipolar-type dc microgrid for super high quality distribution," *IEEE transactions on power electronics*, vol. 25, no. 12, pp. 3066–3075, 2010.
- [14] K.-T. Mok, M.-H. Wang, S.-C. Tan, and S. R. Hui, "Dc electric springs: a technology for stabilizing dc power distribution systems," *IEEE Transactions on Power Electronics*, vol. 32, no. 2, pp. 1088–1105, 2017.
- [15] K. A. Saleh, A. Hooshyar, and E. F. El-Saadany, "Hybrid passive-overcurrent relay for detection of faults in low-voltage dc grids," *IEEE Transactions on Smart Grid*, vol. 8, no. 3, pp. 1129–1138, 2017.
- [16] J. M. Guerrero, M. Chandorkar, T.-L. Lee, and P. C. Loh, "Advanced control architectures for intelligent microgrids: part i: Decentralized and hierarchical

- control,” *IEEE Transactions on Industrial Electronics*, vol. 60, no. 4, pp. 1254–1262, 2013.
- [17] D. Salomonsson, L. Soder, and A. Sannino, “An adaptive control system for a dc microgrid for data centers,” in *Industry Applications Conference, 2007. 42nd IAS Annual Meeting. Conference Record of the 2007 IEEE*. IEEE, 2007, pp. 2414–2421.
- [18] A. Sannino, G. Postiglione, and M. H. Bollen, “Feasibility of a dc network for commercial facilities,” in *Industry Applications Conference, 2002. 37th IAS Annual Meeting. Conference Record of the*, vol. 3. IEEE, 2002, pp. 1710–1717.
- [19] S. Anand and B. Fernandes, “Optimal voltage level for dc microgrids,” in *IECON 2010-36th Annual Conference on IEEE Industrial Electronics Society*. IEEE, 2010, pp. 3034–3039.
- [20] P. Wang, X. Lu, X. Yang, W. Wang, and D. Xu, “An improved distributed secondary control method for dc microgrids with enhanced dynamic current sharing performance,” *IEEE Transactions on Power Electronics*, vol. 31, no. 9, pp. 6658–6673, 2016.
- [21] X. Lu, J. M. Guerrero, K. Sun, J. C. Vasquez, R. Teodorescu, and L. Huang, “Hierarchical control of parallel ac-dc converter interfaces for hybrid microgrids,” *IEEE Transactions on Smart Grid*, vol. 5, no. 2, pp. 683–692, 2014.
- [22] J. He and Y. W. Li, “An enhanced microgrid load demand sharing strategy,” *IEEE Transactions on Power Electronics*, vol. 27, no. 9, pp. 3984–3995, 2012.
- [23] K. Dietrich, J. M. Latorre, L. Olmos, and A. Ramos, “Demand response and its sensitivity to participation rates and elasticities,” in *Energy Market (EEM), 2011 8th International Conference on the European*. IEEE, 2011, pp. 717–716.

- [24] L. Zheng, N. Lu, and L. Cai, "Reliable wireless communication networks for demand response control," *IEEE Transactions on Smart Grid*, vol. 4, no. 1, pp. 133–140, 2013.
- [25] W. Liu, Q. Wu, F. Wen, and J. Østergaard, "Day-ahead congestion management in distribution systems through household demand response and distribution congestion prices," *IEEE Transactions on Smart Grid*, vol. 5, no. 6, pp. 2739–2747, 2014.
- [26] R. Majumder, G. Ledwich, A. Ghosh, S. Chakrabarti, and F. Zare, "Droop control of converter-interfaced microsources in rural distributed generation," *IEEE Transactions on Power Delivery*, vol. 25, no. 4, pp. 2768–2778, 2010.
- [27] D. Guezgouz, D. E. Chariag, Y. Raingeaud, and J.-C. Le Bunetel, "Modeling of electromagnetic interference and plc transmission for loads shedding in a microgrid," *IEEE Transactions on Power Electronics*, vol. 26, no. 3, pp. 747–754, 2011.
- [28] A. Pinomaa, J. Ahola, and A. Kosonen, "Power-line communication-based network architecture for lvdc distribution system," in *Power Line Communications and Its Applications (ISPLC), 2011 IEEE International Symposium on*. IEEE, 2011, pp. 358–363.
- [29] J. Anatory, N. Theethayi, R. Thottappillil, M. Kissaka, and N. H. Mvungi, "The influence of load impedance, line length, and branches on underground cable power-line communications (plc) systems," *IEEE Transactions on Power Delivery*, vol. 23, no. 1, pp. 180–187, 2008.
- [30] H. Liang, B. J. Choi, W. Zhuang, and X. Shen, "Stability enhancement of decentralized inverter control through wireless communications in microgrids," *IEEE Transactions on Smart Grid*, vol. 4, no. 1, pp. 321–331, 2013.
- [31] J. Schonbergerschonberger, R. Duke, and S. D. Round, "Dc-bus signaling: A distributed control strategy for a hybrid renewable nanogrid," *IEEE Transactions on Industrial Electronics*, vol. 53, no. 5, pp. 1453–1460, 2006.

- [32] S. V. Iyer, M. N. Belur, and M. C. Chandorkar, "A generalized computational method to determine stability of a multi-inverter microgrid," *IEEE Transactions on Power Electronics*, vol. 25, no. 9, pp. 2420–2432, 2010.
- [33] J. M. Guerrero, J. Matas, L. G. D. V. De Vicuna, M. Castilla, and J. Miret, "Wireless-control strategy for parallel operation of distributed-generation inverters," *IEEE Transactions on Industrial Electronics*, vol. 53, no. 5, pp. 1461–1470, 2006.
- [34] H. J. Avelar, W. A. Parreira, J. B. Vieira, L. C. G. de Freitas, and E. A. A. Coelho, "A state equation model of a single-phase grid-connected inverter using a droop control scheme with extra phase shift control action," *IEEE Transactions on Industrial Electronics*, vol. 59, no. 3, pp. 1527–1537, 2012.
- [35] W. Yao, M. Chen, J. Matas, J. M. Guerrero, and Z.-M. Qian, "Design and analysis of the droop control method for parallel inverters considering the impact of the complex impedance on the power sharing," *IEEE Transactions on Industrial Electronics*, vol. 58, no. 2, pp. 576–588, 2011.
- [36] M. C. Chandorkar, D. M. Divan, and R. Adapa, "Control of parallel connected inverters in standalone ac supply systems," *IEEE Transactions on Industry Applications*, vol. 29, no. 1, pp. 136–143, 1993.
- [37] P. Karlsson, *DC distributed power systems-Analysis, design and control for a renewable energy system*. IEA-LTH, Box 118, SE-221 00 LUND, SWEDEN,, 2002.
- [38] M. Mahmoodi, G. Gharehpetian, M. Abedi, and R. Noroozian, "Control systems for independent operation of parallel dg units in dc distribution systems," in *Power and Energy Conference, 2006. PECon'06. IEEE International*. IEEE, 2006, pp. 220–224.
- [39] —, "A suitable control strategy for source converters and a novel load-generation voltage control scheme for dc voltage determination in dc distribution systems," in *Power and Energy Conference, 2006. PECon'06. IEEE International*. IEEE, 2006, pp. 363–367.

- [40] B. K. Johnson, R. H. Lasseter, F. L. Alvarado, and R. Adapa, "Expandable multiterminal dc systems based on voltage droop," *IEEE Transactions on Power Delivery*, vol. 8, no. 4, pp. 1926–1932, 1993.
- [41] P. Karlsson and J. Svensson, "Dc bus voltage control for a distributed power system," *IEEE transactions on Power Electronics*, vol. 18, no. 6, pp. 1405–1412, 2003.
- [42] S.-C. Tan, Y.-M. Lai, and C.-K. Tse, *Sliding mode control of switching power converters: techniques and implementation*. CRC press, 2011.
- [43] R. Ridley, "Current mode or voltage mode?" *Switching Power Magazine*, vol. 1, no. 2, pp. 4–6, 2000.
- [44] K. Ogata and Y. Yang, *Modern control engineering*. Prentice hall India, 2002, vol. 4.
- [45] P. Karlsson, *DC distributed power systems-Analysis, design and control for a renewable energy system*. IEA-LTH, Box 118, SE-221 00 LUND, SWEDEN,, 2002.
- [46] A. Kwasinski, "A microgrid architecture with multiple-input dc/dc converters: applications, reliability, system operation, and control," Ph.D. dissertation, University of Illinois at Urbana-Champaign, 2007.
- [47] A. Kwasinski and P. T. Krein, "Stabilization of constant power loads in dc-dc converters using passivity-based control," in *Telecommunications Energy Conference, 2007. INTELEC 2007. 29th International*. IEEE, 2007, pp. 867–874.
- [48] F. A. Himmelstoss, J. W. Kolar, and F. C. Zach, "Analysis of a smith-predictor-based-control concept eliminating the right-half plane zero of continuous mode boost and buck-boost dc/dc converters," in *Industrial Electronics, Control and Instrumentation, 1991. Proceedings. IECON'91., 1991 International Conference on*. IEEE, 1991, pp. 423–428.

- [49] R. Mammano, "Switching power supply topology voltage mode vs. current mode," *Elektron Journal-South African Institute of Electrical Engineers*, vol. 18, no. 6, pp. 25–27, 2001.
- [50] H.-C. Chan, K. Chau, and C. Chan, "A neural network controller for switching power converters," in *Power Electronics Specialists Conference, 1993. PESC'93 Record., 24th Annual IEEE*. IEEE, 1993, pp. 887–892.
- [51] C.-Y. Chan, "A nonlinear control for dc–dc power converters," *IEEE transactions on power electronics*, vol. 22, no. 1, pp. 216–222, 2007.
- [52] K.-H. Cheng, C.-F. Hsu, C.-M. Lin, T.-T. Lee, and C. Li, "Fuzzy–neural sliding-mode control for dc–dc converters using asymmetric gaussian membership functions," *IEEE Transactions on Industrial Electronics*, vol. 54, no. 3, pp. 1528–1536, 2007.
- [53] A. R. Ofoli and A. Rubaai, "Real-time implementation of a fuzzy logic controller for switch-mode power-stage dc–dc converters," *IEEE Transactions on Industry Applications*, vol. 42, no. 6, pp. 1367–1374, 2006.
- [54] K. Viswanathan, R. Oruganti, and D. Srinivasan, "Nonlinear function controller: a simple alternative to fuzzy logic controller for a power electronic converter," *IEEE Transactions on Industrial Electronics*, vol. 52, no. 5, pp. 1439–1448, 2005.
- [55] H. W. Bode, "Relations between attenuation and phase in feedback amplifier design," *Bell System Technical Journal*, vol. 19, no. 3, pp. 421–454, 1940.
- [56] R. C. Dorf and R. H. Bishop, *Modern control systems*. Pearson, 2011.
- [57] W. R. Evans, "Graphical analysis of control systems," *Transactions of the American Institute of Electrical Engineers*, vol. 67, no. 1, pp. 547–551, 1948.
- [58] W. L. Brogan, *Modern control theory*. Pearson education india, 1974.
- [59] A. Kelly and K. Rinne, "Control of dc-dc converters by direct pole placement and adaptive feedforward gain adjustment," in *Applied Power Electronics*

- Conference and Exposition, 2005. APEC 2005. Twentieth Annual IEEE*, vol. 3. IEEE, 2005, pp. 1970–1975.
- [60] F. F. Leung, P. K.-S. Tam, and C. Li, “An improved lqr-based controller for switching dc-dc converters,” *IEEE Transactions on Industrial Electronics*, vol. 40, no. 5, pp. 521–528, 1993.
- [61] F. H. Leung, P. K. Tam, and C. Li, “The control of switching dc-dc converters—a general lwr problem,” *IEEE transactions on industrial electronics*, vol. 38, no. 1, pp. 65–71, 1991.
- [62] L. Camacho-Solorio and A. Sariñana-Toledo, “I-lqg control of dc-dc boost converters,” in *Electrical Engineering, Computing Science and Automatic Control (CCE), 2014 11th International Conference on*. IEEE, 2014, pp. 1–6.
- [63] Z. Liu, L. Xie, A. Bemporad, and S. Lu, “Fast linear parameter varying model predictive control of buck dc-dc converters based on fpga,” *IEEE Access*, vol. 6, pp. 52 434–52 446, 2018.
- [64] T. Hornik, “Power quality in microgrids,” Ph.D. dissertation, The University of Liverpool, 2010.
- [65] C. A. Torres-Pinzón and R. Leyva, “Matlab: A systems tool for design of fuzzy lmi controller in dc-dc converters,” in *MATLAB-A Ubiquitous Tool for the Practical Engineer*. InTech, 2011.
- [66] C. K. Tse and K. M. Adams, “An adaptive control for dc-dc converters,” in *Power Electronics Specialists Conference, 1990. PESC '90 Record., 21st Annual IEEE*. IEEE, 1990, pp. 887–892.
- [67] E. Figueres, G. Garcerá, J. M. Benavent, M. Pascual, and J. A. Martínez, “Adaptive two-loop voltage-mode control of dc-dc switching converters,” *IEEE Transactions on Industrial Electronics*, vol. 53, no. 1, pp. 239–253, 2006.

- [68] G.-J. Jeong, I.-H. Kim, and Y.-I. Son, "Application of simple adaptive control to a dc/dc boost converter with load variation," in *ICCAS-SICE, 2009*. IEEE, 2009, pp. 1747–1751.
- [69] P. Mattavelli, L. Rossetto, G. Spiazzi, and P. Tenti, "General-purpose fuzzy controller for dc/dc converters," in *Applied Power Electronics Conference and Exposition, 1995. APEC'95. Conference Proceedings 1995., Tenth Annual*, vol. 2. IEEE, 1995, pp. 723–730.
- [70] W.-C. So, C. K. Tse, and Y.-S. Lee, "Development of a fuzzy logic controller for dc/dc converters: design, computer simulation, and experimental evaluation," *IEEE Transactions on Power Electronics*, vol. 11, no. 1, pp. 24–32, 1996.
- [71] R. Leyva, L. Martinez-Salamero, B. Jammes, J. C. Marpinard, and F. Guinjoan, "Identification and control of power converters by means of neural networks," *IEEE Transactions on Circuits and Systems I: Fundamental Theory and Applications*, vol. 44, no. 8, pp. 735–742, 1997.
- [72] V. Utkin, J. Guldner, and J. Shi, *Sliding mode control in electro-mechanical systems*. CRC press, 2017.
- [73] K. M. Smedley and S. Cuk, "One-cycle control of switching converters," *IEEE transactions on power electronics*, vol. 10, no. 6, pp. 625–633, 1995.
- [74] D. Goldberg, "Genetic algorithms in search, optimization, and machine learning," 1989.
- [75] C.-Y. Chan, "Simplified parallel-damped passivity-based controllers for dc-dc power converters," *Automatica*, vol. 44, no. 11, pp. 2977–2980, 2008.
- [76] C. Y. Chan, "Investigation of voltage-mode controller for cascade boost converter," *IET Power Electronics*, vol. 7, no. 8, pp. 2060–2068, 2014.
- [77] W. Perruquetti and J.-P. Barbot, *Sliding mode control in engineering*. CRC Press, 2002.

- [78] V. M. Nguyen and C. Lee, "Tracking control of buck converter using sliding-mode with adaptive hysteresis," in *Power Electronics Specialists Conference, 1995. PESC'95 Record., 26th Annual IEEE*, vol. 2. IEEE, 1995, pp. 1086–1093.
- [79] A. Sabanovic *et al.*, "Buck converter regulator operating in the sliding mode," in *proceedings of PCI*, 1893.
- [80] R. Venkataramanan, "Sliding mode control of power converters," Ph.D. dissertation, California Institute of Technology, 1986.
- [81] J. M. Guerrero, P. C. Loh, T.-L. Lee, and M. Chandorkar, "Advanced control architectures for intelligent microgridspart ii: Power quality, energy storage, and ac/dc microgrids," *IEEE Transactions on Industrial Electronics*, vol. 60, no. 4, pp. 1263–1270, 2013.
- [82] H. Kakigano, M. Nomura, and T. Ise, "Loss evaluation of dc distribution for residential houses compared with ac system," in *Power Electronics Conference (IPEC), 2010 International*. IEEE, 2010, pp. 480–486.
- [83] Y. Ito, Y. Zhongqing, and H. Akagi, "Dc microgrid based distribution power generation system," in *Power Electronics and Motion Control Conference, 2004. IPEMC 2004. The 4th International*, vol. 3. IEEE, 2004, pp. 1740–1745.
- [84] D. Chen and L. Xu, "Autonomous dc voltage control of a dc microgrid with multiple slack terminals," *IEEE Transactions on Power Systems*, vol. 27, no. 4, pp. 1897–1905, 2012.
- [85] M. Farhadi and O. A. Mohammed, "Real-time operation and harmonic analysis of isolated and non-isolated hybrid dc microgrid," *IEEE Transactions on Industry Applications*, vol. 50, no. 4, pp. 2900–2909, 2014.
- [86] Y. Gu, X. Xiang, W. Li, and X. He, "Mode-adaptive decentralized control for renewable dc microgrid with enhanced reliability and flexibility," *IEEE Transactions on power electronics*, vol. 29, no. 9, pp. 5072–5080, 2014.

- [87] X. Lu, K. Sun, J. M. Guerrero, J. C. Vasquez, and L. Huang, "State-of-charge balance using adaptive droop control for distributed energy storage systems in dc microgrid applications," *IEEE Transactions on Industrial electronics*, vol. 61, no. 6, pp. 2804–2815, 2014.
- [88] J. J. Justo, F. Mwasilu, J. Lee, and J.-W. Jung, "Ac-microgrids versus dc-microgrids with distributed energy resources: A review," *Renewable and Sustainable Energy Reviews*, vol. 24, pp. 387–405, 2013.
- [89] G. Benysek, M. Kazmierkowski, J. Popczyk, and R. Strzelecki, "Power electronic systems as a crucial part of smart grid infrastructure-a survey," *Bulletin of the Polish Academy of Sciences: Technical sciences*, vol. 59, no. 4, pp. 455–473, 2011.
- [90] J. Meer, A. Bendre, S. Krstic, and D. Divan, "Improved ship power system-generation, distribution, and fault control for electric propulsion and ship service," in *Electric Ship Technologies Symposium, 2005 IEEE*. IEEE, 2005, pp. 284–291.
- [91] M. Noritake, T. Ushirokawa, K. Hirose, and M. Mino, "Verification of 380 vdc distribution system availability based on demonstration tests," in *Telecommunications Energy Conference (INTELEC), 2011 IEEE 33rd International*. IEEE, 2011, pp. 1–6.
- [92] Y. Du, X. Zhou, S. Bai, S. Lukic, and A. Huang, "Review of non-isolated bi-directional dc-dc converters for plug-in hybrid electric vehicle charge station application at municipal parking decks," in *Applied Power Electronics Conference and Exposition (APEC), 2010 Twenty-Fifth Annual IEEE*. IEEE, 2010, pp. 1145–1151.
- [93] D. Izquierdo, R. Azcona, F. L. Del Cerro, C. Fernandez, and B. Delicado, "Electrical power distribution system (hv270dc), for application in more electric aircraft," in *Applied Power Electronics Conference and Exposition (APEC), 2010 Twenty-Fifth Annual IEEE*. IEEE, 2010, pp. 1300–1305.

- [94] D. Salomonsson, L. Soder, and A. Sannino, "An adaptive control system for a dc microgrid for data centers," in *Industry Applications Conference, 2007. 42nd IAS Annual Meeting. Conference Record of the 2007 IEEE*. IEEE, 2007, pp. 2414–2421.
- [95] A. Sannino, G. Postiglione, and M. H. Bollen, "Feasibility of a dc network for commercial facilities," in *Industry Applications Conference, 2002. 37th IAS Annual Meeting. Conference Record of the*, vol. 3. IEEE, 2002, pp. 1710–1717.
- [96] M. Amin, Y. Arafat, S. Lundberg, and S. Mangold, "Low voltage dc distribution system compared with 230 v ac," in *Electrical Power and Energy Conference (EPEC), 2011 IEEE*. IEEE, 2011, pp. 340–345.
- [97] W. Li, X. Mou, Y. Zhou, and C. Marnay, "On voltage standards for dc home microgrids energized by distributed sources," in *Power Electronics and Motion Control Conference (IPEMC), 2012 7th International*, vol. 3. IEEE, 2012, pp. 2282–2286.
- [98] S.-H. Ryu, J.-H. Ahn, B.-K. Lee, and K.-S. Cho, "Single-switch zvzcs quasi-resonant cll isolated dc-dc converter for low-power 32 lcd tv," in *Energy Conversion Congress and Exposition (ECCE), 2013 IEEE*. IEEE, 2013, pp. 4887–4893.
- [99] C.-H. Tsai, Y.-W. Bai, M.-B. Lin, R. J. R. Jhang, and C.-Y. Chung, "Reduce the standby power consumption of a microwave oven," *IEEE Transactions on Consumer Electronics*, vol. 59, no. 1, pp. 54–61, 2013.
- [100] K. Techakittiroj and V. Wongpaibool, "Co-existence between ac-distribution and dc-distribution: in the view of appliances," in *Computer and Electrical Engineering, 2009. ICCEE'09. Second International Conference on*, vol. 1. IEEE, 2009, pp. 421–425.
- [101] M.-H. Ryu, H.-S. Kim, J.-H. Kim, J.-W. Baek, and J.-H. Jung, "Test bed implementation of 380v dc distribution system using isolated bidirectional

- power converters,” in *Energy Conversion Congress and Exposition (ECCE), 2013 IEEE*. IEEE, 2013, pp. 2948–2954.
- [102] G. Reed, “Dc technologies: Solutions to electric power system advancements [guest editorial],” *IEEE Power and Energy Magazine*, vol. 10, no. 6, pp. 10–17, 2012.
- [103] B. T. Patterson, “Dc, come home: Dc microgrids and the birth of the” enernet”,” *IEEE Power and Energy Magazine*, vol. 10, no. 6, pp. 60–69, 2012.
- [104] T.-F. Wu, C.-H. Chang, L.-C. Lin, G.-R. Yu, and Y.-R. Chang, “Dc-bus voltage control with a three-phase bidirectional inverter for dc distribution systems,” *IEEE Transactions on Power Electronics*, vol. 28, no. 4, pp. 1890–1899, 2013.
- [105] B. A. Thomas, “Edison revisited: Impact of dc distribution on the cost of led lighting and distributed generation,” in *Applied Power Electronics Conference and Exposition (APEC), 2010 Twenty-Fifth Annual IEEE*. IEEE, 2010, pp. 588–593.
- [106] W. Yu, J.-S. Lai, H. Ma, and C. Zheng, “High-efficiency dc–dc converter with twin bus for dimmable led lighting,” *IEEE Transactions on Power Electronics*, vol. 26, no. 8, pp. 2095–2100, 2011.
- [107] L. Zhang, F. Jabbari, T. Brown, and S. Samuelson, “Coordinating plug-in electric vehicle charging with electric grid: Valley filling and target load following,” *Journal of Power Sources*, vol. 267, pp. 584–597, 2014.
- [108] G. Mills and I. MacGill, “Potential power system and fuel consumption impacts of plug in hybrid vehicle charging using australian national electricity market load profiles and transportation survey data,” *Electric Power Systems Research*, vol. 116, pp. 1–11, 2014.

- [109] M. Tabari and A. Yazdani, "A dc distribution system for power system integration of plug-in hybrid electric vehicles," in *Power and Energy Society General Meeting (PES), 2013 IEEE*. IEEE, 2013, pp. 1–5.
- [110] A. Mohamed, V. Salehi, T. Ma, and O. Mohammed, "Real-time energy management algorithm for plug-in hybrid electric vehicle charging parks involving sustainable energy," *IEEE Transactions on Sustainable Energy*, vol. 5, no. 2, pp. 577–586, 2014.
- [111] B. E. Noriega, R. T. Pinto, and P. Bauer, "Sustainable dc-microgrid control system for electric-vehicle charging stations," in *Power Electronics and Applications (EPE), 2013 15th European Conference on*. IEEE, 2013, pp. 1–10.
- [112] L. Roggia, C. Rech, L. Schuch, J. E. Baggio, H. L. Hey, and J. R. Pinheiro, "Design of a sustainable residential microgrid system including phev and energy storage device," in *Power Electronics and Applications (EPE 2011), Proceedings of the 2011-14th European Conference on*. IEEE, 2011, pp. 1–9.
- [113] C. Dierckxsens, K. Srivastava, M. Reza, S. Cole, J. Beerten, and R. Belmans, "A distributed dc voltage control method for vsc mtdc systems," *Electric Power Systems Research*, vol. 82, no. 1, pp. 54–58, 2012.
- [114] M. Aragüés-Peñalba, A. Egea-Àlvarez, S. G. Arellano, and O. Gomis-Bellmunt, "Droop control for loss minimization in hvdc multi-terminal transmission systems for large offshore wind farms," *Electric Power Systems Research*, vol. 112, pp. 48–55, 2014.
- [115] A. Al-Diab and C. Sourkounis, "Integration of flywheel energy storage system in production lines for voltage drop compensation," in *IECON 2011-37th Annual Conference on IEEE Industrial Electronics Society*. IEEE, 2011, pp. 3882–3887.
- [116] B. H. Kenny, R. Jansen, P. Kascak, T. Dever, and W. Santiago, "Integrated power and attitude control with two flywheels," *IEEE transactions on aerospace and electronic systems*, vol. 41, no. 4, pp. 1431–1449, 2005.

- [117] D. J. Becker and B. Sonnenberg, "Dc microgrids in buildings and data centers," in *Telecommunications Energy Conference (INTELEC), 2011 IEEE 33rd International*. IEEE, 2011, pp. 1–7.
- [118] P. Gross and K. L. Godrich, "Total dc integrated data centers," in *Telecommunications Conference, 2005. INTELEC'05. Twenty-Seventh International*. IEEE, 2005, pp. 125–130.
- [119] S. Rajagopalan, B. Fortenbery, and D. Symanski, "Power quality disturbances within dc data centers," in *Telecommunications Energy Conference (INTELEC), 32nd International*. IEEE, 2010, pp. 1–7.
- [120] G. AlLee and W. Tschudi, "Edison redux: 380 vdc brings reliability and efficiency to sustainable data centers," *IEEE Power and Energy Magazine*, vol. 10, no. 6, pp. 50–59, 2012.
- [121] D.-H. Kim, T. Yu, H. Kim, H. Mok, and K.-S. Park, "300v dc feed system for internet data center," in *Power Electronics and ECCE Asia (ICPE & ECCE), 2011 IEEE 8th International Conference on*. IEEE, 2011, pp. 2352–2358.
- [122] A. Pratt, P. Kumar, and T. V. Aldridge, "Evaluation of 400v dc distribution in telco and data centers to improve energy efficiency," in *Telecommunications Energy Conference, 2007. INTELEC 2007. 29th International*. IEEE, 2007, pp. 32–39.
- [123] G. Sulligoi, A. Tessarolo, V. Benucci, M. Baret, A. Reborra, and A. Taffone, "Modeling, simulation, and experimental validation of a generation system for medium-voltage dc integrated power systems," *IEEE Transactions on industry applications*, vol. 46, no. 4, pp. 1304–1310, 2010.
- [124] I.-Y. Chung, W. Liu, K. Schoder, and D. A. Cartes, "Integration of a bi-directional dc–dc converter model into a real-time system simulation of a shipboard medium voltage dc system," *Electric Power Systems Research*, vol. 81, no. 4, pp. 1051–1059, 2011.

- [125] D. Boroyevich, I. Cvetković, D. Dong, R. Burgos, F. Wang, and F. Lee, “Future electronic power distribution systems a contemplative view,” in *Optimization of Electrical and Electronic Equipment (OPTIM), 2010 12th International Conference on*. IEEE, 2010, pp. 1369–1380.
- [126] I. Cvetkovic, D. Dong, W. Zhang, L. Jiang, D. Boroyevich, F. C. Lee, and P. Mattavelli, “A testbed for experimental validation of a low-voltage dc nanogrid for buildings,” in *Power Electronics and Motion Control Conference (EPE/PEMC), 2012 15th International*. IEEE, 2012, pp. LS7c–5.
- [127] W. A. Tabisz, M. M. Jovanovic, and F. C. Lee, “Present and future of distributed power systems,” in *Applied Power Electronics Conference and Exposition, 1992. APEC’92. Conference Proceedings 1992., Seventh Annual*. IEEE, 1992, pp. 11–18.
- [128] S. Peyghami, P. Davari, H. Mokhtari, P. C. Loh, and F. Blaabjerg, “Synchronverter-enabled dc power sharing approach for lvdc microgrids,” *IEEE Transactions on Power Electronics*, vol. 32, no. 10, pp. 8089–8099, 2017.
- [129] Shivam and R. Dahiya, “Robust decentralized control for effective load sharing and bus voltage regulation of dc microgrid based on optimal droop parameters,” *Journal of Renewable and Sustainable Energy*, vol. 9, no. 4, p. 045301, 2017.
- [130] S. Luo, Z. Ye, R.-L. Lin, and F. C. Lee, “A classification and evaluation of paralleling methods for power supply modules,” in *Power Electronics Specialists Conference, 1999. PESC 99. 30th Annual IEEE*, vol. 2. IEEE, 1999, pp. 901–908.
- [131] B. T. Irving and M. M. Jovanovic, “Analysis, design, and performance evaluation of droop current-sharing method,” in *Applied Power Electronics Conference and Exposition, 2000. APEC 2000. Fifteenth Annual IEEE*, vol. 1. IEEE, 2000, pp. 235–241.

- [132] J. S. Glaser and A. F. Witulski, "Output plane analysis of load-sharing in multiple-module converter systems," *IEEE Transactions on Power Electronics*, vol. 9, no. 1, pp. 43–50, 1994.
- [133] C. Jamerson, T. Long, and C. Mullett, "Seven ways to parallel a magamp," in *Applied Power Electronics Conference and Exposition, 1993. APEC'93. Conference Proceedings 1993., Eighth Annual*. IEEE, 1993, pp. 469–474.
- [134] I. Batarseh, K. Siri, and H. Lee, "Investigation of the output droop characteristics of parallel-connected dc-dc converters," in *Power Electronics Specialists Conference, PESC'94 Record., 25th Annual IEEE*, vol. 2. IEEE, 1994, pp. 1342–1351.
- [135] D.-W. Cheng, Y.-S. Lee, and Y. Chen, "A current-sharing interface circuit with new current-sharing technique," *IEEE transactions on power electronics*, vol. 20, no. 1, pp. 35–43, 2005.
- [136] H. R. Muhammad, "Power electronics-circuits, devices, and applications," *Upper Saddle River, NJ, Pearson Prentice Hall*, 2004.
- [137] S. K. Mishra, S. Zhou, W. Huang, and G. Schuellein, "Design of a redundant paralleled voltage regulator module system with improved efficiency and dynamic response," in *Industry Applications Conference, 2006. 41st IAS Annual Meeting. Conference Record of the 2006 IEEE*, vol. 5. IEEE, 2006, pp. 2524–2528.
- [138] S. D. Tavakoli, M. Mahdavyfakhr, M. Hamzeh, K. Sheshyekani, and E. Afjei, "A unified control strategy for power sharing and voltage balancing in bipolar dc microgrids," *Sustainable Energy, Grids and Networks*, vol. 11, pp. 58–68, 2017.
- [139] S. Peyghami, H. Mokhtari, P. C. Loh, P. Davari, and F. Blaabjerg, "Distributed primary and secondary power sharing in a droop-controlled lvdc microgrid with merged ac and dc characteristics," *IEEE Transactions on Smart Grid*, 2016.

- [140] L. Zifa, L. Ya, Z. Ranqun, and J. Xianlin, “Distributed reinforcement learning to coordinate current sharing and voltage restoration for islanded dc microgrid,” *Journal of Modern Power Systems and Clean Energy*, pp. 1–11, 2017.
- [141] S. Peyghami, H. Mokhtari, and F. Blaabjerg, “Hierarchical power sharing control in dc microgrids,” in *Microgrid*. Elsevier, 2017, pp. 63–100.
- [142] W. Qiu and Z. Liang, “Practical design considerations of current sharing control for parallel vrm applications,” in *Applied Power Electronics Conference and Exposition, 2005. APEC 2005. Twentieth Annual IEEE*, vol. 1. IEEE, 2005, pp. 281–286.
- [143] T. Dragicevic, J. M. Guerrero, and J. C. Vasquez, “A distributed control strategy for coordination of an autonomous lvdc microgrid based on power-line signaling,” *IEEE Transactions on Industrial Electronics*, vol. 61, no. 7, pp. 3313–3326, 2014.
- [144] A. Kwasinski and C. N. Onwuchekwa, “Dynamic behavior and stabilization of dc microgrids with instantaneous constant-power loads,” *IEEE Transactions on Power Electronics*, vol. 26, no. 3, pp. 822–834, 2011.
- [145] I.-S. Bae and J.-O. Kim, “Reliability evaluation of distributed generation based on operation mode,” *IEEE Transactions on Power Systems*, vol. 22, no. 2, pp. 785–790, 2007.
- [146] M. Rashad, M. Ashraf, A. I. Bhatti, D. M. Minhas, and B. A. Ahmed, “Mathematical modeling and stability analysis of dc microgrid using sm hysteresis controller,” *International Journal of Electrical Power & Energy Systems*, vol. 95, pp. 507–522, 2018.
- [147] C. Edwards and S. Spurgeon, *Sliding mode control: theory and applications*. Crc Press, 1998.
- [148] V. Utkin, “Sliding modes in control and optimization, ser. communications and control engineering series,” 1992.

- [149] W. Perruquetti and J.-P. Barbot, *Sliding mode control in engineering*. CRC Press, 2002.
- [150] J.-J. E. Slotine, W. Li *et al.*, *Applied nonlinear control*. Prentice hall Englewood Cliffs, NJ, 1991, vol. 199, no. 1.
- [151] L. Martinez, A. Poveda, J. Majo, L. Garcia-de Vicuna, F. Guinjoan, J. Marpinard, and M. Valentin, “Lie algebras modelling of bidirectional switching converters,” in *Proceedings, European Conference on Circuit Theory and Design (ECCTD)*, vol. 2, 1993, pp. 1425–1429.
- [152] L. Martinez-Salamero, J. Calvente, R. Giral, A. Poveda, and E. Fossas, “Analysis of a bidirectional coupled-inductor cuk converter operating in sliding mode,” *IEEE Transactions on Circuits and Systems I: Fundamental Theory and Applications*, vol. 45, no. 4, pp. 355–363, 1998.
- [153] J. Ackermann and V. Utkin, “Sliding mode control design based on ackermann’s formula,” *IEEE transactions on automatic control*, vol. 43, no. 2, pp. 234–237, 1998.
- [154] W. L. Brogan, *Modern control theory*. Pearson education india, 1982.
- [155] A. Esmaeli, “Retracted: Stability analysis and control of microgrids by sliding mode control,” 2016.
- [156] M. Rashad, U. Raoof, M. Ashraf, and B. Ashfaq Ahmed, “Proportional load sharing and stability of dc microgrid with distributed architecture using sm controller,” *Mathematical Problems in Engineering*, vol. 2018, 2018.
- [157] S. Singh, D. Fulwani, and V. Kumar, “Robust sliding-mode control of dc/dc boost converter feeding a constant power load,” *IET Power Electronics*, vol. 8, no. 7, pp. 1230–1237, 2015.
- [158] S. I. Serna-Garcés, D. Gonzalez Montoya, and C. A. Ramos-Paja, “Sliding-mode control of a charger/discharger dc/dc converter for dc-bus regulation in renewable power systems,” *Energies*, vol. 9, no. 4, p. 245, 2016.

- [159] N. Vázquez, Y. Azaf, I. Cervantes, E. Vázquez, and C. Hernández, “Maximum power point tracking based on sliding mode control,” *International Journal of Photoenergy*, vol. 2015, 2015.
- [160] J. Cabiles-Magsino, R. C. Guevara, and M. Escoto, “Implementation of sliding mode control for current sharing in fixed frequency voltage regulator modules,” in *TENCON 2012-2012 IEEE Region 10 Conference*. IEEE, 2012, pp. 1–6.
- [161] R. Silva-Ortigoza, V. M. Hernández-Guzmán, M. Antonio-Cruz, and D. Muñoz-Carrillo, “Dc/dc buck power converter as a smooth starter for a dc motor based on a hierarchical control,” *IEEE Transactions on Power Electronics*, vol. 30, no. 2, pp. 1076–1084, 2015.
- [162] Y. Zhao, W. Qiao, and D. Ha, “A sliding-mode duty-ratio controller for dc/dc buck converters with constant power loads,” *IEEE Transactions on Industry Applications*, vol. 50, no. 2, pp. 1448–1458, 2014.
- [163] K. K. Leung and H. S. Chung, “Derivation of a second-order switching surface in the boundary control of buck converters,” *IEEE Power Electronics Letters*, vol. 2, no. 2, pp. 63–67, 2004.
- [164] V. R. Module, “and enterprise voltage regulator-down (evrd) 11.1 design guidelines,” *Intel Corp., Santa Clara, CA*, 2009.
- [165] W. Theodore *et al.*, *Electrical machines, drives and power systems, 6/E*. Pearson Education India, 2007.